ธรณีวิทยาโครงสร้างของแนวสันเขาหินปูนอุทัยธานี บริเวณชัยนาทดูเพลค ประเทศไทย

นางสาวพรชนก จินดามณี

รายงานนี้เป็นส่วนหนึ่งของการศึกษาตามหลักสูตรปริญญาวิทยาศาสตร์บัณฑิต ภาควิชา

ธรณีวิทยา คณะวิทยาศาสตร์ จุฬาลงกรณ์มหาวิทยาลัย

ปีการศึกษา 2554

STRUCTURAL GEOLOGY OF THE UTHAI THANI LIMESTONE RIDGE WITHIN THE CHAINAT DUPLEX, THAILAND

MS.PORNCHANOK CHINDAMANEE

A REPORT SUBMITTED IN PARTIAL FULFILMENT OF THE REQUIREMENTS

FOR THE DEGREE OF THE BACHELOR OF SCIENCE,

DEPARTMENT OF GEOLOGY, FACULTY OF SCIENCE,

CHULALONGKORN UNIVERSITY, 2011

วันที่ส่ง ...../……/….....

วันที่อนุมัติ ...../……/…..

ลงชื่อ.....

(อาจารย์ ดร. พิษณุพงศ์ กาญจนพยนต์)

อาจารย์ที่ปรึกษาโครงงาน

Acknowledgement

At the beginning and sincerely, I appreciate to thanks project advisor Dr. Pitsanupong Kanjanapayont for advice and suggestion throughout the beginning to the end of my bachelor's degree. All of my project, I feel carefulness and intention to pass on knowledge of him. Moreover he instituted Microtectonic class for teaching microstructure that is necessary for my senior project.For thank you to Assis.Prof.Dr.Thasinee Charoentitirat for suggestion about the Uthai Thai limestone. Thank you to Assis.Prof.Dr.Chakkaphan Sutthirat for great helpful in deform mineral. Thank you to Piyapong Chainreay for good suggestion and Global Mapper program to use in macroscopic scale.

Most of all, I would like to thanks Department of Geology, Faculty of Science, Chulalongkorn University for supporting the budget during this project and many useful laboratory instruments.

At last, special thanks are given to my friend and my senior, Ms.Piyanuch Keidaupratum, Ms.Pimporn Choemprapai, Mr.Boworn Butchaingam, Mr.Nutchapond Kachonthum, Ms.Kultirat phongpun and Mr.Ekapost Meenak for support and encourage.

STRUCTURAL GEOLOGY OF THE UTHAI THANI LIMESTONE RIDGE WITHIN THE CHAINAT DUPLEX, THAILAND

Pornchanok Chindamanee* and Pitsanupong Kanjanapayont

Department of Geology, Faculty of Science, Chulalongkorn University;

Tel: 083-762-1512, e-mail: pchindamanee@gmail.com

Abstract: Uthai Thani limestone ridge, which is located in Changwat Uthai Thani, lies in N-S direction on the central plane of Thailand. It is a southwestern part of Chainat duplex. Below the Mae Ping fault zone. This ridge is a part of Uthai Thani limestone. It is consist of Permian limestone. The evidences of macroscopic, mesoscopic and microscopic scales can be combined for the structural style of the Uthai Thani limestone ridge. Remote sensing interpretation show major lineament trends to N-S composite and minor NE-SW and ENE-WSW that conform to bed, fault, fracture and joint. The limestone was developed by sinistral ductile shear motion that was shown by sigmoid texture in calcite and chert nodule with strain shadow in outcrops and thinsection. Deformation of limestone widely spread which shown by stylolites, kink bands, the recrystallisation of twin boundary migration and bulging (BLG) recrystallisation. The temperature gauge of calcite twin geometry indicates temperatures at above 200 ^{o}C. In part of brittle deformation, dip slip fault was found and related with tend of bedding. All of characteristic of structural geology fit with the flexural slip and flexural shear fold models and the sinistral shear relates with the Chainat duplex and the Mae Ping fault zone during Tertiary.

Keywords: structural geology, Uthai Thani limestone ridge, Chainat duplex

บทคัดย่อ

สันเขาหินปูนอุทัยธานีตั้งอยู่ในเขตจังหวัดอุทันธานี โดยจะวางตัวอยู่ในแนวเหนือ -ใต้ และโดดเด่นขึ้นมา ในบริเวณที่ราบภาคกลาง ซึ่งอยู่ทางตะวันตกเฉียงใต้ของพื้นที่ชัยนาทดูเพลคในแนวรอยเลื่อนแม่ปิง ลักษณะทางธรณีวิทยาของสันเขาดังกล่าวประกอบด้วยกลุ่มหินปูนอายุเพอร์เมียน และเป็นส่วนหนึ่งของหินปูนอุทัยธานี

การศึกษาและวิเคราะห์ร่วมกันในระดับมหภาค มัจฉิมภาค และจุลภาค สามารถอธิบายลักษณะพฤติกรรมและธรณีโครงสร้างของสันเขาหินปูนอุทันธานีได้ โครงสร้างเส้นหลักจากการแปรภาพถ่ายดาวเทียมอยู่ในแนวเหนือใต้ซึ่งสัมพันธ์กับแนวการวางตัวของชั้นหินและรอยเลื่อน และโครงสร้างเส้นรองอยู่ในแนวตะวันออกเฉียงเหนือ -ตะวันตกเฉียงใต้ และในแนวเกือบเหนือ -ใต้ ซึ่งสัมพันธ์กับแนวการวางตัวของแนวแตกและรอยแยกในพื้นที่ศึกษา หลักฐานภาคสนามบงชี้ หินในพื้นที่ศึกษามีการบิดเบี้ยวและมีการแปรสภาพบางส่วนภายใต้การเฉือนแบบยืดเคลื่อนที่ทวนเข็มนาฬิกา (sinistral ductile shear) ซึ่งสังเกตได้จากลักษณะแร่แคลไซต์ และกระเปราะเชิตร์ ที่มีเขตเงาความเครียด (strain shadow) ทั้งในแนวหินโผล่และภายใต้กล้องจุลทรรศน์ การเปลี่ยนแปลงลักษณะของหินปูนพบได้โดยทั่วไปในพื้นที่ โดยสังเกตได้จาก stylolites, kink bands, twin boundary migration และ bulging (BLG). การบอกอุณหภูมิของการเปลี่ยนแปลงบอกได้จากลักษณะรูปร่างของของผลึกแฝดของแร่แคลไซต์ที่พบจากการศึกษาภายใต้กล้องจุลทรรศน์ โดยมีอุณหภูมิมากกว่า 200 °C การเปลี่ยนแปลงแบบแตกเปราะ (brittle deformation) พบว่ามีการเคลื่อนที่ในแนวระดับที่สัมพันธ์กับแนวการวางตัวของชั้นหิน จากลักษณะพฤติกรรมและธรณีโครงสร้างของสันเขาหินปูนอุทันธานีทั้งหมดที่พบสอดคล้องกับแบบจำลองของ ชั้นหินคดโค้ง (Fold) ที่เป็นแบบผสมของ flexural slip และ flexural shear fold ร่วมกัน และการเฉือนแบบอ่อนนิ่มเคลื่อนที่ทวนเข็มนาฬิกาสัมพันธ์กับชัยนาทดูเพลค และแนวรอยเลื่อนแม่ปิงในระว่างช่วงอายุเทอร์เทียรี

คำสำคัญ: ธรณีวิทยาโครงสร้าง สันเขาหินปูนอุทัยธานี ชัยนาทดูเพลค

Contents

Page

Acknowledgement I

Abstract (English) II

Abstract (Thai) III

Chapter 1 ..... **1-8**

Introduction 1

1.1 Location 4

1.2 Objective 5

1.3 Scope of Work 5

1.4 Expected Output 5

1.5 Regional Geology 5

1.6 Tectonic Setting 8

Chapter 2 ..... **9-18**

Methodology 9

Data Acquisition 10

2.1 Data and previous works reviews 10

2.2 Remote Sensing Interpretation 10

2.2.1 Lineament analysis 11

2.2.2 Landsat Thematic Mapper (TM) 11

2.2.3 SRTM digital elevation model 12

2.3 Field observation 13

2.3.1 Spatial data 13

2.3.2 Rocks oriented sampling 13

2.3.2.1 Collecting Rock Samples 13

Contents (conct.)

Page

2.3.2.2 Oriented of hand specimen for thin sections 15

Data Analysis 15

2.4 Laboratory 15

2.4.1 Structural analysis from stereographic nets and rose diagrams (Mesoscopic scale) 15

2.4.2 Microstructure analysis in thin sections (Microscopic scale) 16

- Cutting Sample 16
- Microstructure analysis 16

Data interpretation 18

2.5 Interpretation and discussion 18

2.5.1 Macroscopic scale 18

2.5.2 Mesoscopic scale 18

2.5.3 Microscopic scale 18

2.6 Conclusion and presentation 18

Chapter 3 ..... **19-54**

3.1 Remote Sensing Interpretation 19

3.1.1 STRM Digital Elevation Model (DEM) 19

3.1.2 Satellite images 23

3.2 Geology 26

3.2.1 Limestone 26

3.2.2 Limestone classification in thin section 28

3.3 Structural Geology 30

3.3.1 Mesoscopic scale 30

3.3.1.1 Brittle Deformation 31

Contents (conct.)

Page

- Fractures and joints 31
- En echelon joint or Tension gash 32
- Fault 34

3.3.1.2 Ductile Deformation 35

3.3.2 Microscopic scale 37

Calcite 38

Quartz 38

3.3.2.1 Sense of Shear 39

- Pure Shear 39
- Simple Shear 40

3.3.2.2 Deformation Mechanism 42

- Brittle Fracturing 42
- Shear band type fragmented porphyroclasts 43
- Pressure solution 44
- Stylolites 45
- Kink bands 45
- Twin boundary migration recrystallisation 46
- Temperature gauges 48
- Undulose extinction in calcite 52
- Bulging (BLG) Recrystallisation 53

Chapter 4 ..... **55-63**

Discussion 55

4.1 Structural style 55

4.2 Structural Evolution 57

4.3 Tectonics Evolution 61

Chapter 5 ..... **64**

Contents (conct.)

Page

Conclusion 64

References **65**

Appendix **68-74**

A : Field observation 68

B : Field Structural Measurement Data 69

C : Microtectonic 71

List of Figures

Figure		Page
1.1	Oblique DEM of SE Indochina illustrating key Tertiary geological features and their link with topography (Morley, 2002).	2
1.2	(a) to (c) Regional location maps and satellite image showing structural geology of the Mae Ping fault zone and (b) Chainat duplex in central Thailand (Smith et al., 2007).	3
1.3	Satellite image of the geometry and structure of Uthai Thani limestone ridge within the Chainat duplex. Linear north–south ridges where a number of fault strands splay from the NW–SE-trending Ayutthaya-Ban Klong Pong Fault and curve to a north–south direction (Smith et al., 2007).	3
1.4	The Landsat 7 image band 7,5 and 4 showing the northern-central plain of Thailand and the location of the Uthai Thani limestone ridge.	4
1.5	Geology of the Uthai Thani limestone ridge dominated by Permian limestone (Department of Mineral Resources, 1976).	6
2.1	Flow chart shows methodology for study in this project is presented.	9
2.2	Method to obtain an orientated sample from an outcrop and orientated thin section from a sample (Passchier and Trouw, 2005)	14
2.3	Concept of the fabric attractor. In both pure shear a. and simple shear b. deformation, material lines rotate towards and concentrate near an attractor direction, as shown in the stereograms (Passchier and Trouw, 2005).	17
3.1	Hillshead map in 3D of the Uthai Thani limestone ridge showed N-S major lineament that conform to the topographic ridge. c. and d. show the mountain range a. and b. show side view. Stimulated by Global mapper software.	20
3.2	Hillshade map with lineament interpretation in white lines generated form STRM digital elevation.	21

List of Figures (conct.)

Figure		Page
3.3	Lineament map, interpreted form hillshade map, presents the three main directions in rose diagram. The major strike is 010° NNE-SSW and two minor strikes are 060° NE-SW and 100° E-W.	22
3.4	The Landsat 5 TM images generated from bands 6-5-4 with lineament interpretation in red lines.	24
3.5	Lineament map with rose diagram based on Landsat 5 TM images presents three main directions. The major strike is 010° NNE-SSW and two minor strikes are 040° NE-SW and 090° E-W respectively.	25
3.6	The limestone outcrop in eastern area generally shows their texture, a. limestone doesn't have chert nodules, and b. shared grain of calcite.	26
3.7	The limestone outcrop in western area generally shows their texture, a. chert nodules wall, b. chert nodules mostly indicates deformed shape, and c. bedding	27
3.8	The Dunham (1962) classification of limestones according to depositional texture, as modified by Embry and Klovan (1971). For descriptions detailing the textural components of sediments and sedimentary rocks are describe by Dunham, 1962. **Mudstone** contains less than 10% grains (usually assessed by area in cut or thin section), supported by a lime mud. **Wackestone** consists of more than 10% grains, supported by a lime mud. **Packstone** contains lime mud, but is grain supported. **Grainstone** lacks mud, and is grain supported. **Boundstone is** Carbonate rocks that showing signs of being bound during deposition. Crystalline carbonate does not have recognizable depositional structures.	28
3.9	Packstone is carbonate rocks that is grain-supported and have a matrix of micrite (lime mud). Grains within a packstone are largely in contact with each other. The term packstone is part of the Dunham Classification (1962) of carbonate rocks.	

List of Figures (conct.)

Figure Page

The grains consist of most calcite and some quartz. Sometime calcite grains show graded from small to large size. In grain boundary don't clearly because of pressure solution. In limestone has mud residual between grain boundaries. Moreover they have grain boundary sliding, which is plastic flow evidence. 29

3.10 Packstone is carbonate rocks that is grain-supported and have a matrix of micrite (lime mud). Grains within a packstone are largely in contact with each other. The term packstone is part of the Dunham Classification (1962) of carbonate rocks. In limestone shows switching of calcite grains which notice by loop of small and large. Sometime stylolite can be preserved (Top of thin section). This is the thin section of sample from limestone in eastern area. 29

3.11 The rock shown in this thin section of a packstone is composed of most calcite and some quartz in a lime-mud matrix. The texture shows grain support that is part of the Dunham Classification (1962) of carbonate rocks. The calcite grains are very small size. This is the thin section of sample from limestone in western area. 30

3.12 Stereographic plots of the brittle deformation of bed. Contour poles of the direction showing 50° to 80° dipping mainly N-S 31

3.13 Show two sets of mutually intersecting joints. Joints in each set cut joints of the other set. There is no consistent relationship whereby joints of one set terminate on joints of the other set. 31

3.14 Stereographic plots of the brittle deformation of joint. Contour poles of the direction showing 50° to 80° dipping mainly in 2 directions, which consist of NEE-SWW and NE-SW. 32

List of Figures (conct.)

Figure Page

3.15 a. En echelon joint or Tension gash in limestone outcrop and between bed b. Tension gash fracture with weak zone that are arrayed en echelon along a shear fracture form as extension fractures during shearing, and c. Gash fractures form an en echelon array along a shear zone with each fracture perpendicular to the minimum compressive stress. 33

3.16 En echelon joint or Tension gash preserve in chert nodule. Chert is easy to brittle more ductile at low T, while limestone is more ductile. 33

3.17 The outcrop shows vertical fault movement. a. Fault plane is in the same direction as bedding plane that is N-S direction. There are both of normal fault and reverse in this fault plane. So the movement has more than one time, b. Chatter mark shows reverse fault, and c. Chatter mark shows normal fault. 34

3.18 Stereographic plots of the fault plain. Contour poles of the direction showing 70° to 80° dipping mainly NNE-SSW. 35

3.19 Rose diagram plots of the lineation in fault plain. The lineation is in ENE-WSW trending. It point to vertical movement of bed. 35

3.20 The limestone ridge in western area is folded. 36

3.21 Limestone outcrops showing ductile shear, a. chert nodules wall, and b. stretching chert nodules. 36

3.22 a. This outcrop shows chert nodule sheared. b. Interpretation of chert nodule sheared. Zigma shape of chert nodule sheared shows sinistral shear movement. Minor fault found in core of chert nodule that indicates vertical moment. 36

3.23 a. σ-shape of chert nodule sheared show distort core grain and strain shadow b. Sinistral sense of shear. 37

3.24 Bed folded relate with fault movement. This evidence shows deformation of ductile to brittle. Fault plain is N-S trending parallel to the trend of ridge. 37

List of Figures (conct.)

Figure Page

3.25 Concept of the fabric attractor (FA). In both **a.** pure shear and **b.** simple shear deformation, material lines rotate towards and concentrate near an attractor direction, as shown in the stereograms (Passchier and Trouw, 2005). 39

3.26 The calcite (**a.** and **b.**) and quartz (**c.**) grain example of irrotational strain in which a body is elongated in one direction. Pure shear derive from the compression, without shearing 40

3.27 Polycrystal of quartz show sigmoid texture. Sense of shear in sinistral. 40

3.28 Single crystal of quartz (**a.**and **b.**) calcite (**c.-e.**) show σ- type. Sense of sheared in sinistral. 42

3.29 Singelr crystal of calcite shows δ-type. Calcite grain shears and rotates. Sense of sheared in sinistral. 42

3.30 Single crystal of 2 calcite grain show mineral fish shapes. Sense of shear in sinistral. 42

3.31 Two sets of mutually intersecting micro fractures in calcite. Micro fractures of two sets cut each other. There is no consistent relationship whereby micro fractures of one set terminate on micro fractures of the other set. This micro fractures relate with joint in the field. 43

3.32 Microfaults transecting calcite grain in a section shows sliding in vertical movement which have normal (**a.**) and reverse (**b.**). Sense of sheared is dextral (**a.**) and sinistral (**b.**). 44

3.33 In Uthai Thani limestone, pressure solution is common that indicate low-grade metamorphic deformation. Pressure solution is usually active throughout a rock volume on the grain scale, leading to development of foliations and grain-scale dissolution and deposition features. The surfaces are normally highly indented

List of Figures (conct.)

Figure Page

and consist in three dimensions of surfaces mud in grain boundary (red arrow). Compressive strength is perpendicular with surfaces mud. 44

3.34 Stylolites formed by pressure solution. The surfaces are normally highly indented and consist in three dimensions of interlocking teeth of wall rock. These surfaces are therefore known as stylolites. 45

3.35 Kinking is common in crystals with a single slip system at low temperature. Sense of shear is sinistral kink fold. The kink bands are revealed by differences in absorption color, owing to their orientation differences. 46

3.36 Deformation twins are commonly wedge-shaped or tabular or tapered. Twin boundary is not sharp but curve. The small picture in right corner shows boundary migration recrystallisation in calcite, which can sweep whole crystals by migration of twin boundaries (Ramsay, 1967and Hobbs et al., 1988). 46

3.37 Deformation twins are commonly wedge-shaped or tabular or tapered. Some calcite twin absents in middle but in grain boundary still remain. The small picture in right corner shows boundary migration recrystallisation in calcite, which can sweep whole crystals by migration of twin boundaries. It is higher stage than figure 3.36 (Ramsay, 1967and Hobbs et al., 1988). 47

3.38 **a** Schematic illustration of the influence of temperature on deformation by calcite twinning (after Burkhard 1993; Ferrillet al. 2004). **b–e** Photomicrograph examples of different twin types (all in crossed-polarized light).**b** At temperatures below 200 C and dominate below 170 C. Narrow straight twins indicate Type I. **c** At temperatures dominate above 200 C up to 300 C. Wider twins which can be optically resolved ;Type II. **d.** At temperatures above 200 C, Type III intersecting twins and bent twins are present. **e.** At temperatures above 250 C, twins obtain serrated boundaries due to twin boundary migration recrystallisation; Type IV (Ramsay, 1967and Hobbs et al., 1988). 48

List of Figures (conct.)

Figure Page

3.39 Calcite grain has thick twin. Wider twins can be optically resolved; Type II. At temperatures dominate above 200 °C up to 300 °C that is a deformation temperature. 49

3.40 Calcite twin become curved, tapered and lensoid thick twins; Type III. The temperature above 200 °C is a deformation temperature. 50

3.41 Calcite twins obtain serrated boundaries due to twin boundary migration recrystallisation; Type IV. At temperatures above 250 °C that is a deformation temperature. 54

3.42 Undulose extinction is occurred in deformation calcite grain. Dislocations distributed over the crystal give rise to undulose extinction. 52

3.43 In calcite grain boundary show bulging (BLG) recrystallisation. At low temperature, the grain boundary may bulge into the crystal with high dislocation density and form new, independent small crystals. 53

3.44 Diagram show relationship between evidence from microscopic scale and mesoscopic scale 54

4.1 Show evident in mesoscopic and microscopic scale in field observation and thinsection that was found in the Uthai Thani limestone ridge. Those evident contribute to the fold model of flexural shear combine with flexural slip (Fig. 4.2); A, B, C, and D show stereographic projection plotted; E, F, M, and O; G, H, J, K and L show microstructure in thin section. 56

4.2 Geometry of flexural shear and flexural slip folding. **a.** The flexural shear fold is accommodated by simple and pure shear which is stretching into fold. The sense of shear on the rims of fold changes across the fold axial surface and the magnitude of the shear decreases toward the hinge. **b.** The flexural slip fold from an originally planar multilayer, showing relative displacement on layer surfaces.

List of Figures (conct.)

Figure Page

Layers on the convex side of a surface slip toward the hinge line relative to those on the concave side. 57

4.3 **a.** Fractures associated with folds. The stereographic projections show the orientations of the coordinate system, the bedding where it is not horizontal (dotted great circles), and the fractures (solid great circles). **b.** The stereographic projections show the orientations of joint and fracture in study area. They are associated with rim of fold. 58

4.4 **1st stage;** Digenesis of limestone in Permian; **2nd stage;** Fold stage that is combination with flexural shear and flexural slip. The flexural shear show sinistral and dextral shear in each rim of fold.; **3th stage** ; The sinistral ductile shear stage is developed on limestone as the affect of Mae Ping fault zone motion.; **4th stage** ; The result from continuous transpressional tectonic of Mae Ping fault zone probably leads to the N-S ridges in Chainat duplex. The reverse fault is possible to associate with uplift process of this ridge and others. 59

4.5 **a.** The SRTM digital elevation model show regional scale of northern central plain of Thailand and lineament interpretation to the restraining ben d duplex that modified form Smith et al. (2007). **b.** Model for structural style of the Uthai Thani-Nakhorn Sawan ridge (Phasongthum, 2011) **c.** Model for structural style of the Uthai Thani rhyolite ridge (Kachondham, 2012). 60

List of Tables

Tables		Page
2.1	Oblique DEM of SE Indochina illustrating key Tertiary geological features and their link with topography (Morley, 2002).	11
2.2	Evaluation of TM color combinations (after Sabins, 1996). *TM bands are listed in the sequence of projection colors: blue-green-red	12
4.1	The table shows summary of tectonic events and structural style in Uthai limestone ridge within Chainat duplex.	63

Chapter 1

Introduction

The collision of continental blocks of West Burma and Shan-Thai was during late Cretaceous-Early Tertiary (Bunopas, 1981, 1983; Charusiri et al., 2002; Polachan et al., 1991) (Fig. 1.1). Mae Ping Fault zone first developed during a Late Cretaceous-Early Tertiary transpressional event related with collision the West Burma and the western of Shan-thai (Morley, 2004). This early transpression was an initially developed to the main Indian-Eurasian collision when the fault zone underwent further (probably greatest) sinistral motion during the Oligocene (Lacassin et al. 1997).

The Mae Ping fault zone is extended to the Central Plains area by a low-lying major strike-slip duplex. This duplex called the Chainat Duplex related to the Himalayan Orogeny (Morley, 2002). The duplex is about 100 km long in a N-S direction. It was developed by sinistral motion on Mae Ping Fault zone, where the N-S and NW-SE fault orientation acted as a restraining bend during the Miocene. Minor episodic dextral motion may also have been of Late Oligocene-Miocene and/or Pliocene-resent (Smith el al., 2007).Both related with the Central Basin (Pliocene-Recent post-rift basin) which have or possibly possess petroleum potential as the superior target for petroleum exploration in Thailand.

The Chainat Duplex, that is in the Mae Ping fault zone, has been studied by Bunopas (1981), O'Leary and Hill (1989), and Smith et al. (2007) in regional morphology and analog model. However, a detailed interpretation of the geometry of faults with in Uthai Thani area (past of area in the Chainat Duplex) was not made. The geology the Chainat Ridge is composed of series of N-S striking isolated ridges of Paleozoic-Mesozoic sedimentary, meta-sedimentary, and igneous rocks (Smith et al, 2007) that has a complex structure and less clear data (Fig. 1.2).This area includes limestone ridge that prominently lies on southern zone of the Chainat Duplex about 19 km. The limestone ridge was named as "Uthai Thani limestone ridge" (Fig. 1.3). This ridge is a part of Uthai Thani limestone, which is proposed by Ueno et al. (2011).

This study focuses on the Uthai Thani limestone ridge where no previous works have in structural geology and their evolution .The aims of this study are to the structural geology and

structural evolution in this ridge. There are 3 main analysis including remote sensing interpretation, field observation and microstructure analysis.

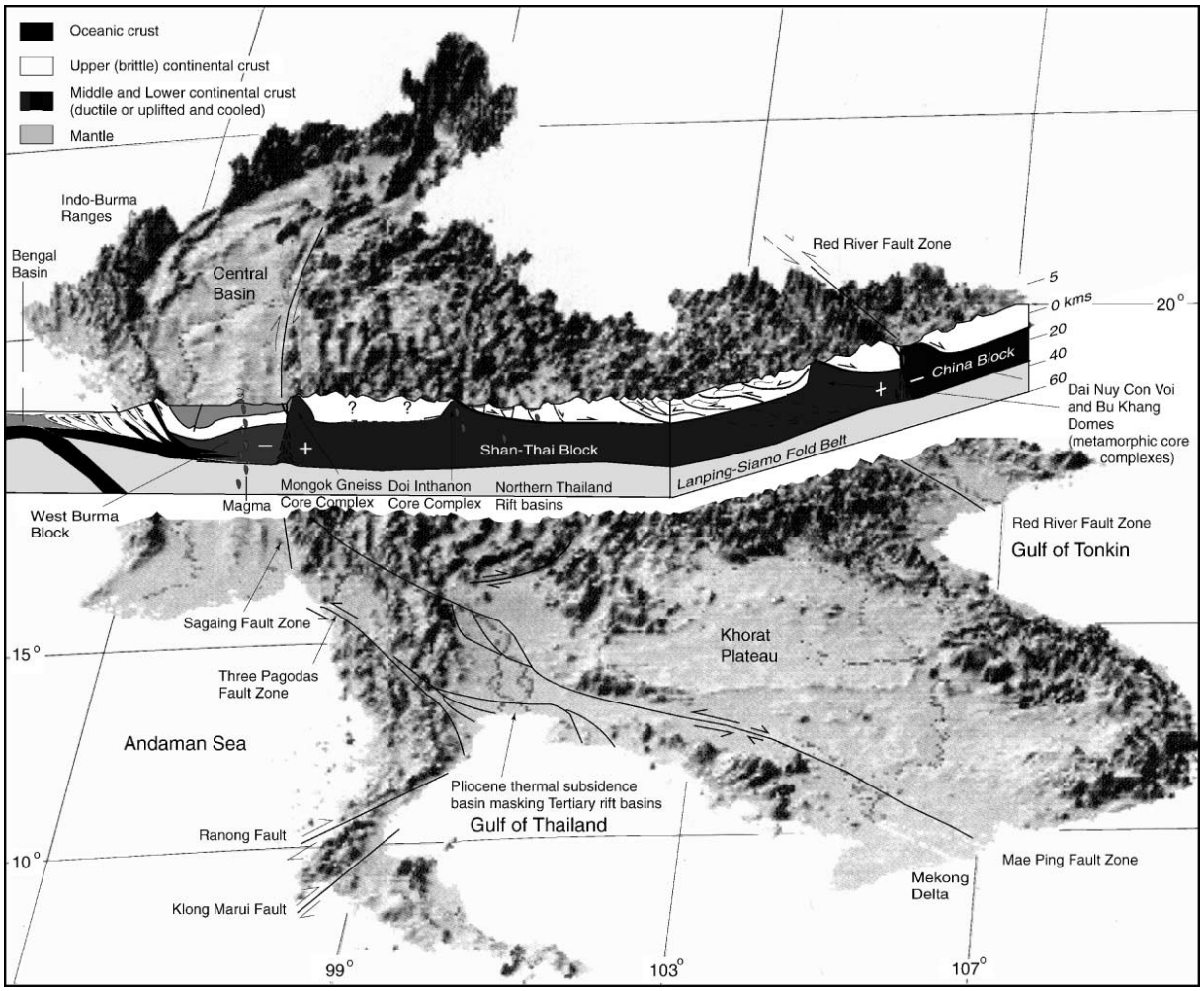

Figure 1.1 Oblique DEM of SE Indochina illustrating key Tertiary geological features and their link with topography (Morley, 2002).

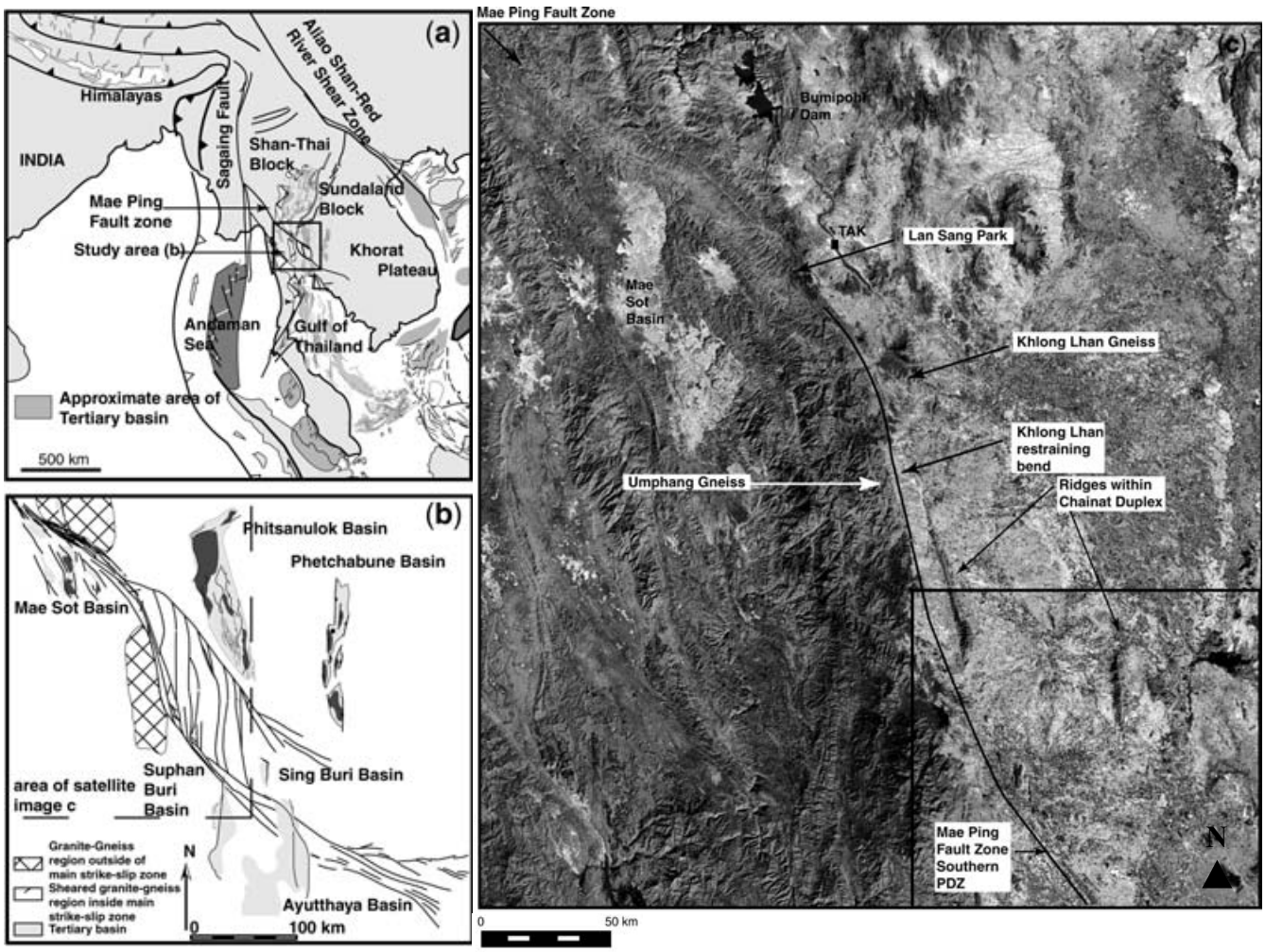

Figure 1.2 (a) to (c) Regional location maps and satellite image showing structural geology of the Mae Ping fault zone and (b) Chainat duplex in central Thailand (Smith et al., 2007).

Figure 1.3 Satellite image of the geometry and structure of Uthai Thani limestone ridge within the Chainat duplex. Linear north–south ridges where a number of fault strands splay from the NW–SE-trending Ayutthaya-Ban Klong Pong Fault and curve to a north–south direction (Smith et al., 2007).

1.1 Location

The Uthai Thani limestone ridge lies on the central plane of Thailand. It is in the southwestern part of the Chainat duplex. The Uthai Thani limestone ridge is located in Uthai Thani province, western part of Thailand between UTM 565000 to 578000, and 1685250 to 170630 (Fig. 1.2). This ridge long about 19 km in a N-S direction. The geology in the ridge is Permian limestone which obviously shows lineaments in the satellite image (Fig. 1.4). This ridge is parallel to the Uthai Thani-Nakhorn Sawan ridge which related to Chainat duplex (Prasongthum, 2011) (Fig. 1.2).

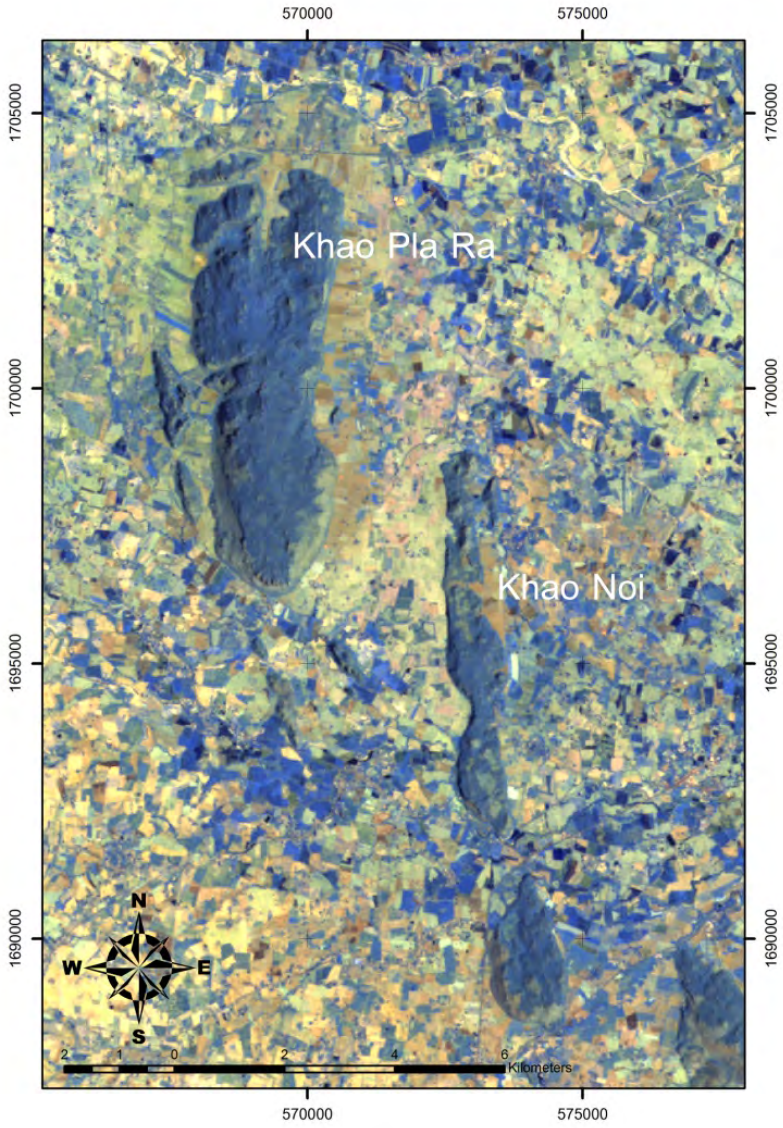

Figure 1.4 The Landsat 7 image band 7,5 and 4 showing the northern-central plain of Thailand and the location of the Uthai Thani limestone ridge.

1.2 Objective

- Characterize the structural geology of the Uthai Thani limestone ridge
- Interpret the structural evolution of the Uthai Thani limestone ridge with in Chainat duplex

1.3 Scope of Work

This study focuses on the structural geology of Uthai Thani limestone ridges. There are 2 main analysis including field observation and microstructure analysis. Initial form thoroughly literature reviews and methods are briefed and compiled for general geologic data and fundamental knowledge. The first main analysis is mesoscopic scale. Field observation is an important method to explain detail spatial data such as beddings, joints, lineations, and faults that have been measured and sampling. The rocks oriented samplings in the field observation are studied through the thin sections for microscopic scale. Spatial data from field observation are plotted and calculated in the equal-area stereographic projections and rose diagrams for structural analysis. The data from 2 main interpretation scales can be interpreted for structural geology and structural evolution of the Uthai Thani limestone ridge.

1.4 Expected Output

- Structural geology of the Uthai Thani limestone ridge within the Chainat duplex
- Structural evolution of the Uthai Thani limestone ridge

1.5 Regional geology

The Uthai limestone ridge, which is Permian limestone, is in southern of Mae Ping fault zone. The adjacent area consists of various rock ages from Silurian-Devonian to Quaternary. The all rock in study area is Permian Ratburi Group. In the part of the Chainat ridges is composed of series of N-S striking that are isolated ridges of Paleozoic-Mesozoic sedimentary, meta-sedimentary, and igneous rocks. Quaternary sediment deposits are surrounding in flat areas. The geology in the Uthai limestone ridge and nearly area is demonstrating the result in geological map sheet Changwat Nakhorn Sawan ND47-3 scale 1:250,000 of Department of

Mineral Resources in 1976 (Fig. 1.5) and the expressive geology in the study area by rock units is below in the geological map.

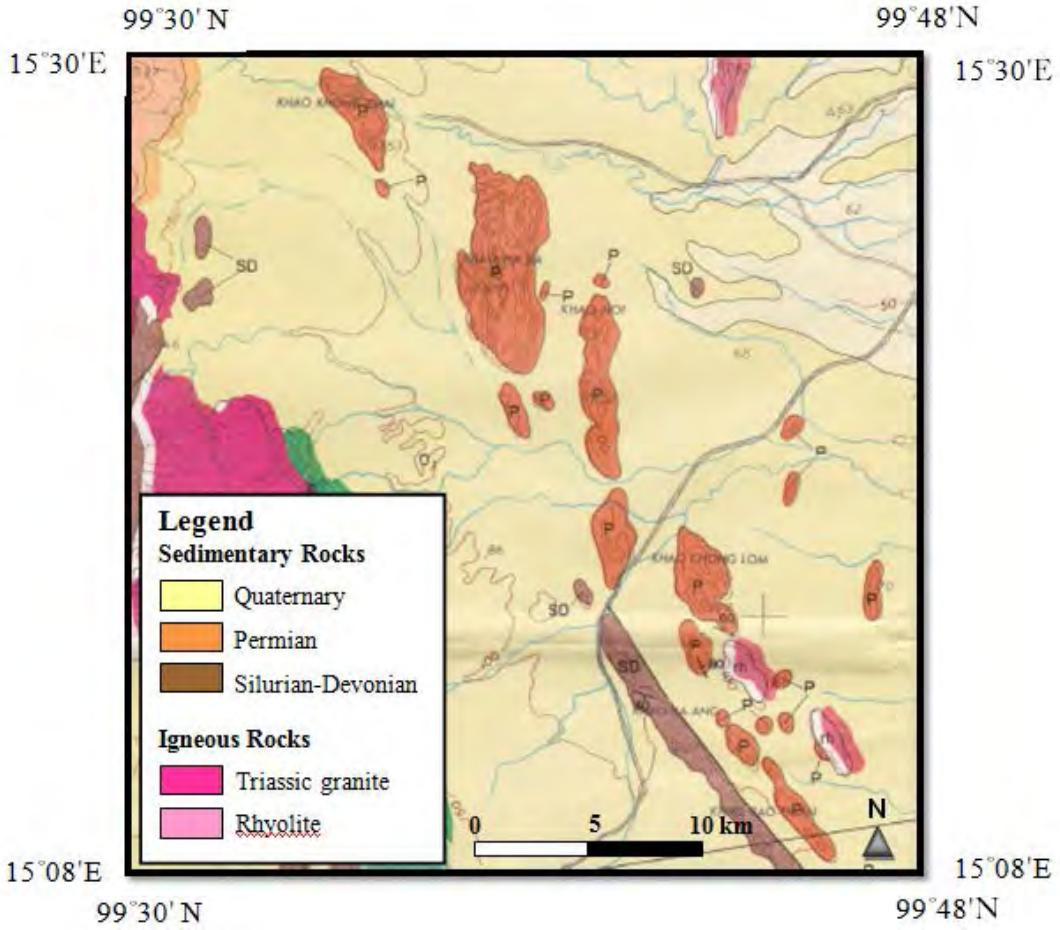

Figure 1.5 Geology of the Uthai Thani limestone ridge dominated by Permian limestone (Department of Mineral Resources, 1976).

Silurian-Devonian Unit

This unit is in south of the Uthai limestone ridge. According to geological map (DMR, 2008) group this unit is Ban Rai formation. Ban Rai formation is undifferentiated sequences of quartzite, phylite, greywacke, chert beds and local conglomerate.

Permain unit

This unit is the most of Uthai limestone ridge. The Permian limestone is in Khao Khad formation in Saraburi group, which comprised of beded to massive limestone, dolomitic limestone, dolomite, gray, well bedded, thin to very thick bedded, with fossils of fusulinid, brachiopods, corals, sponge and algae, miner shale, chert, and conglomerate.

The Saraburi Goup can be subdivided into 7 formations based on its lithologic character and stratigraphic position. The platform to basin margin belt consists of the Khao Khwang, the Khao Phaeng Ma and the Sap Bon Formations respectively in ascending order. The newly established Khao Phaeng Ma Formation consists of thin-to thick-bedded limestone and interbedded shale, chert and limestone conglomerate. Limestone is normally characterized by hummocky cross-bedding and graded bedding. Some beds show poorly sorted texture of a typical debris flow deposit. The basin belt comprises the lower Nong Pong Formation and the upper Pang Asok Formation. The fold and thrust belt proper includes the lower Nam Duk and the upper Nam Nao Formations (Chonglakmani, 2001).

Recently, Ueno et al. (2011) has suggested that there are some, N-S trending monadnock ranges in central Nakhon Sawan and eastern Uthai Thani provinces. They are composed of several limestone mountains which consist of massive, shallow-marine limestone, and bioclastic grainstone and packstone. They are the major microfacies. In places, boundstone observe skeletal metazoans and found Late Triassic foraminifers. Based on the foraminiferal contents and lithology, it can be correlated to a limestone member of the Lampang Group in the Sukhothai Zone of Northern Thailand. In western Uthai Thani Province, there is a outstanding ridge consisting of karstified limestone, which is called the Uthai Thani limestone. It is generally weakly metamorphosed and deformed. But Permian age is evident based on the occurrence of rare and poorly preserved fusulines from some localities. The Uthai Thani limestone can be distinguished from the eastern Late Triassic limestone by distinctive NNW-SSE extension and different deformation and metamorphic records. It is more reasonable to correlate it with the Sai Yok and the Ratburi limestones. The Uthai Thani limestone is widely distributed in the Sibumasu Block of Western and Peninsular Thailand.

Quaternary unit

Quaternary sediments deposits are surround in flat area are represented by old alluvial fan, colluvial and old flood in deposit of high and low terraces (Q1) and recent flood plain alluvial sediments (Q). Q1 consisting of gravels, sands, silts and laterite. Q is consisting of sands, silts and back swamps sediments.

Rhyolite unit

This unit also refers to Permo-Triassic age (DMR, 2008), which compose of undifferentiated volcanic rocks: rhyolite, andesite, dacite and tuff

Granitic rock

There are granitic rock in west of the Uthai limestone ridge that belongs to the north-south Cestern Belt Granite (Charusiri et al., 1993). The lithologies consist of megacrystic biotite granite, foliated biotite granite, alkaline complex, and migmatite granite.

1.6 Tectonic setting

The structural geology of Thailand related with the Himalayan Orogeny that is the Cenozoic orogenic processes (Morley, 2002). It was developed by Indian-Asian Collision and leading to the southeast extrusion of the Indochina block (Lacassin et al., 1997; Tapponnier et al., 1986). The India plate migrated northward, stresses rotated > 100 ^{o} clockwise between the middle Eocene and middle Miocene. It was given the NW-SE strike of these faults such as Mae Ping Fault Zone and Three Pagodas Fault Zone. The changing stresses orientations should have resulted in a reversal of strike-slip from Eocene-Oligocene left-lateral to Miocene right-lateral (Rhodes et al., 2005). In western and central Thailand was dominated by NW-SE trending Mae Ping Fault Zone and Three Pagodas Fault Zone. These faults cut the western part of the Indochina block and lie parallel to the Red River Fault. Evidence of extreme ductile left-lateral shear is found in the Lansang gneisse, which is in a transpressional environment. Dating by $^{40}Ar/^{39}Ar$ in this zone shows around 30.5 Ma. It suggests that the ductile left-lateral slip is pre-late Oligocene (Lacassin et al., 1993, 1997).

The Mae Ping fault zone has undergone predominantly sinistral strike-slip motion (Lacassin et al., 1993, 1997). Along the Mae Ping fault zone, where is in the Central Plains area, developed strike-slip duplex, called the Chainat Duplex (Smith et al., 2007). The duplex has N-S and NW-SE strike and developed during sinistral displacement on Mae Ping Fault zone. The N-S fault orientation leads to a restraining bend. The restraining bend form major topographic uplifts that call ridge (Cunningham et al., 2007). The geology of the Chainat ridges is composed of series of N-S striking that are isolated ridges of Paleozoic-Mesozoic sedimentary, meta-sedimentary, and igneous rocks. The Chainat ridges are surrounding Quaternary sediment and the Central Basin (Pliocene-Recent post-rift basin) (Smith et al, 2007).

Chapter 2

Methodology

Methodology for study in this project is presented in the flow chart. There are 3 main parts; Data Acquisition, Data Analysis and Data Interpretation.

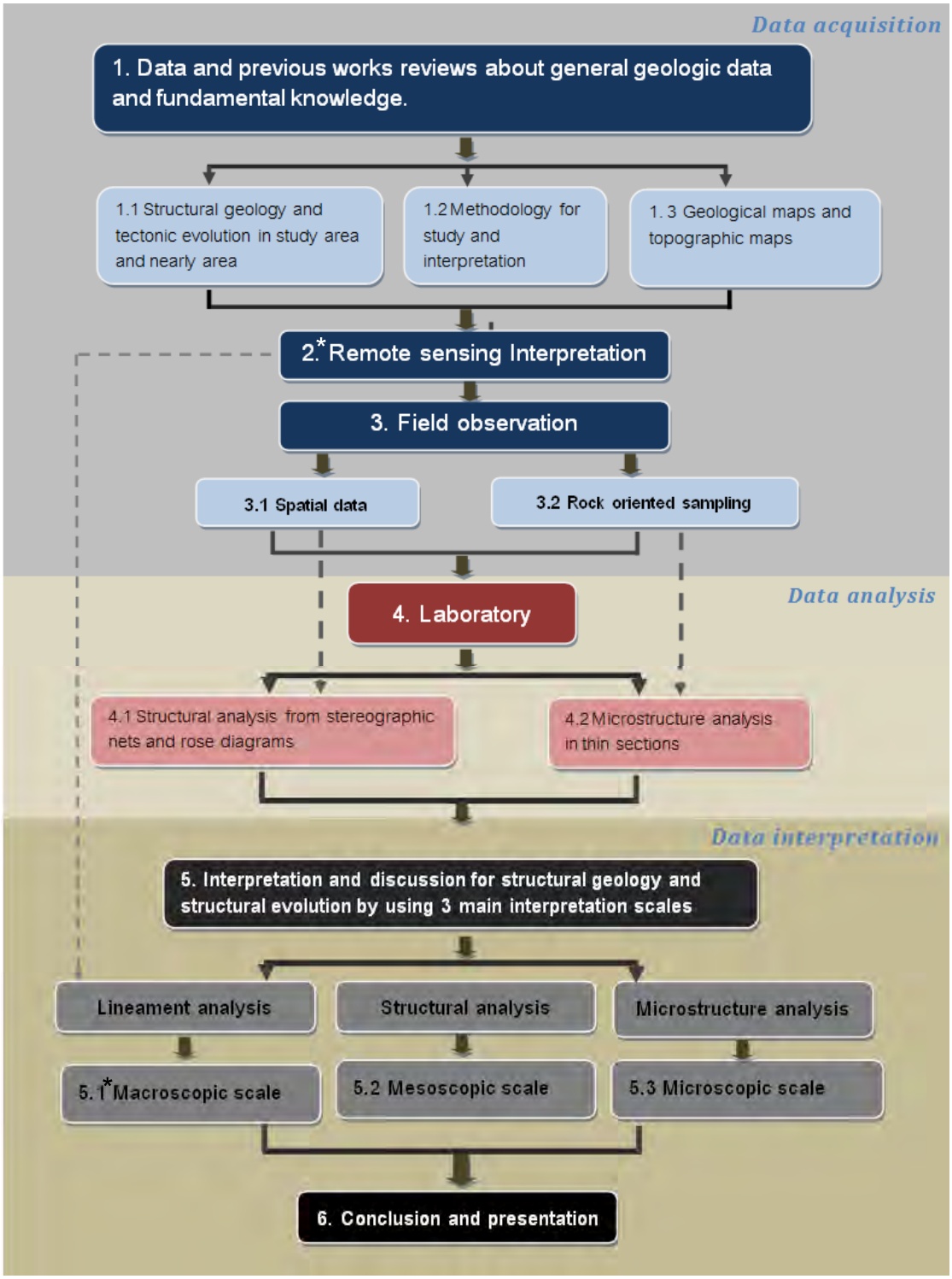

Figure 2.1 Flow chart **shows** methodology for study in this project is presented.

Remark * Remote sensing interpretation and Macroscopic scale out of my scope and add in laster.

Data Acquisition

2.1 Data and previous works reviews about general geologic data and fundamental knowledge

Data acquisition is profiling and collecting the data in geology. Data acquisition was done for initial data (previous works) and fact data (field observations). Initial data is about previous works, general geologic data, fundamental knowledge in structural geology and tectonic evolution, topographic maps, and satellite images in the study area and adjacent area. Geological data for the field observation is important to understand geological and structure in the region. This data used to be a guideline for planning. On the other hand previous works may be not informed in detail. So field observations are needed for detail data. They are important evidences which using for the interpretation.

2.2 Remote sensing interpretation

Remote sensing gives the information about the Earth's surface without actually being in contact with it. This is done by sensing and recording reflected or emitted energy. These dates were processing, analyzing, and applying for geological information in regional scale. Several types of satellite images with multiwavelength bands and medium-to-high spatial resolution have become available and can be processed easily on a personal computer. Digital satellite image data provide information on spectral characteristics of surface materials. Particularly in the field of geology, the application patterns on satellite images can be divided broadly into two categories: lineament enhancement and lineament extraction for characterization of geologic structure image classification. The surface facial expression such as fractures, bed, and fault are strikingly expressed as lineaments. So remote sensing image an important in order to use for reginal scale studies including lineament analysis.

The data from remote sensing interpretation are an important in order to use for reginal scale studies including lineament analysis. The remote sensing data used in this study are LANSAT 5 TM images, and STRM digital elevation model (DEM). Two different data sources are integrated in Global Mapper and ArcGIS software for quantitative spatial lineament interpretation.

2.2.1 Lineament analysis

Lineament analysis, which integrates the analyses of linear patterns, geometry, kinematics and dynamics, can be applied to study geological structures on the basis of tectonic contexts. Brittle structure such as fracture and faults may correspond with lineaments appearing on remote sensensing images.

Lineaments used in this study are two different remote sensing data sources: (1) satellite images with resolution 30 m^2/pixel, and (2) the SRTM Digital Elevation Model with resolution 90 m^2/pixel. Satellite images were processed by selected 3 band mixing of thematic mapper with false-color composites. The SRTM 90 m DEM was processed to generate the hillshade map for the lineament analysis. A LANDSAT Thematic Mapper (TM) subscene was used for the analysis. The band 4 subscene of the LANDSAT 5 TM image was determined to be appropriate for the lineament analysis by comparing several images with a shaded-relief image derived from a digital elevation model (DEM).

2.2.2 Landsat Thematic Mapper (TM)

Landsat Thematic Mapper (TM) images consist of seven spectral bands with a spatial resolution of 30 meters for Bands 1 to 5 and 7 (Table 2.1). Spatial resolution for Band 6 (thermal infrared) is 120 meters, but is resampled to 30-meter pixels(Table 2.1). Approximate scene size is 170 km north-south by 183 km east-west (106 mi by 114 mi).

Table 2.1 Landsat thematic mapper (TM) Sensor Band designations. (Geological Survey (USGS) and the National Aeronautics and Space Administration (NASA), 2006).

Spectral Bands		Wavelength, μm	Use
1	Blue-green	0.45-0.52	Bathymetric mapping; distinguishes soil from vegetation; deciduous from coniferous vegetation
2	Green	0.52-0.60	Emphasizes peak vegetation, which is useful for assessing plant vigor
3	Red	0.63-0.69	Emphasizes vegetation slopes

4	Reflected IR	0.76-0.90	Emphasizes biomass content and shorelines
5	Reflected IR	1.55-1.75	Discriminates moisture content of soil and vegetation; penetrates thin clouds
6	Thermal IR	10.40-12.50	Useful for thermal mapping and estimated soil moisture
7	Reflected IR	2.08-2.35	Useful for mapping hydrothermally altered rocks associated with mineral deposits

Table 2.2 Evaluation of TM color combinations (after Sabins, 1996). *TM bands are listed in the sequence of projection colors: blue-green-red.

Display colors	Advantages	Disadvantages
1-2-3	Normal color image. Optimum for mapping shallow bathymetric features.	Lower spatial resolution due to band 1. Limited spectral diversity because no reflected IR bands are used.
2-3-4	IR color image. Moderate spatial resolution.	Limited spectral diversity.
4-5-7	Optimum for humid regions. Maximum spatial resolution.	Limited spectral diversity because no visible bands are used.
2-4-7	Optimum for temperate to arid regions. Maximum spectral diversity.	Unfamiliar color display, but interpreters quickly adapt.

2.2.3 SRTM digital elevation model

The Shuttle Radar Topography Mission (SRTM) got elevation data on a near-global scale to generate the most complete high-resolution digital topographic database of Earth. The digital elevation data (DEMs) is had provide by the NASA Shuttle Radar Topographic Mission (SRTM) for over 80% of the earth. A digital elevation model (DEM) is a digital model or 3-D representation of surface to vary along to elevation. A DEM shows that elevation is available

continuously at each location in the study area. The quality of a DEM is measures of how correct elevation is at each pixel and how correctly are the morphology presented.

2.3 Field observation

2.3.1 Spatial data

Field data have two important data that are spatial data and orientated rock samples. Spatial data including structural geology data consist of attitude of bedding, foliation, lineation and fault for plotting on stereographic projection and rose diagram. Orientated rock samples in the field are used for microstructure analysis in thin the section, rock chip microstructure and rock descriptions.

2.3.2 Rocks oriented sampling

2.3.2.1 Collecting Rock Samples

In the field we can collect the sample for studying in the laboratory. Rock Samples from out crop can use to 4 procedures. The first, we make petrographic identification. The second, we measure small-scale planar and linear structures. Then, we trace mineral reactions. Finally, we compare rocks from different parts of the area (Compton, 1985). If interest is in the rock types of an area, we can collect. This will take effort, for typical rocks tend to become an unnoticed background to ones that are unusual from different area.

In addition to being representative, samples must be as fresh as possible for identified rock types. In structural study should collect representative in structure characteristic such as foliation and lineation. Rock samples are numbered, marked, and labeled to realize and wrapped or placed in bags to protect them from abrasion.

In figure 2.1 discusses the steps of sample collection and choice of sectioning plane. The choice of samples for thin sections depends on the topic of interest and methods that are going to be used. Thin section studies usually give best results if they are undertaken to solve a specific problem that has been defined before the sections were cut (Passchier et al. 1990). Rock Samples or hand specimens for structural studies should be oriented in the field. This is best done by marking dip and strike of a planar surface of the specimen on that surface (Fig.

12.1). If a sample is taken in a major fold, it is useful to know from which limb or part of the hinge it was taken. Shear zones should be sampled in the high strain, in the low strain rim and in the wall rock. In many ductile shear zones, fine-grained samples representing highly strained parts of the shear zone give better results than samples of coarse-grained or low strain domains (Passchier and Trouw, 2005).

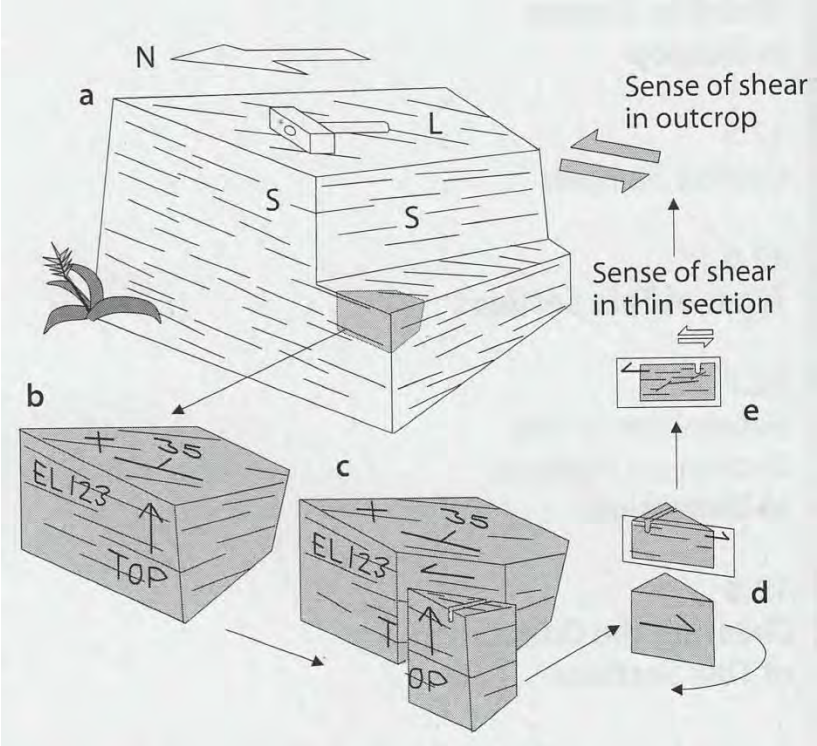

Figure 2.2 Method to obtain an orientated sample from an outcrop and orientated thin section from a sample (Passchier and Trouw, 2005) .

Method to obtain an orientated sample from an outcrop and orientated thin section from a sample is illustrated in the Fig. 2.2. An outcrop where targeted to collect sample (a). To make strike-dip symbol on the planar top surface of the sample and a cross (marking on the top) fix the orientation of the sample in a space (b). A thin section is cut parallel to the lineation and anticlinal to foliation. A chip is cut from the sample. In order to orient the chip, direction of the top surface can use an arrow and draw on both the sample and the chip (c). Care should be taken that this arrow is copied correctly onto the thin section (d). Alternatively, a small saw-cut scar can be made in the top surface of the chip, which can be found back in the thin section.

Shear sense determined in thin section. This thin section is directly related to the sample and through the sample to the original outcrop (e).

2.3.2.2 Oriented of hand specimen for thin sections

Samples or hand specimens for structural studies have to orient in the field (Fig 2.1). Oriented samples are collected for later field in microstructure of fabrics or small features in rocks that must be related to the major structure in field. Examples are sandstone with possible current oriented fabric; metamorphic rocks with folded lineation; igneous rocks cut by sets of thin veins; and orientations of crystallographic axes of quartz. Most samples can be collected by: (1) Measuring the strike and dip of a planar surface on the rock and (2) Drawing a strike-and-dip symbol on the surface before breaking the sample from the outcrop, or after fitting it back exactly to its original position. An arrowhead in added to the strike line and a geographic direction to the dip line to insure that the orientation will be unambiguous. The compass direction of the arrow is included in the note, as is a notation as to whether the planar surface faces upward or downward (Compton, 1985). Photograph or simple sketch of the samples is useful when the samples are confused. If there are structures of interest in the sample (foliations, lineation, etc.) it is important to make the cut at an angle of interest in thin sections.

Data Analysis

2.4 Laboratory

This study focuses on the structural geology and Structural evolution of Uthai Thani limestone ridges. There are 2 mains analysis including spatial data and rocks oriented sampling. Spatial data in field observation use for structural analysis (Mesoscopic scale). Rocks oriented sampling use for microstructure analysis in thin sections (Microscopic scale).Those data analysis can bring about to purpose of studying.

2.4.1 Structural analysis from stereographic nets and rose diagrams (Mesoscopic scale)

Outcrops, or exposures, consist of earth materials that can be examined in place. Exposed rocks may also develop forms characteristic of certain rock unit. A hypothesis is a statement about what you expect to observe. Field observation is important to prove the hypothesis. It is a basic method of geologists for collecting geological data such as attitude of

bedding, foliation, lineation, joint, fracture, fault and fold that are spatial data. In the field observation, geologists can measure small-scale planar and linear structures in sample, which they interested and wanted more detail to study. Example in this study, oriented samples is collected for later field in microstructure of fabrics or small features in rocks that must be related to the major structure in field. All attitude data will be statistically plotted in stereographic net and rose diagram to analyze the structural geology in mesoscopic scale. All of data in field is important to interpret and analyze structural geology or other point in geology.

2.4.2 Microstructure analysis in thin sections (Microscopic scale)

Cutting Sample

When oriented sample are cut to make thin sections, they must have orientation data. Method to obtain an orientated sample from an outcrop and orientated thin section from a sample is in figure 2.1. After saw-cut is cut from the sample, the orientation of the sample should be copied on both sides of the saw-cut in mirror image (Fig. 2.1). We should mark a symbol in which an arrow with a single barb is drawn parallel to the lineation, with the barb indicating the top of the sample. Be careful when preparing the rock chips for thin sections that the orientation is not lost or confused.

Microstructure analysis

Thin section preparation is needed orderly for rock samples in the Uthai Thani limestone Ridge to be inspected microscopically for analyze the characteristics of the rock. Polarized light microscope is also widely used for study in microstructure and petrography and this technique requires the surface of the sample to be flat and highly polished for the best results to be achieved.

Microstructure or fabric of a rock in thin section can be used in two major fields that are mechanism of rock deformation and metamorphism. Thin section mostly studies in the latter field. Because in thin section can serve to reconstruct tectonic evolution in the microtectonic term. In theory, one could expect that a sedimentary rock which is buried, metamorphosed and uplifted into the surface should have the same mineral composition as the original serve to sediment if perfect original equilibrium conditions were to be attained at each stage. A simple fabric should be developed in such a case in response to gradual changes in the stress field

and in metamorphic condition. The aim is interpret overprinting relations in terms of deformation phase and metamorphic events. Once deformation phases and metamorphic events are defined, it is necessary to determine to what extent they correspond to tectonic event or metamorphic cycles, i.e. events on a larger scale such as those associated with plate motion or collision (Passchier and Trouw, 2005).

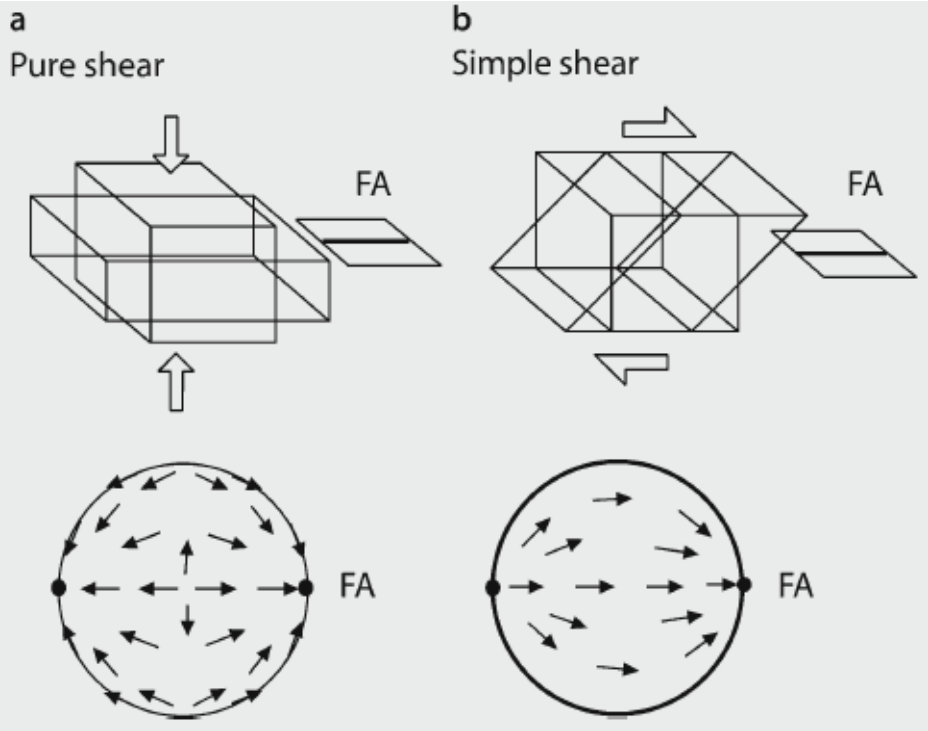

Figure 2.3 Concept of the fabric attractor. In both pure shear **a** and simple shear **b** deformation, material lines rotate towards and concentrate near an attractor direction, as shown in the stereogram (Passchier and Trouw, 2005) .

The concept of deformation phases has been used extensively in the geological literature in reconstruction of the structure evolution of rock units with complex deformation patterns (Ramsay, 1967; Hobbs et al., 1988). A metamorphic evolution can be subdivided into metamorphic event defined by the growth of particular metamorphic minerals, in a way similar to the concept of deformation phase. Microstructure may include grain shape, grain boundaries, deformation lamellae, aggregates of grain with similar shape, lattice preferred orientation, and shear sense indicators (Figure 2.2). Those textures and other microstructures will be observed, classified and photographed in thin sections for structural geology in microscopic scale.

Data interpretation

2.5 Interpretation and discussion

Interpretation and discussion for structural geology and structural evolution are using 2 main scales for interpretation.

2.5.1 Macroscopic scale

Lineament analysis, which integrates the analyses of linear patterns, geometry, kinematics and dynamics form LANSAT 5 TM images, and STRM digital elevation model (DEM), are an important in order to use for regional scale studies. The spatial lineament orientations are plotted, and analyzed in rose diagrams. Each different source data are compared and complied with major lineament trend of the area. Lineament analysis can be applied to study geological structures on the basis of tectonic contexts.

2 5.2 Mesoscopic scale

Spatial data in the outcrop such as attitude of bedding, foliation, lineation and fault plus detailed rock descriptions are use for structural geology analysis. The result from structural analysis can be interpreted to the structural evolution in study area that relate to tectonic setting in Thailand.

2.5.3 Microscopic scale

Rock microstructure is studied in the thin sections which describe the texture of a rock and the small scale rock structures. Thin section preparation is needed to be inspected microscopically for analyze the characteristics of the rock. Microstructure analysis support to structure analysis from mesoscopic scale which can explain and support to tectonic evolution in study area.

2.6 Conclusion and presentation

The last methodology, which refers to achieve the study's aim, is conclusion. The accurate conclusion is integrated from the interpretation and discussion of both mesoscopic and microscopic scales. Finally, report and present project's objection and output.

Chapter 3

The results of Remote sensing interpretation, field observation and microstructure analysis of the Uthai Thani limeston ridge with in Chainat duplex are reported in this chapter. All results can compare to each other.

3.1 Remote Sensing Interpretation

The data from remote sensing interpretation are an important in order to use for reginal scale studies including lineament analysis. The remote sensing data used in this study are LANSAT 5 TM images, and STRM digital elevation model (DEM). Two different data sources are integrated in Global Mapper and ArcGIS software for quantitative spatial lineament interpretation. The spatial lineament orientations are plotted, and analyzed in rose diagrams. Each different source data are compared and complied with major lineament trend of the area. Remote sensing techniques are necessary for understanding the regional geology in the Uthai Thani limeston ridge because of the high weathering and erosion in the tropical climate. So the limestone ridge show krast topography and rich of solution limestone outcrop.

3.1.1 STRM Digital Elevation Model (DEM)

The SRTM 90 m DEM is used for qualification of the topographic signal. The STRM digital elevation model is processed and analyzed by Global mapper software to produce hillshade maps. Topography in 3D views in hillshaed map is used to interpret major lineament trend of ridge, which controlled by geological structures.

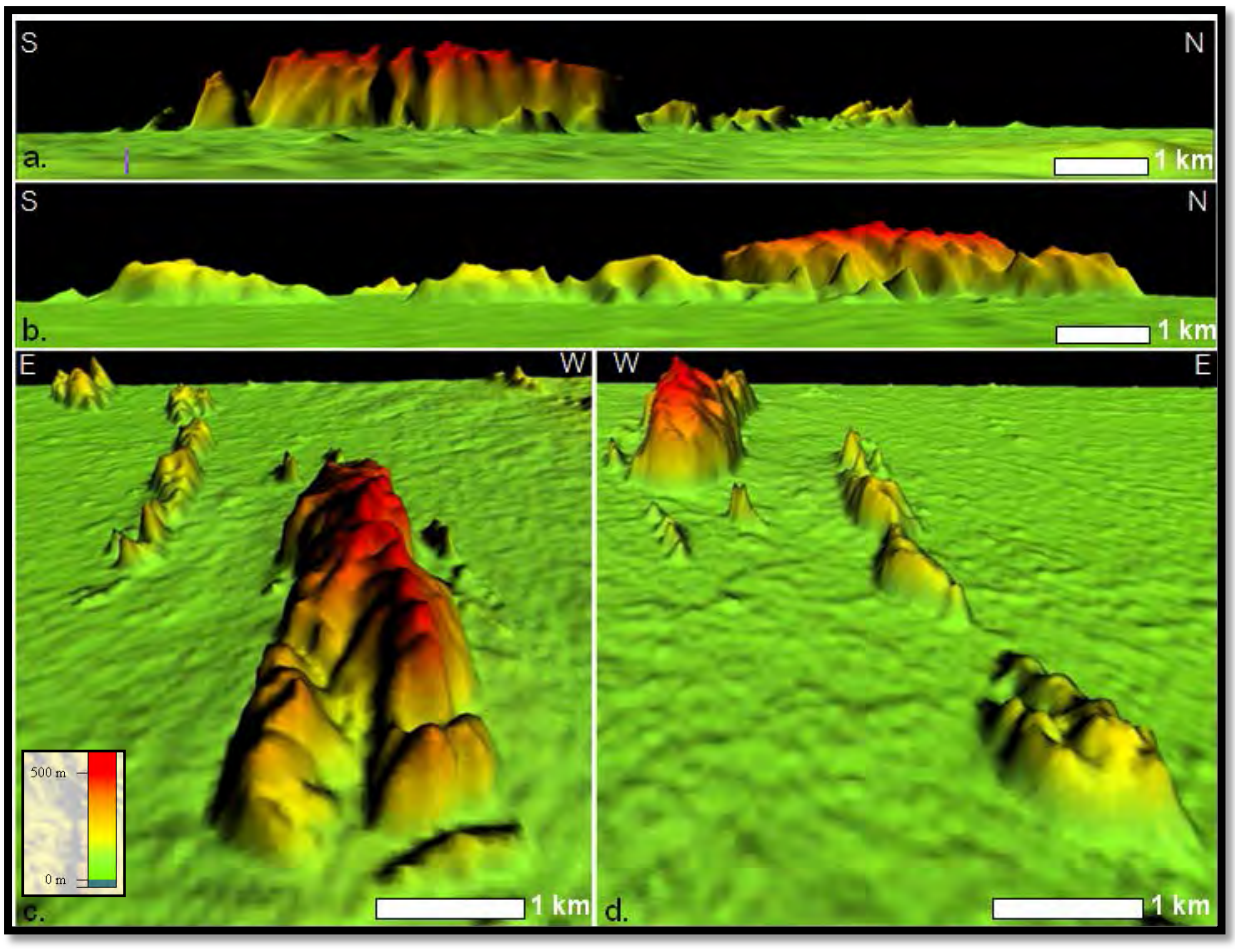

Figure 3.1 Hillshead map in 3D of the Uthai Thani limeston ridge showed N-S major lineament that conform to the topographic ridge. **c.** and **d.** show the mountain range **a.** and **b.** show side view. Stimulated by Global mapper software.

Form SRTM DEM, the 43 lineaments (Fig. 3.2) which were plotted in rose diagram show three main directions (Fig. 3.3). The major strike is 010° NNE-SSW and two minor strikes are 060° NE-SW and 100° E-W

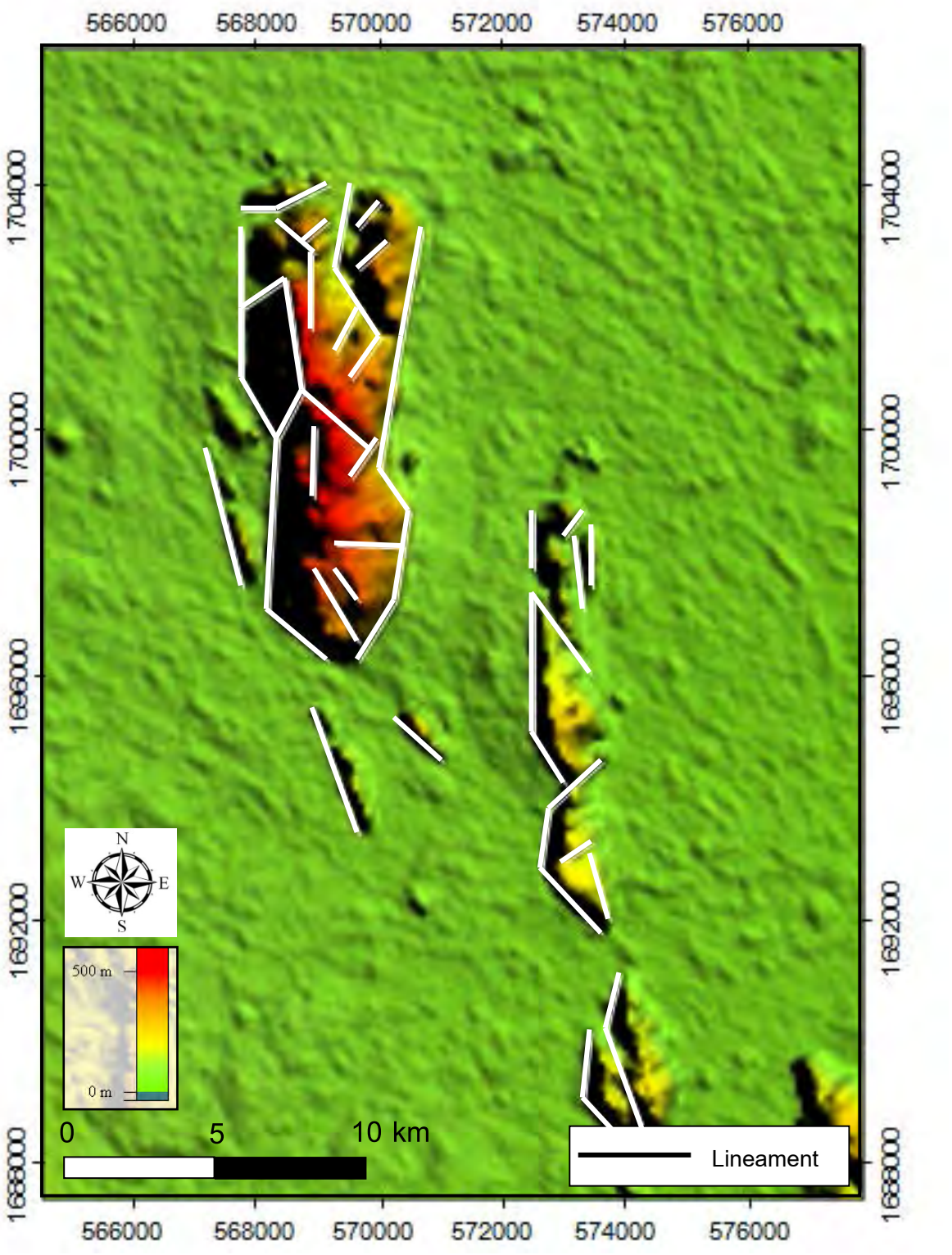

Figure 3.2 Hillshade map with lineament interpretation in white lines generated form STRM digital elevation

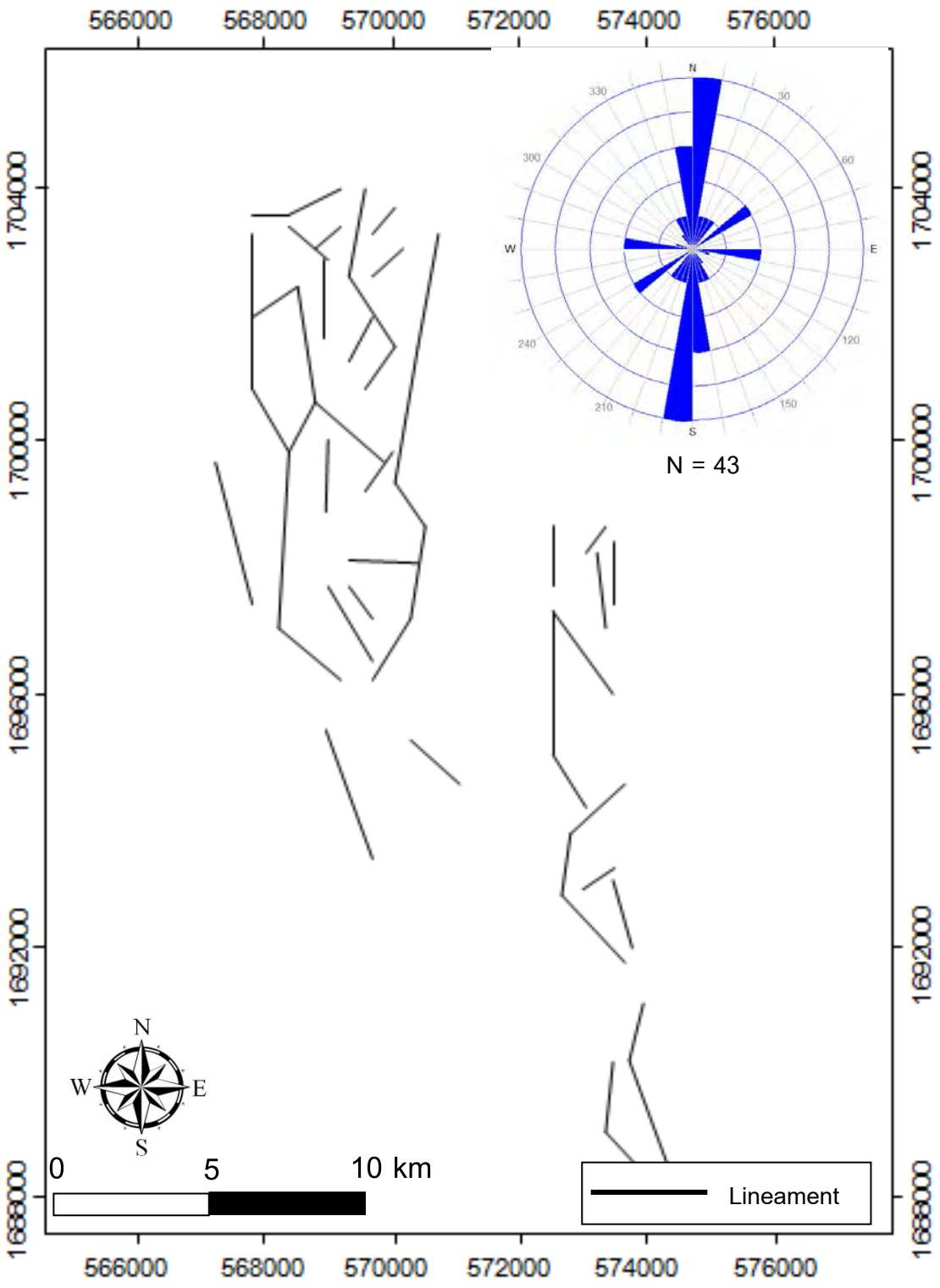

Figure 3.3 Lineament map, interpreted form hillshade map, presents the three main directions in rose diagram. The major strike is 010° NNE-SSW and two minor strikes are 060° NE-SW and 100° E-W

3.1.2 Satellite images

Optical remote sensing techniques over more than three decades have shown a great promise for mapping geological feature variations over wide scale. Lineament information extractions from satellite image can be divided broadly into lineament enhancement and lineament extractions for characterization of geologic structure. This study uses Landsat 5 TM data (path 129 row 49, path 129 row 50, path 130 row 49, and path 130 row 50). The topical mapper bands are classified by wavelengths which have different characteristics at the Earth's surface in table. The identification of lineaments from the 6-5-4 Landsat image is mainly based on geomorphologic features such as slope-break and valley-strike (Fig. 3.4). The lineaments in study were interpreted in the Landsat 5 TM images (Fig. 3.5).

Rose diagram of 62 lineaments form satellite image shows in three main directions (Fig. 3.5). The major strike is 010^{o} NNE-SSW and two minor strikes are 040^{o} NE-SW and 090^{o} E-W respectively.

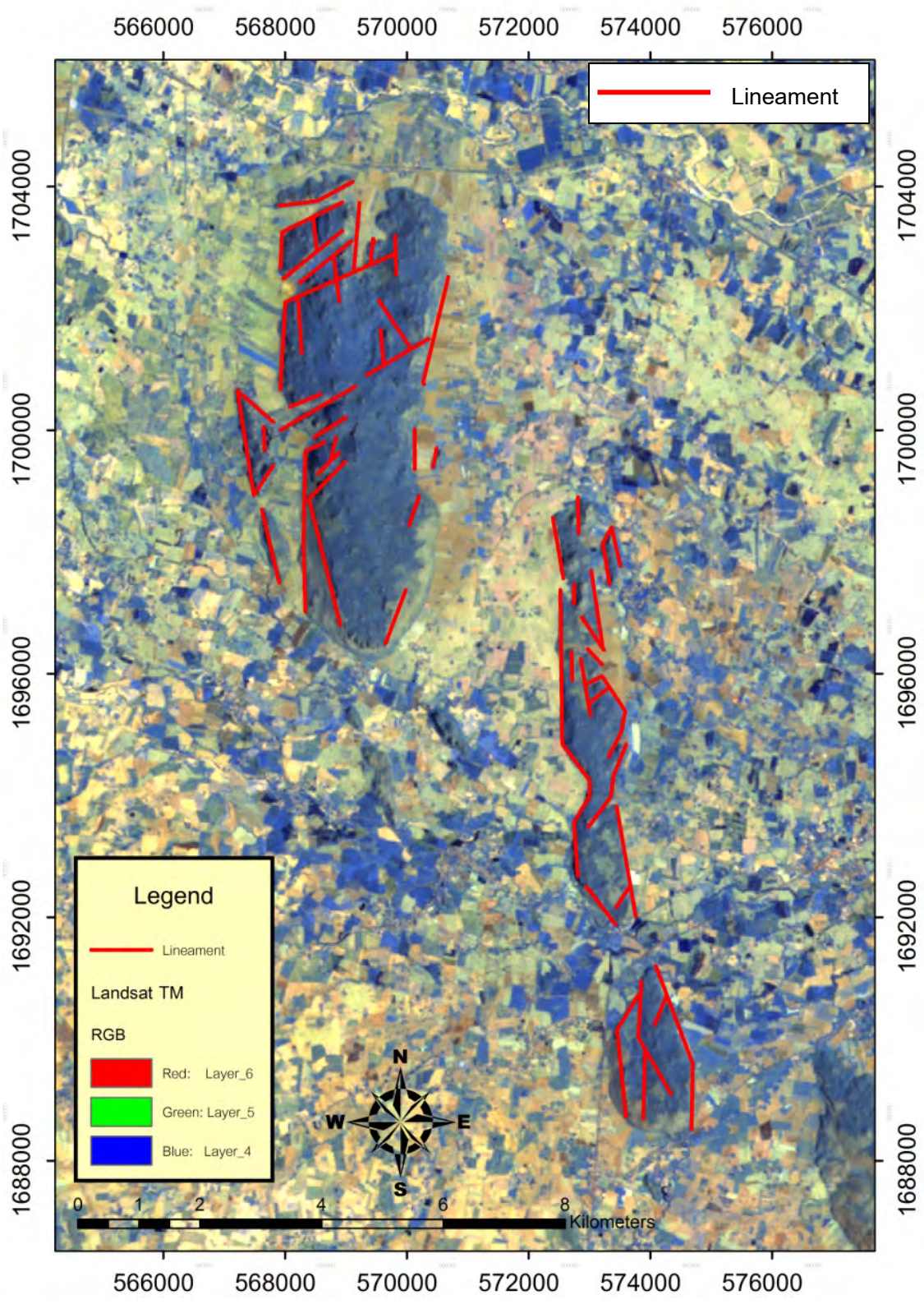

Figure 3.4 The Landsat 5 TM images generated from bands 6-5-4 with lineament interpretation in red lines.

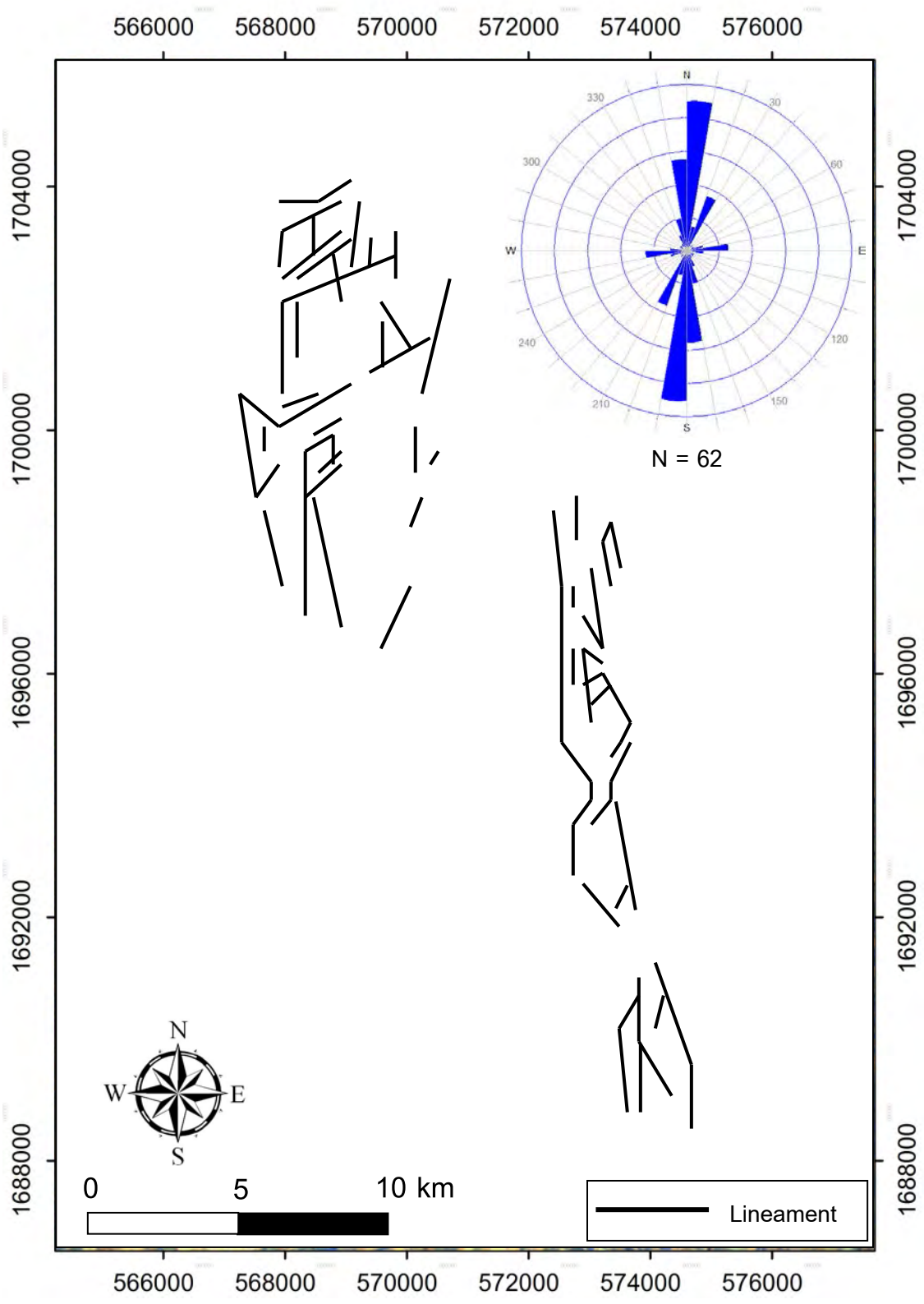

Figure 3.5 Lineament map with rose diagram based on Landsat 5 TM images presents three main directions. The major strike is 010° NNE-SSW and two minor strikes are 040° NE-SW and 090° E-W respectively.

3.2 Geology

The Uthai Thani limestone ridge lies on the western part of Uthai Thani Province. It is in the southwestern part of the Chainat duplex and formed by N-S trending karstified limestone ridge. The Uthai Thani limestone ridge is a part of Uthai Thani limestone, which is proposed by Ueno et al. (2011). The Uthai Thani limestone ridge is commonly packstone based on Dunham (1962). This rock is generally weakly metamorphosed and deformed. It is Permian limestone because of occurrence of rare and poorly preserved fusulines from some localities. The Uthai Thani limestone is widely distributed in the Sibumasu Block of Western and Peninsular Thailand (Ueno et al., 2011).

3.2.1 Limestone

From evident in field observation, the rocks of The Uthai Thani limestone ridge were classified base on the composition. There are 2 type of limestone 1) limestone with chert nodules 2) limestone without chert nodules. Limestone in eastern area generally doesn't have chert nodules that show shared grain (Fig. 3.6). Limestone in western area generally shows chert nodules (Fig. 3.7). The chert nodules mostly indicate deformed shape, which conform to bedding plane. Bedding and Foliation planes are parallel and orientate in N-S to NNW-SSE that related with this ridge orientation.

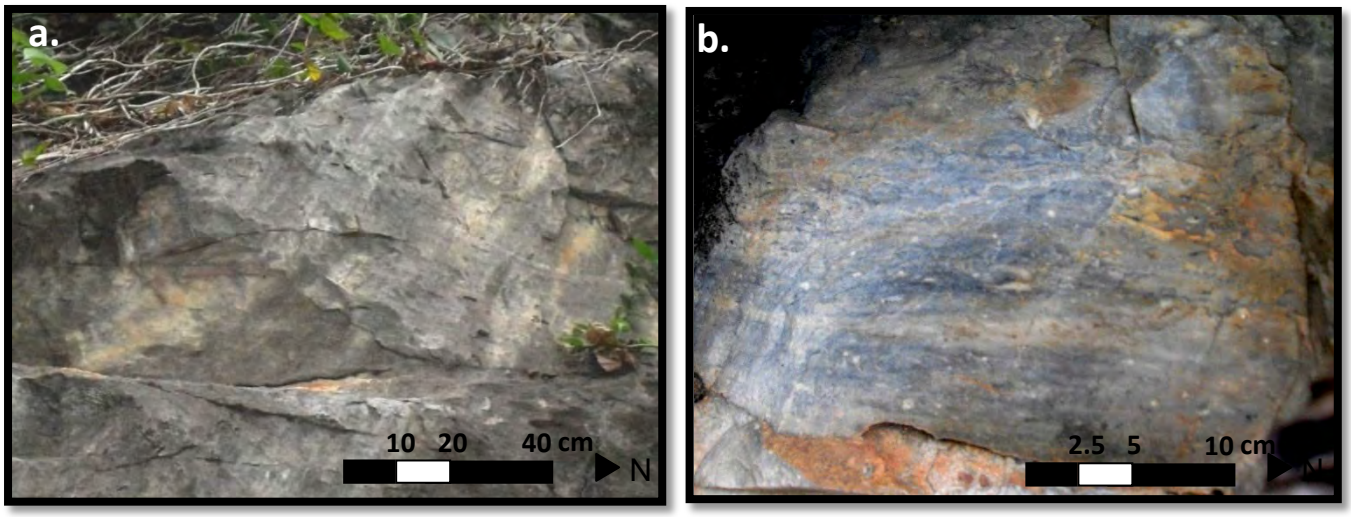

Figure 3.6 The limestone outcrop in eastern area generally shows their texture, a. limestone doesn't have chert nodules, and b. shared grain of calcite.

Figure 3.7 The limestone outcrop in western area generally shows their texture, **a.** chert nodules wall, **b.** chert nodules mostly indicates deformed shape, and c. bedding

3.2.2 Limestone classification in thin section

In the Dunham's classification (1964), the rock of the Uthai Thani limestone ridge was classified to packstone in the thin section (Fig. 3.8).

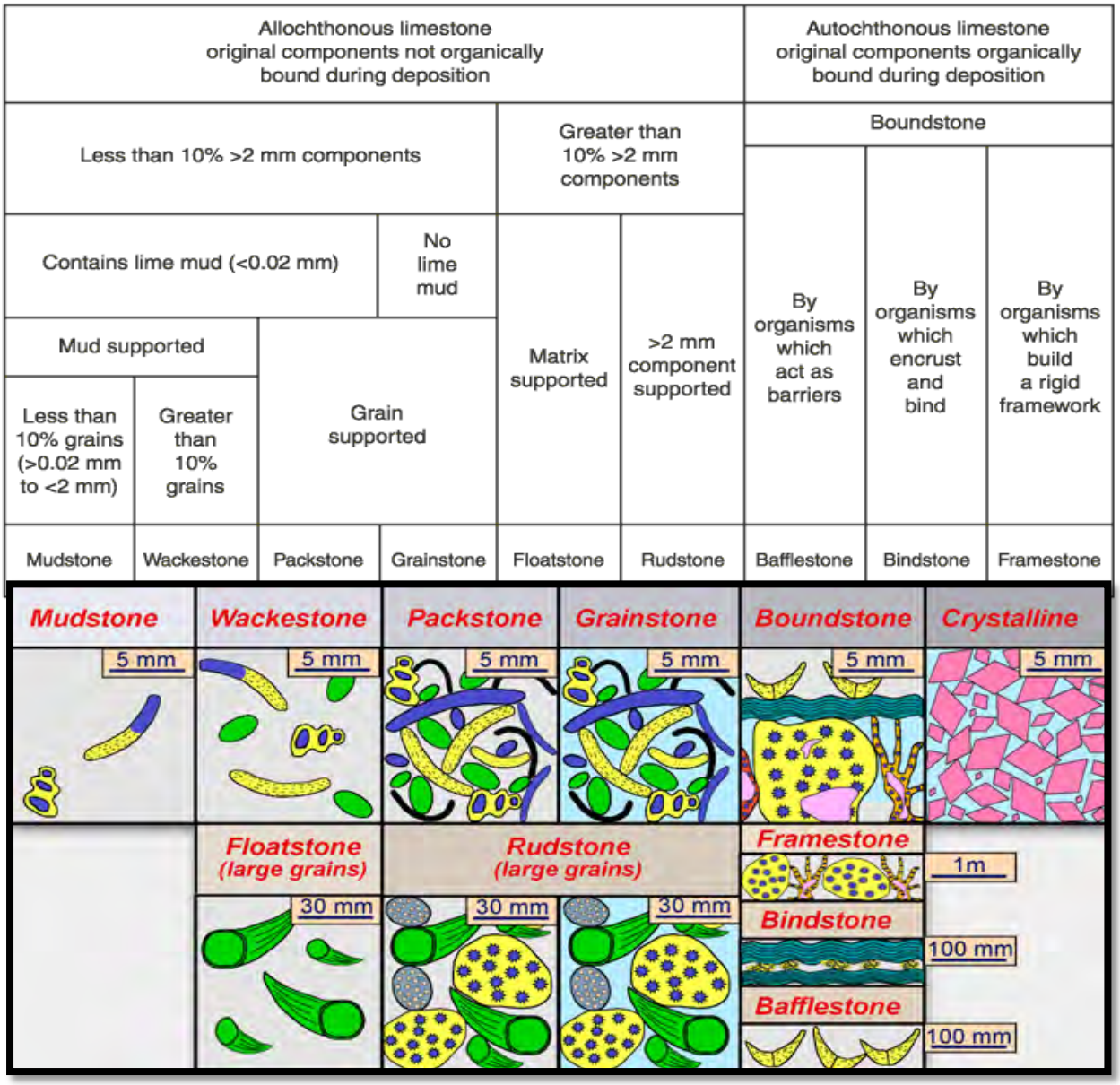

Figure 3.8 The Dunham (1962) classification of limestone according to depositional texture, as modified by Embry and Klovan (1971). For descriptions detailing the textural components of sediments and sedimentary rocks are describe by Dunham, 1962. **Mudstone** contains less than 10% grains (usually assessed by area in cut or thin section), supported by a lime mud. **Wackestone** consists of more than 10% grains, supported by a lime mud. **Packstone** contains lime mud, but is grain supported. **Grainstone** lacks mud, and is grain supported. **Boundstone**

is Carbonate rocks that showing signs of being bound during deposition. Crystalline carbonate does not have recognizable depositional structures.

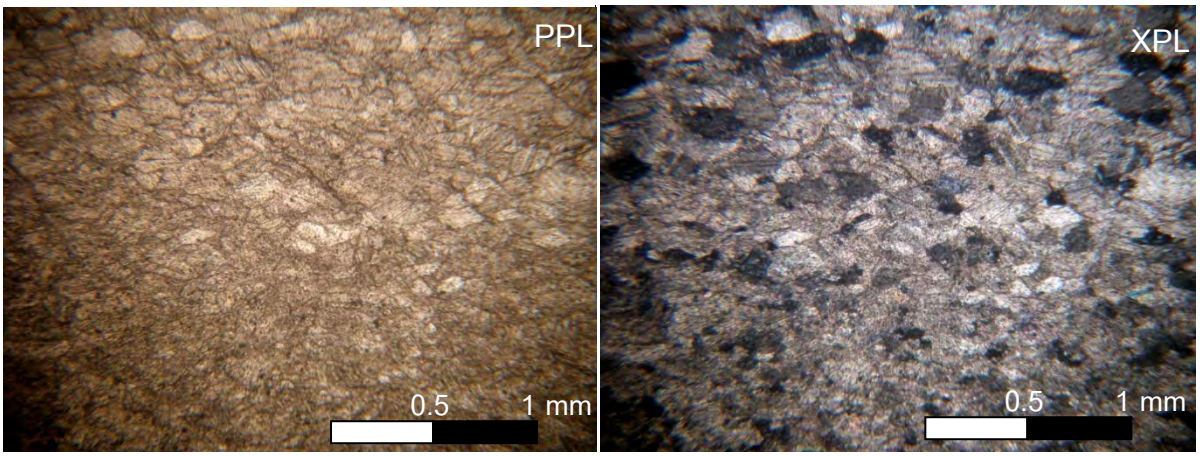

Figure 3.9 Packstone is carbonate rocks that is grain-supported and have a matrix of micrite (lime mud). Grains within a packstone are largely in contact with each other. The term packstone is part of the Dunham Classification (1962) of carbonate rocks. The grains consist of most calcite and some quartz. Sometime calcite grains show graded from small to large size. In grain boundary don't clearly because of pressure solution. In limestone has mud residual between grain boundaries. Moreover they have grain boundary sliding, which is plastic flow evidence.

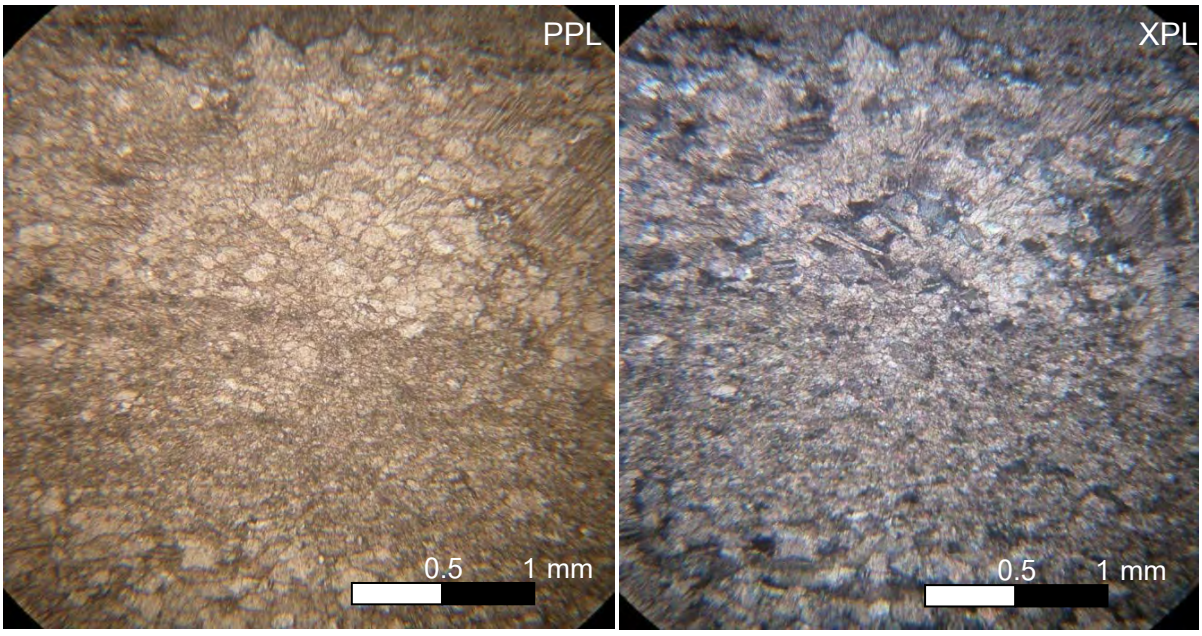

Figure 3.10 Packstone is carbonate rocks that is grain-supported and have a matrix of micrite (lime mud). Grains within a packstone are largely in contact with each other. The term

packstone is part of the Dunham Classification (1962) of carbonate rocks. In limestone shows switching of calcite grains which notice by loop of small and large. Sometime stylolite can be preserved (Top of thin section). This is the thin section of sample from limestone in eastern area.

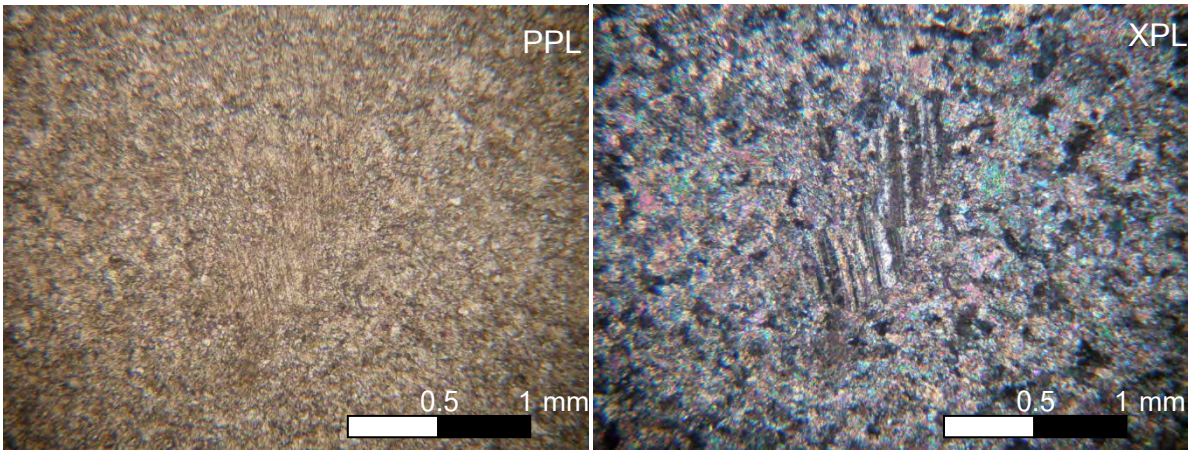

Figure 3.11 The rock shown in this thin section of a packstone is composed of most calcite and some quartz in a lime-mud matrix. The texture shows grain support that is part of the Dunham Classification (1962) of carbonate rocks. The calcite grains are very small size. This is the thin section of sample from limestone in western area.

3.3 Structural Geology

Discussion for structural geology and structural evolution are using 2 main scales for interpretation. There are mesoscopic scale and microscopic scale. Evidence for mesoscopic scale is spatial data from the field observation. Evidence for microscopic scale is studied for the microstructure in the thin section. From study in 2 main scales were classified and described into the brittle deformation and ductile deformation.

3.3.1 Mesoscopic scale

Spatial data in the outcrop such as attitude of bedding, joint, foliation, lineation and fault plus detailed rock descriptions are use for structural geology analysis. The result from structural analysis can be interpreted to the structural evolution in the study area.

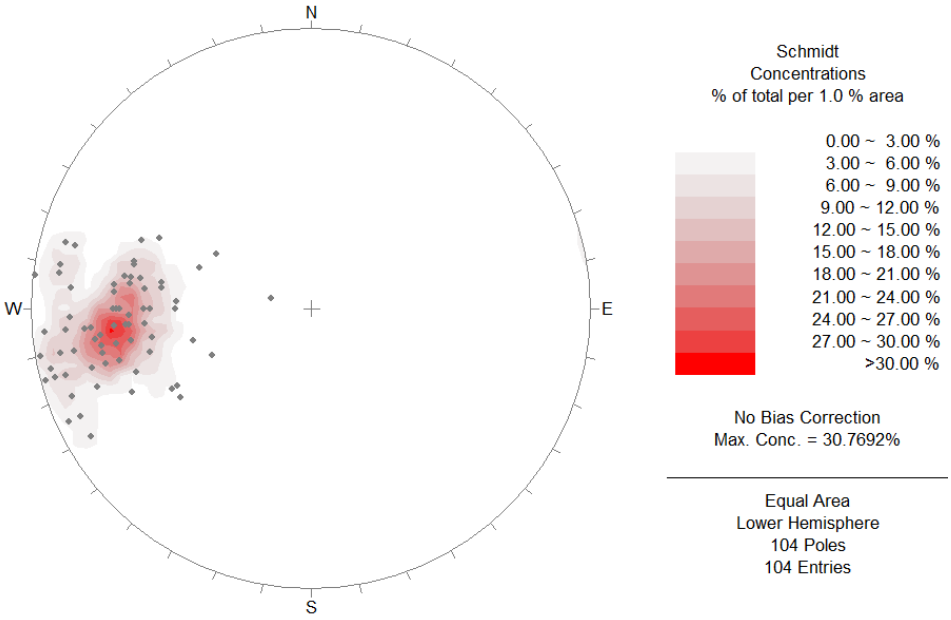

Figure 3.12 Stereographic plots of the brittle deformation of bed. Contour poles of the direction showing 50° to 80° dipping mainly N-S

3.3.1.1 Brittle Deformation

The brittle deformations in study area are general to observe because limestone responses easily to the force. Fractures and joints are common in the area and they show 2 sets of mutually intersecting joints. Those joints mainly in 2 directions consist of NEE-SWW and NE-SW. En echelon or Tension gash can be observed in limestone outcrop. Fault, which oriented in NNW-SSE direction, found in eastern and western area.

Fractures and joints

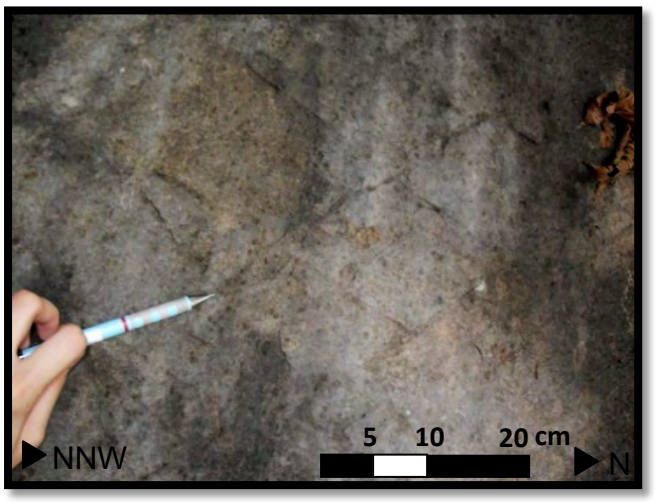

Figure 3.13 Show two sets of mutually intersecting joints. Joints in each set cut joints of the other set. There is no consistent relationship whereby joints of one set terminate on joints of the other set.

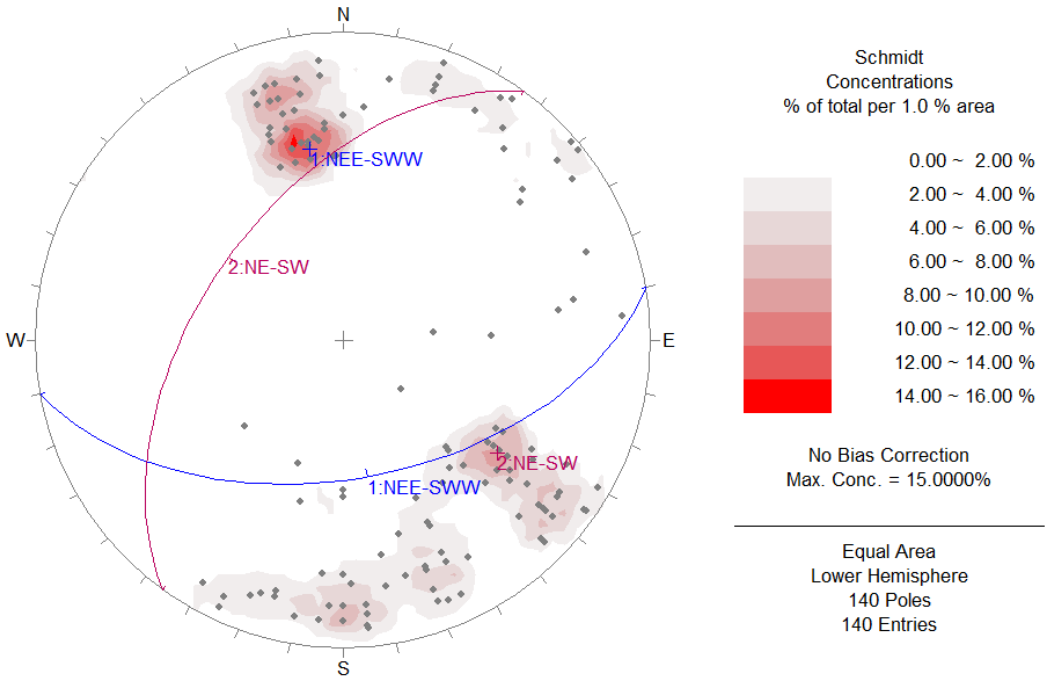

Figure 3.14 Stereographic plots of the brittle deformation of joint. Contour poles of the direction showing 50° to 80° dipping mainly in 2 directions, which consist of NEE-SWW and NE-SW.

En echelon joint or Tension gash

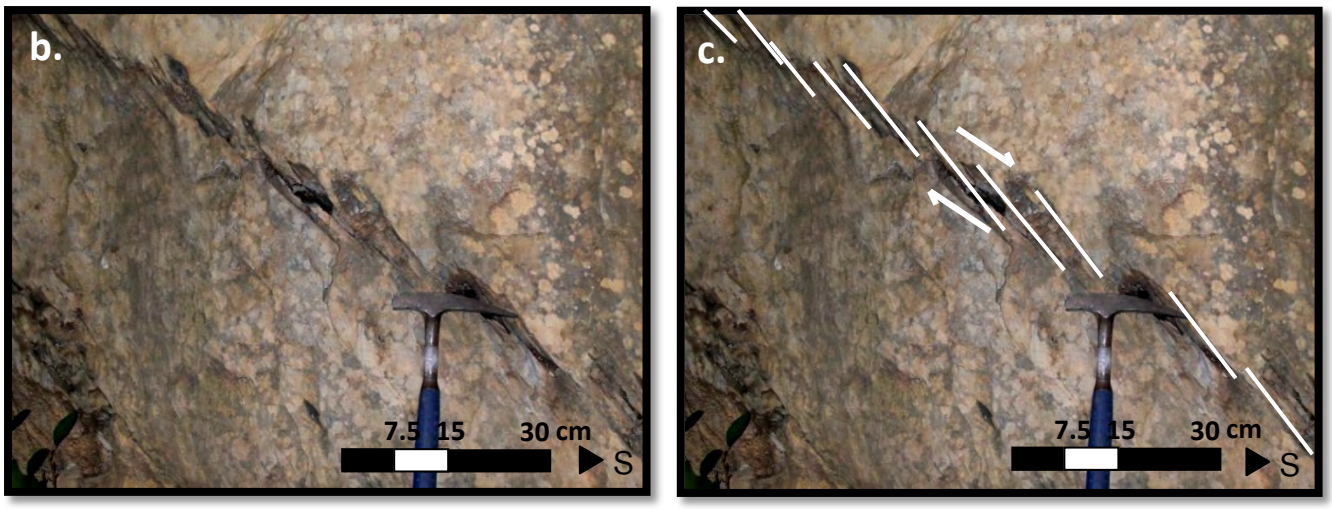

Figure 3.15 a. En echelon joint or Tension gash in limestone outcrop and between bed **b.** Tension gash fracture with weak zone that are arrayed en echelon along a shear fracture form as extension fractures during shearing, and **c.** Gash fractures form an en echelon array along a shear zone with each fracture perpendicular to the minimum compressive stress.

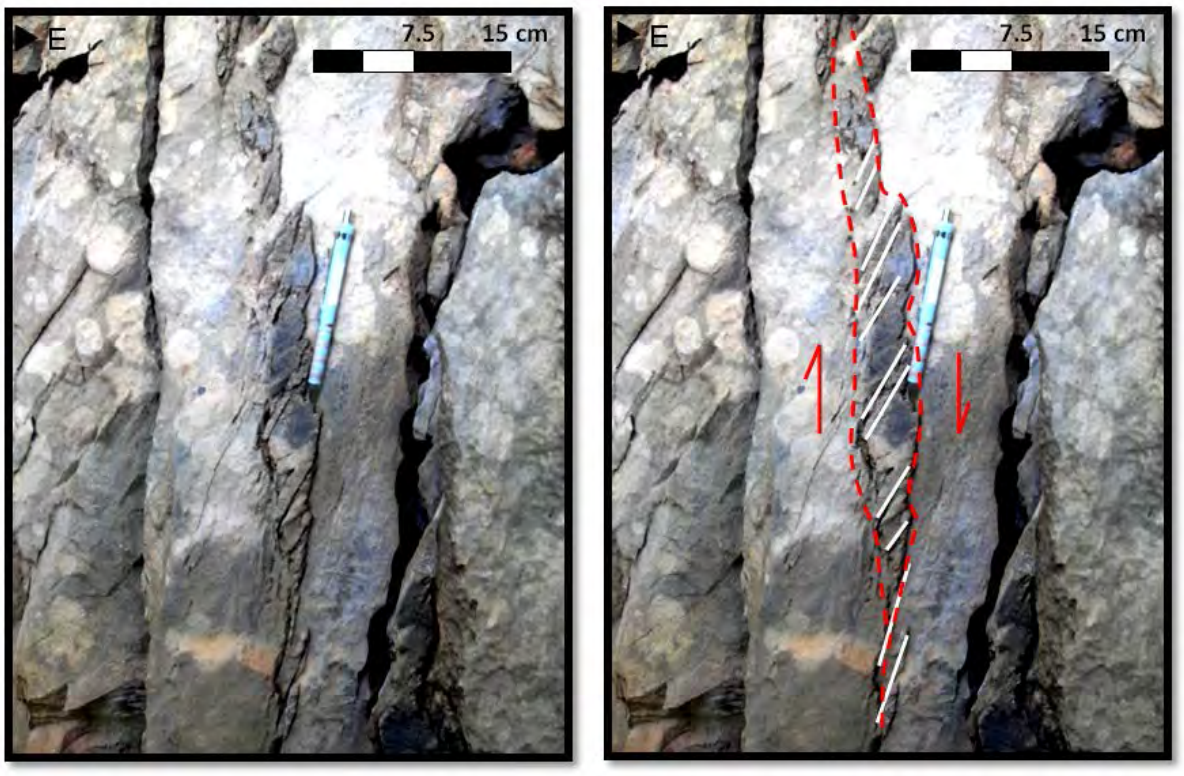

Figure 3.16 En echelon joint or Tension gash preserve in chert nodule. Chert is easy to brittle more ductile at low T, while limestone is more ductile.

Fault

Figure 3.17 The outcrop shows vertical fault movement. **a.** Fault plane is in the same direction as bedding plane that is N-S direction. There are both of normal fault and reverse in this fault plane. So the movement has more than one time, **b.** Chatter mark shows reverse fault, and **c.** Chatter mark shows normal fault.

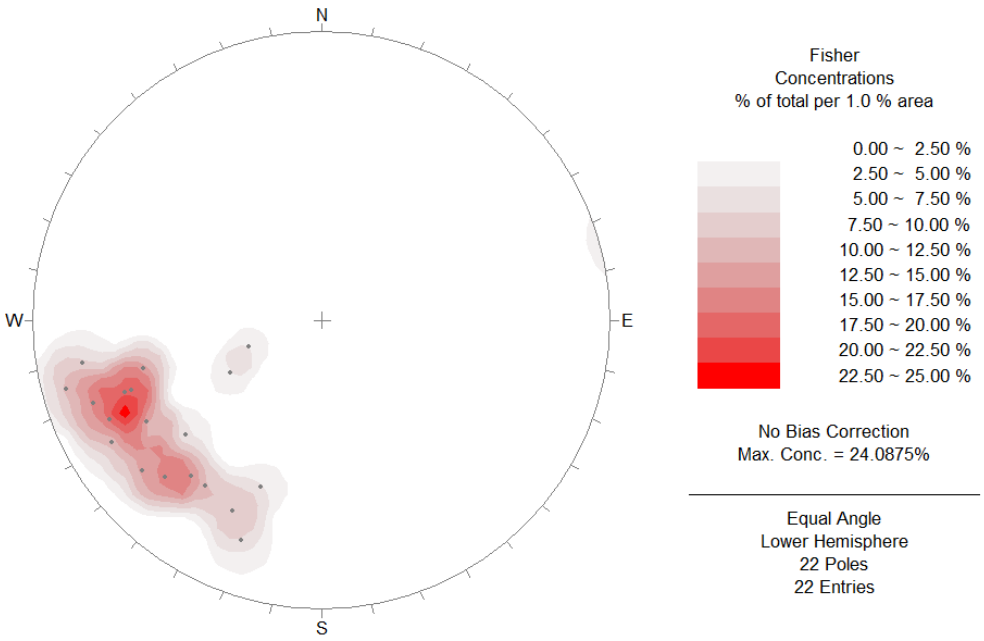

Figure 3.18 Stereographic plots of the fault plain. Contour poles of the direction showing 70° to 80° dipping mainly NNE-SSW.

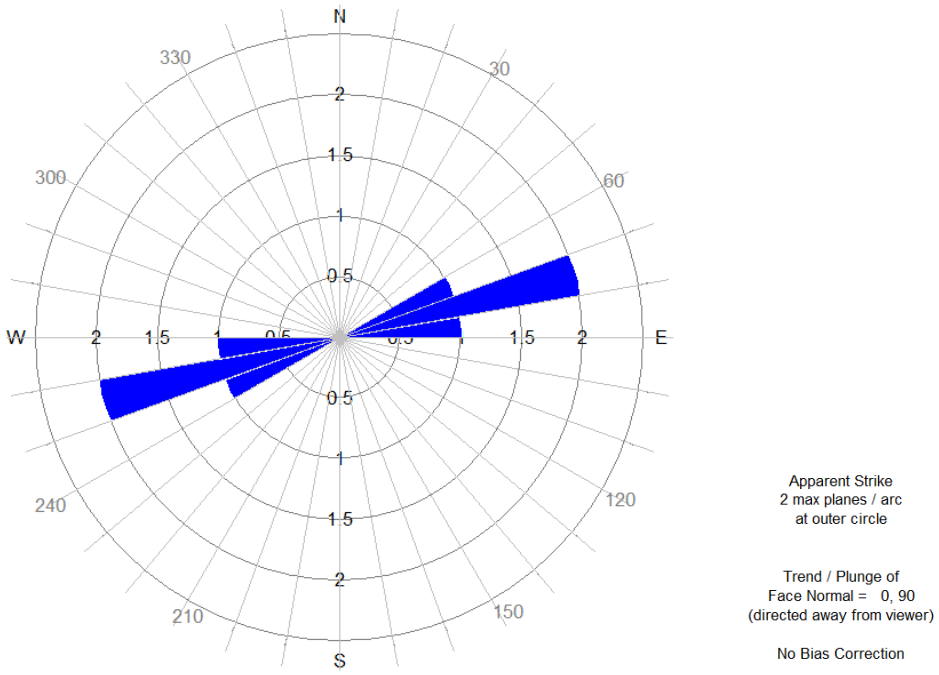

Figure 3.19 Rose diagram plots of the lineation in fault plain. The lineation is in ENE-WSW trending. It point to vertical movement of bed

3.3.1.2 Ductile Deformation

The Uthai Thani limestone ridge is dominant by the ductile deformation. The limestone generally shows chert nodules (Fig. 3.7). The chert nlodules mostly indicate deformed shape, which conform to bedding orientation. Calcite grains in limestone shows shared grain. Sense of shear in chert nodules and calcite grains is sinistral. In calcite without chert nodule sometime can be observed shared grain calcite in limestone (Fig. 3.22 and 3.23). In western area found fold in top of ridge (Fig. 3.20).

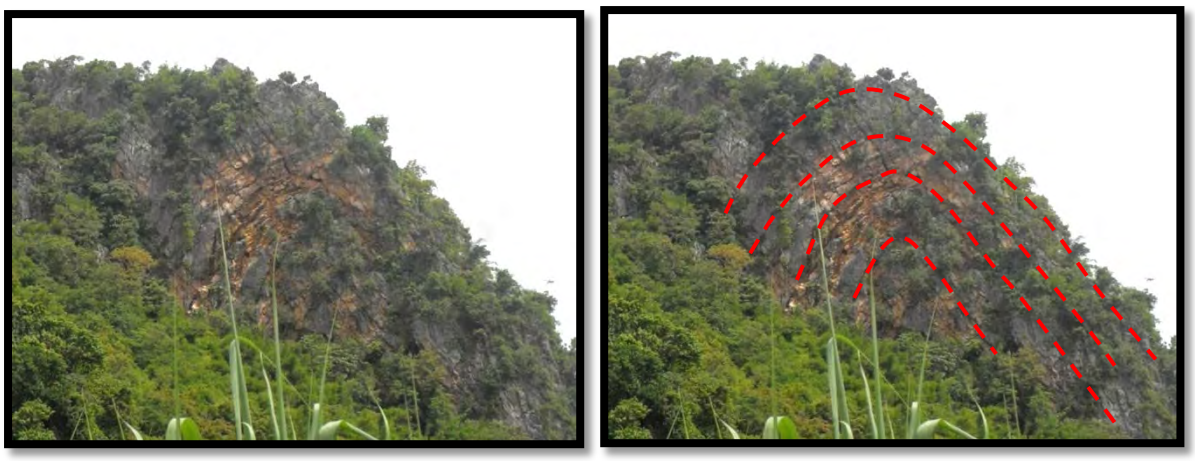

Figure 3.20 The limestone ridge in western area is folded.

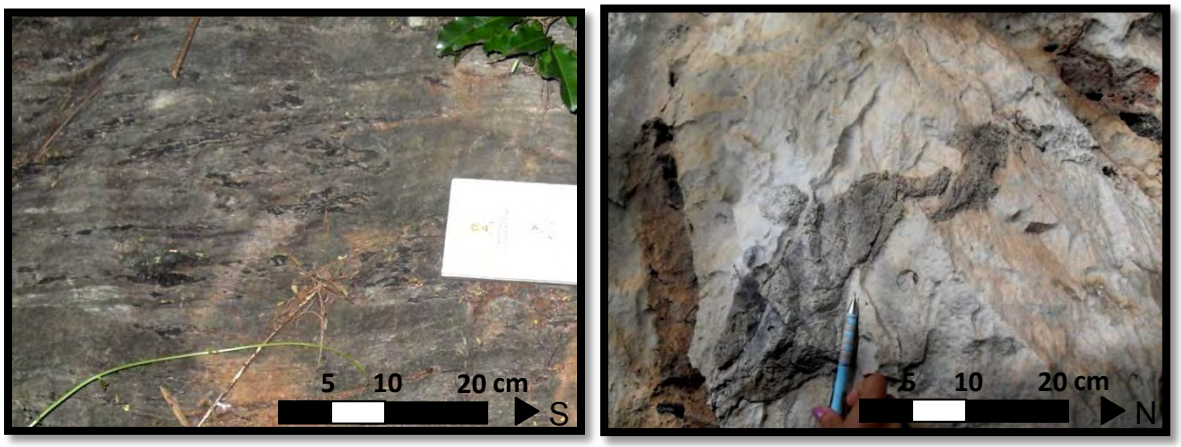

Figure 3.21 Limestone outcrops showing ductile shear, a. chert nodules wall, and b. stretching chert nodules.

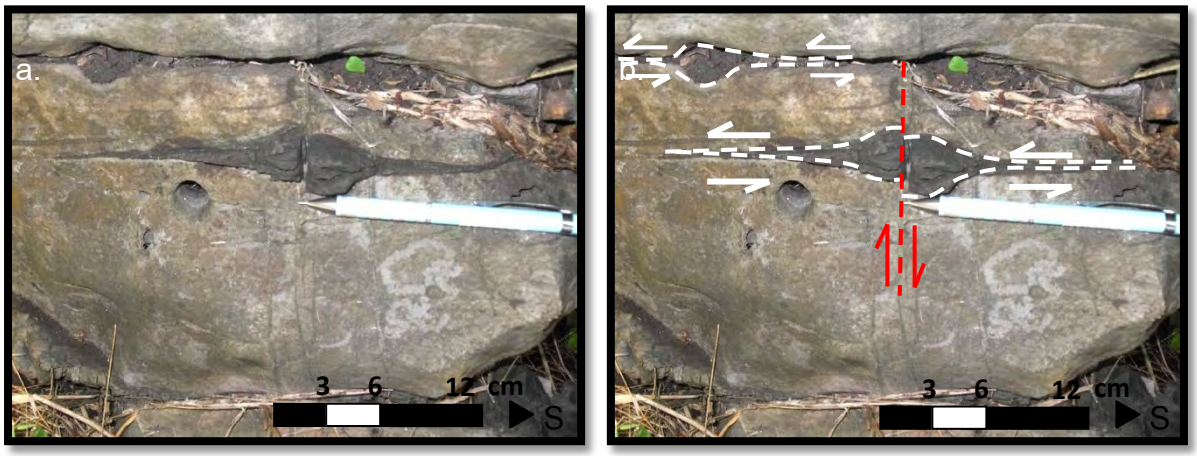

Figure 3.22 a. This outcrop shows chert nodule sheared. b. Interpretation of chert nodule sheared. Zigma shape of chert nodule sheared shows sinistral shear movement. Minor fault found in core of chert nodule that indicates vertical moment.

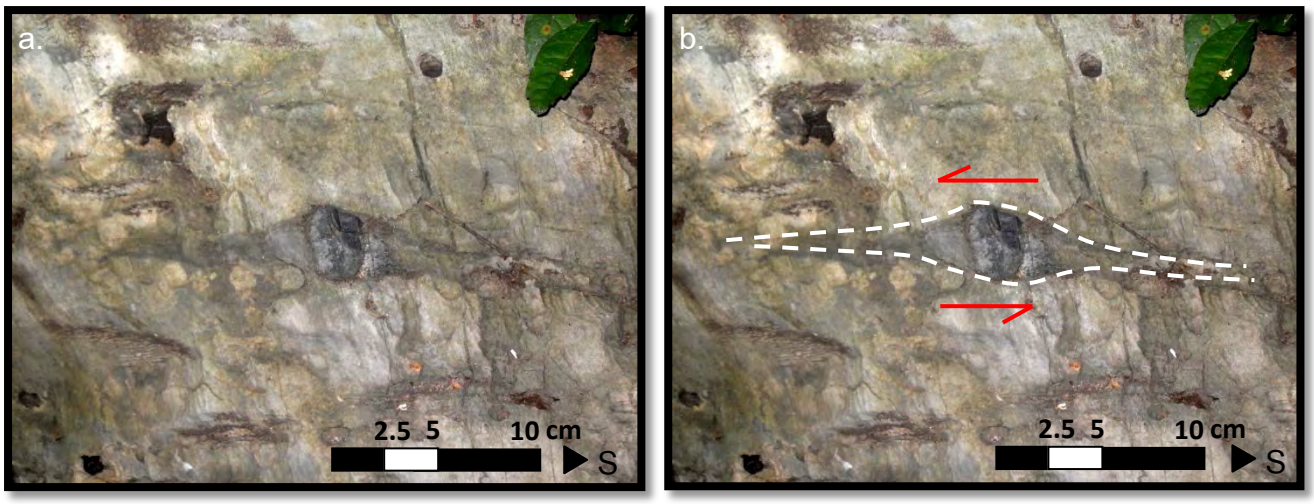

Figure 3.23 a. σ-shape of chert nodule sheared show distort core grain and strain shadow **b.** Sinistral sense of shear.

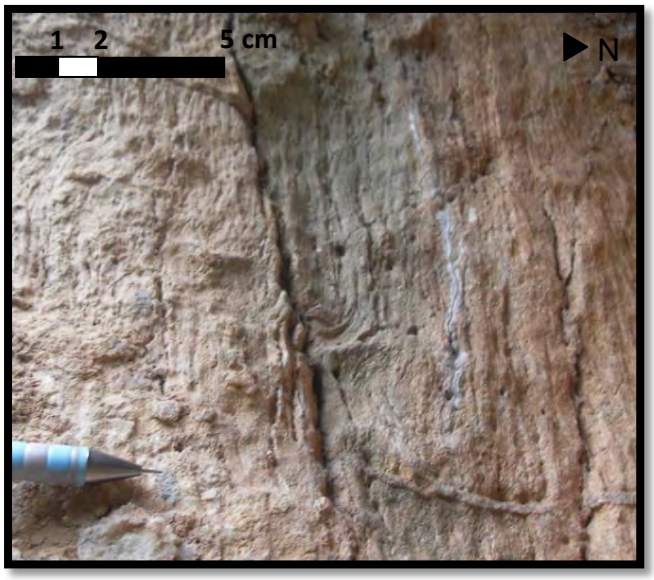

Figure 3.24 Bed folded relate with fault movement. This evidence shows deformation of ductile to brittle. Fault plain is N-S trending parallel to the trend of ridge.

3.3.2 Microscopic scale

Rock microstructure is studied in the thin sections which describe the texture of a rock and the small scale rock structures. Thin section preparation is needed to be inspected microscopically for analyze the characteristics of the rock. Microstructure analysis support to structure analysis from mesoscopic scale. The deformation and metamorphism processes of the rocks in microscopic scale can be explained. Sense of shear and deformation mechanisms in rock are evident in the thin sections which are support to tectonic evolution in study area.

Microstructure may include grain shape, grain boundaries, aggregates of grain with similar shape, lattice preferred orientation, and shear sense indicators. Those textures and other

microstructures will be observed, classified and photographed in thin sections for structural geology in microscopic scale.

In thin section, mineral assemblage is most calcite and some quartz. Each mineral have specific deformation structures and deformation mechanisms in some common rock-forming minerals. A simple fabric in calcite or quartz should be developed in such a case in response to gradual changes in the stress field and in metamorphic condition. The aim is interpret overprinting relations in terms of deformation phase and metamorphic events. Sometime temperature of deformation can be approximately predicting form deformation indicator. Once deformation phases and metamorphic events are defined, it is necessary to determine to what extent they correspond to tectonic event, namely events on a larger scale such as those associated with plate motion or fault. In this study, microstructure can be explain in 2 topic that consist of sense of shear and deformation mechanism

Calcite

At very low-grade metamorphic conditions calcite deforms by fracturing and cataclastic flow (Kennedy and Logan 1998). The coarse grain fragments are heavily twinned and show undulose extinction, and are cut by veins and stylolites while small matrix grains can be strain and twin free. Brittle deformation is originated by solution transfer, twinning and, especially in the fine grain matrix. At low-grade metamorphic conditions and if water is present, pressure solution is dominant in calcite and leads to stylolite development although other mechanisms may also contribute. The amount of strain that can be achieved by twinning is limited. The strain must be observed at grain boundaries by pressure solution, grain boundary migration or grain boundary sliding. Twins can be used as indicators of temperature, strain and stress. Grain boundary sliding and 'superplastic' behaviour may be important in calcite if the grain size is very small (Schmid 1982; Schmid et al. 1987; Walker et al. 1990; Casey et al. 1998; Brodie and Rutter 2000; Bestmann and Prior 2003).

Quartz

Quartz is one of the most common minerals in the crust. The Uthai Thani limestone Ridge sometime found quartz. At very low-grade conditions (below 300 ^{o}C) brittle fracturing, pressure solution and solution transfer of quartz are dominant deformation mechanisms. Characteristic structures are fractures in grains, undulose extinction and evidence for pressure

solution and redeposition of material, sometimes in veins. BLG recrystallisation may locally occur at very low-grade conditions in strongly deformed quartz. Sometime shear of quartz can be observed in section

3.3.2.1 Sense of Shear

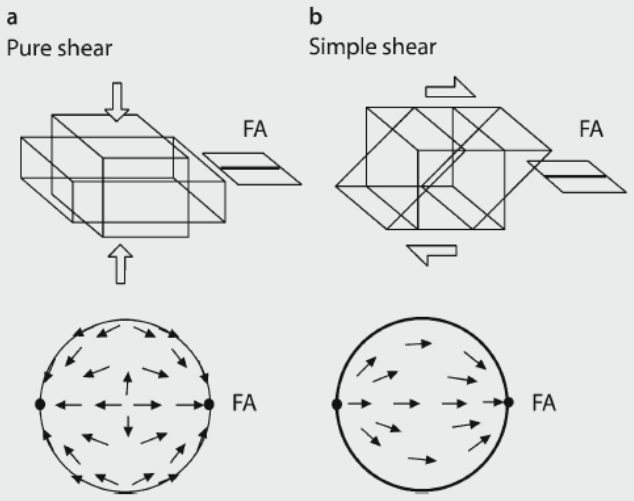

Figure 3.25 Concept of the fabric attractor (FA). In both **a.** pure shear and **b.** simple shear deformation, material lines rotate towards and concentrate near an attractor direction, as shown in the stereograms (Passchier and Trouw, 2005).

Pure Shear

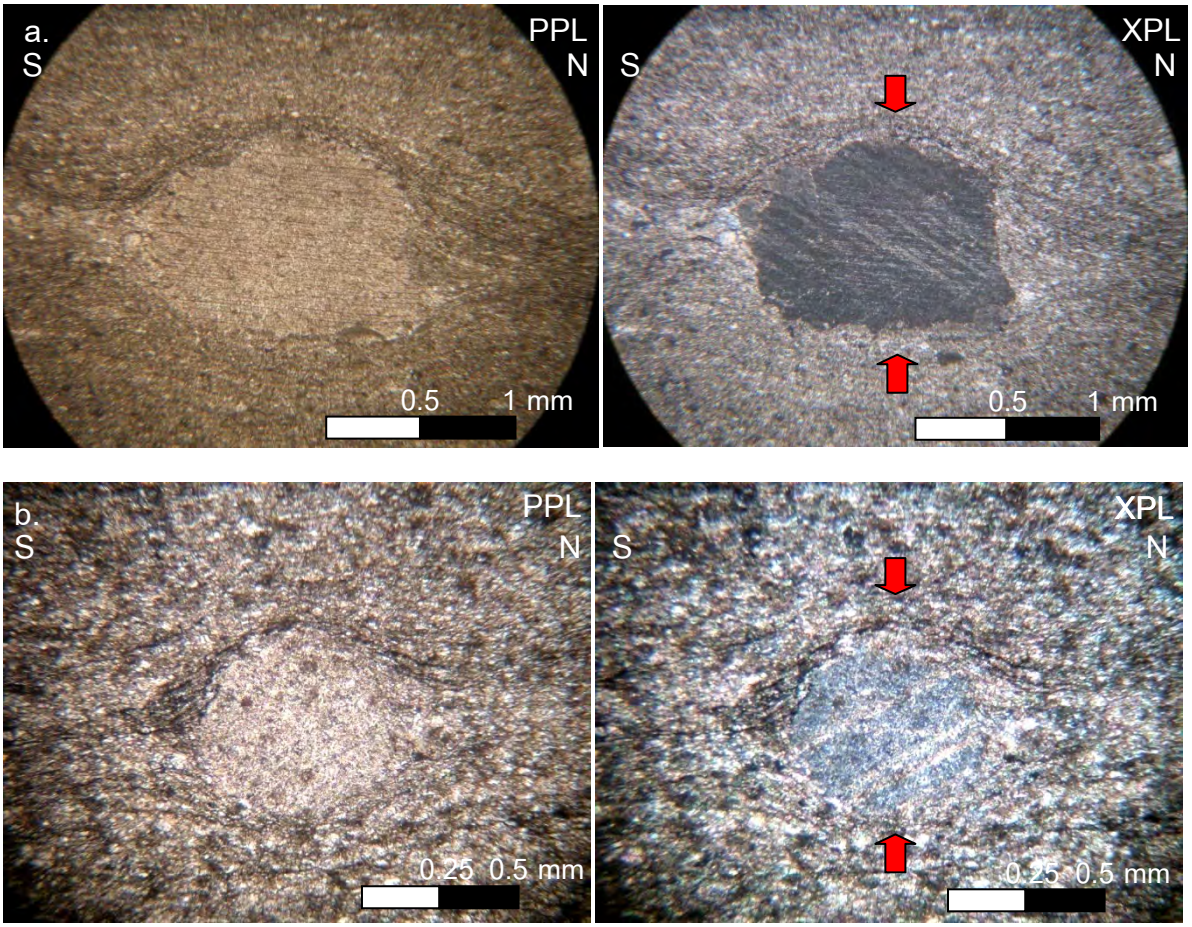

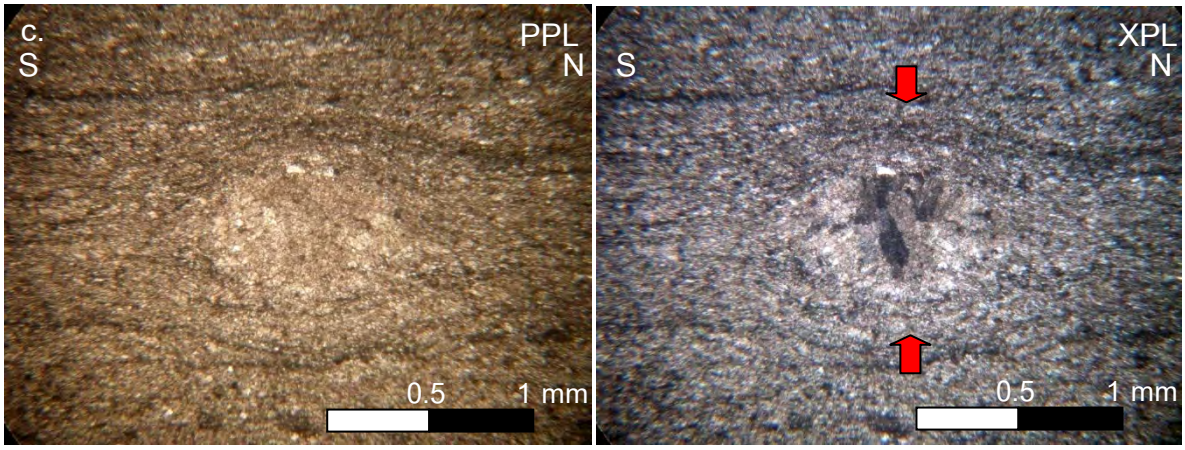

Figure 3.26 The calcite (**a.** and **b.**) and quartz (**c.**) grain example of irrotational strain in which a body is elongated in one direction. Pure shear derive from the compression, without shearing.

Simple Shear

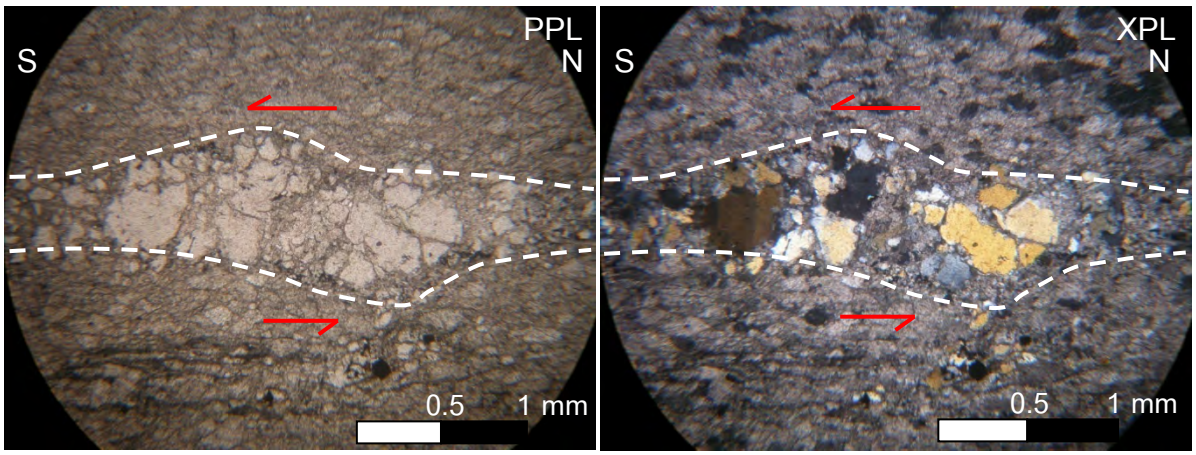

Figure 3.27 Polycrystal of quartz show sigmoid texture. Sense of shear in sinistral.

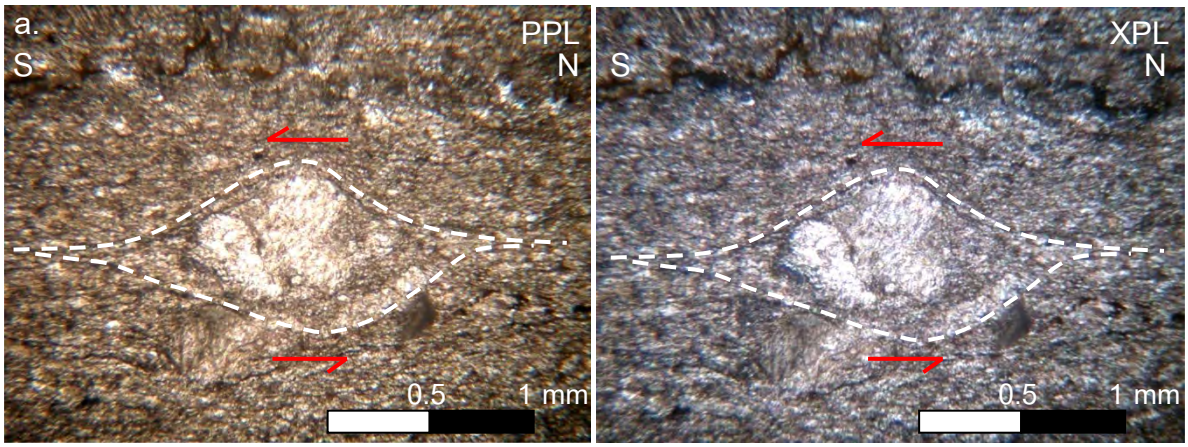

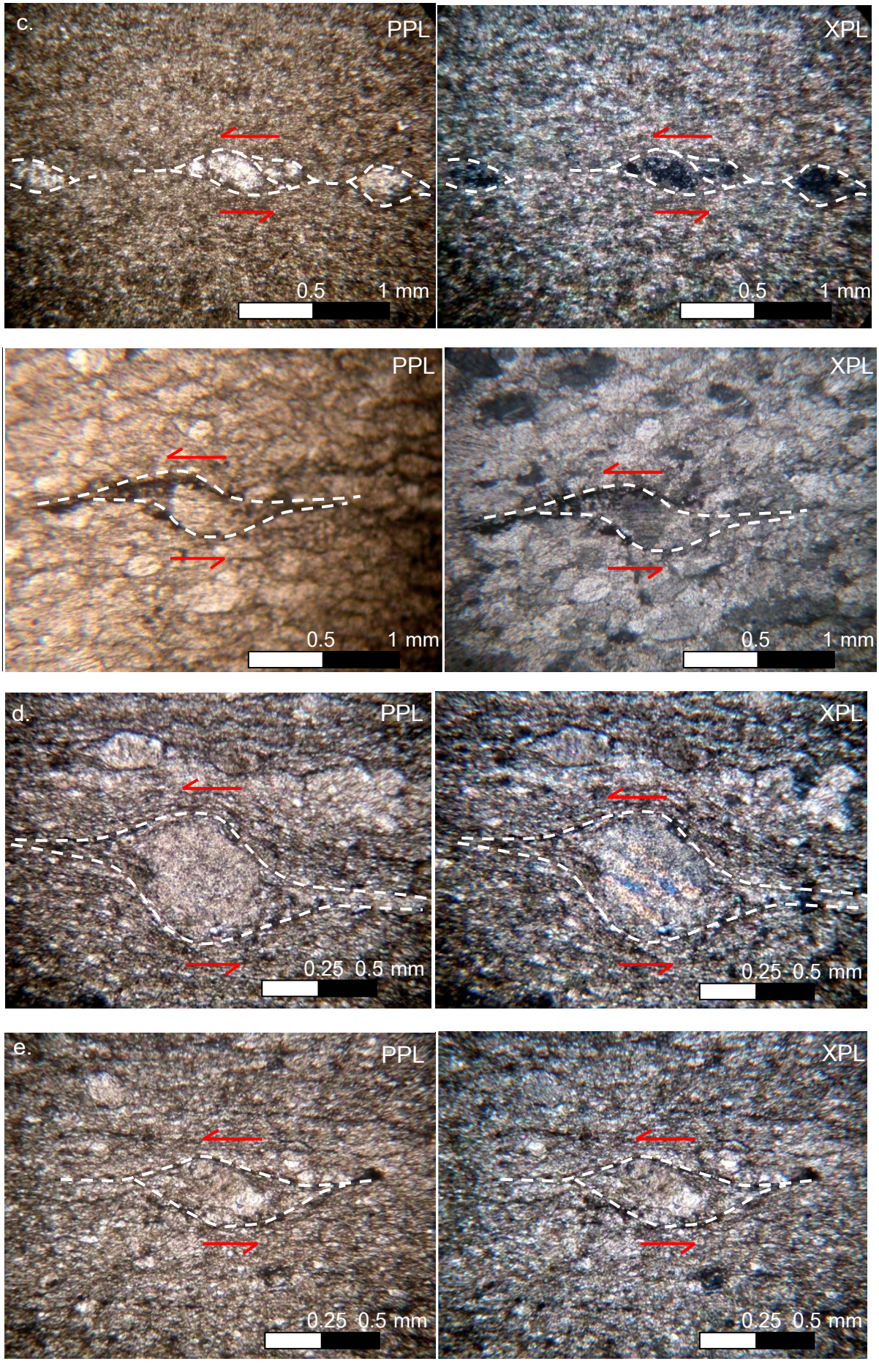
c.
PPL
0.5 1 mm
XPL
0.5 1 mm
PPL
0.5 1 mm
XPL
0.5 1 mm
d.
PPL
0.25 0.5 mm
XPL
0.25 0.5 mm
e.
PPL
0.25 0.5 mm
XPL
0.25 0.5 mm

Figure 3.28 Single crystal of quartz (**a.** and **b.**) calcite (**c.-e.**) show σ- type. Sense of sheared in sinistral.

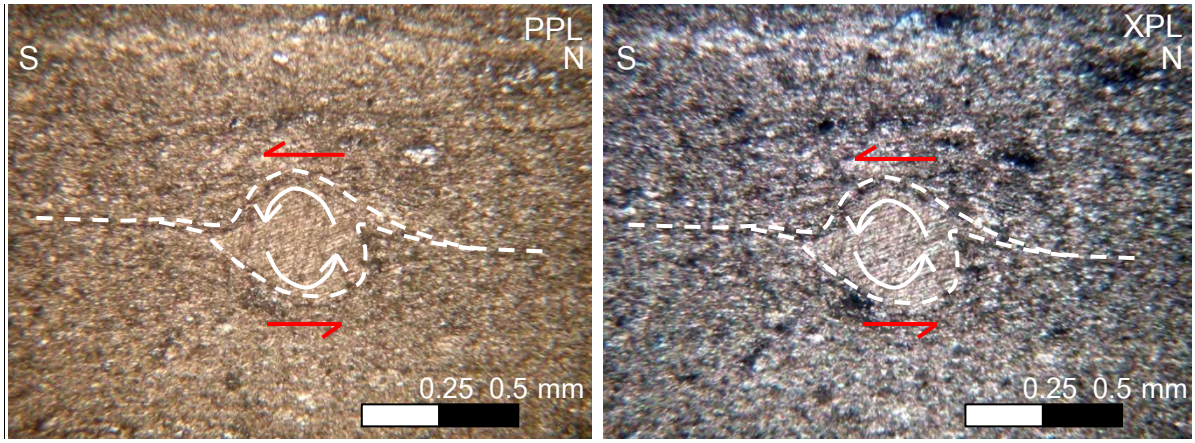

Figure 3.29 Single crystal of calcite shows δ-type. Calcite grain shears and rotates. Sense of sheared in sinistral.

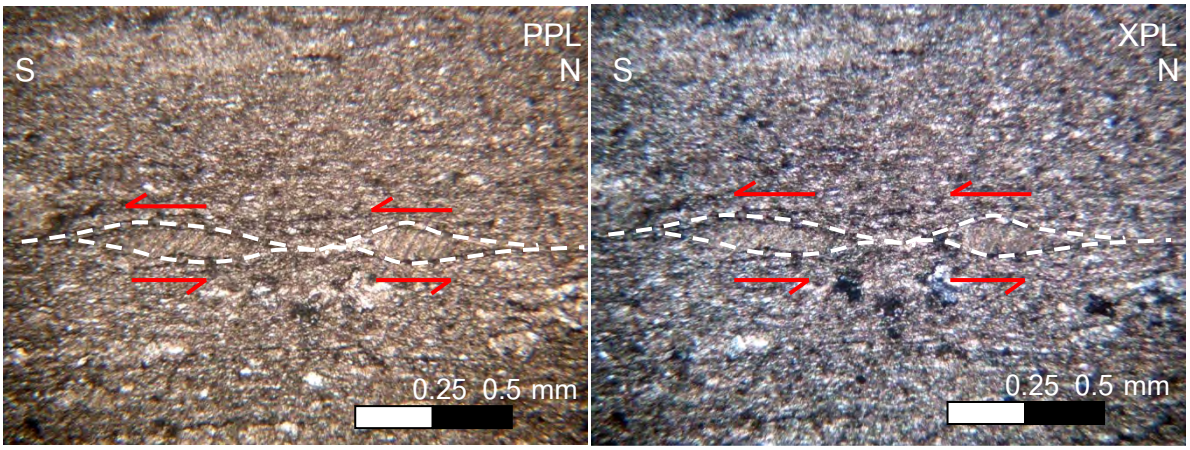

Figure 3.30 Single crystal of 2 calcite grain show mineral fish shapes. Sense of shear in sinistral.

3.3.2.2 Deformation Mechanism

Brittle Fracturing

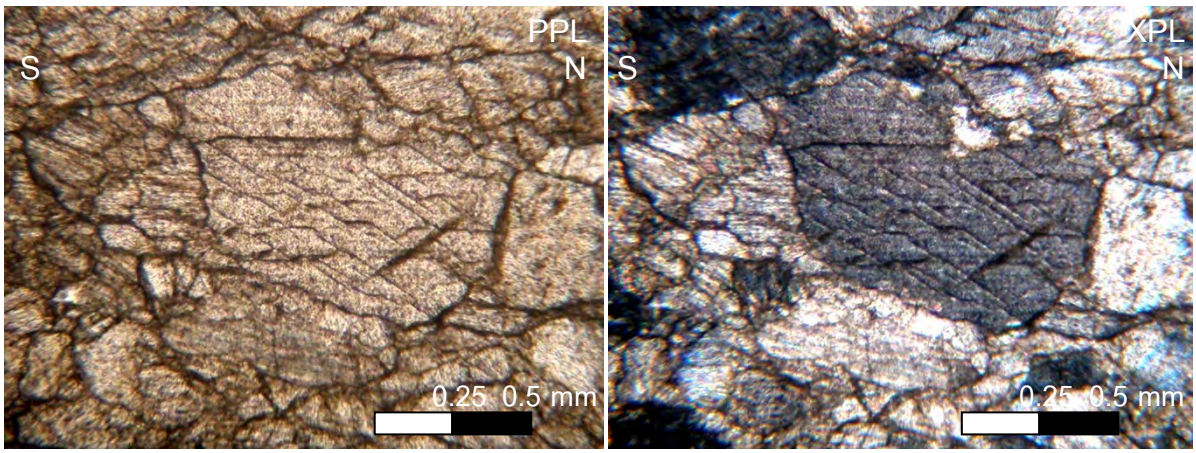

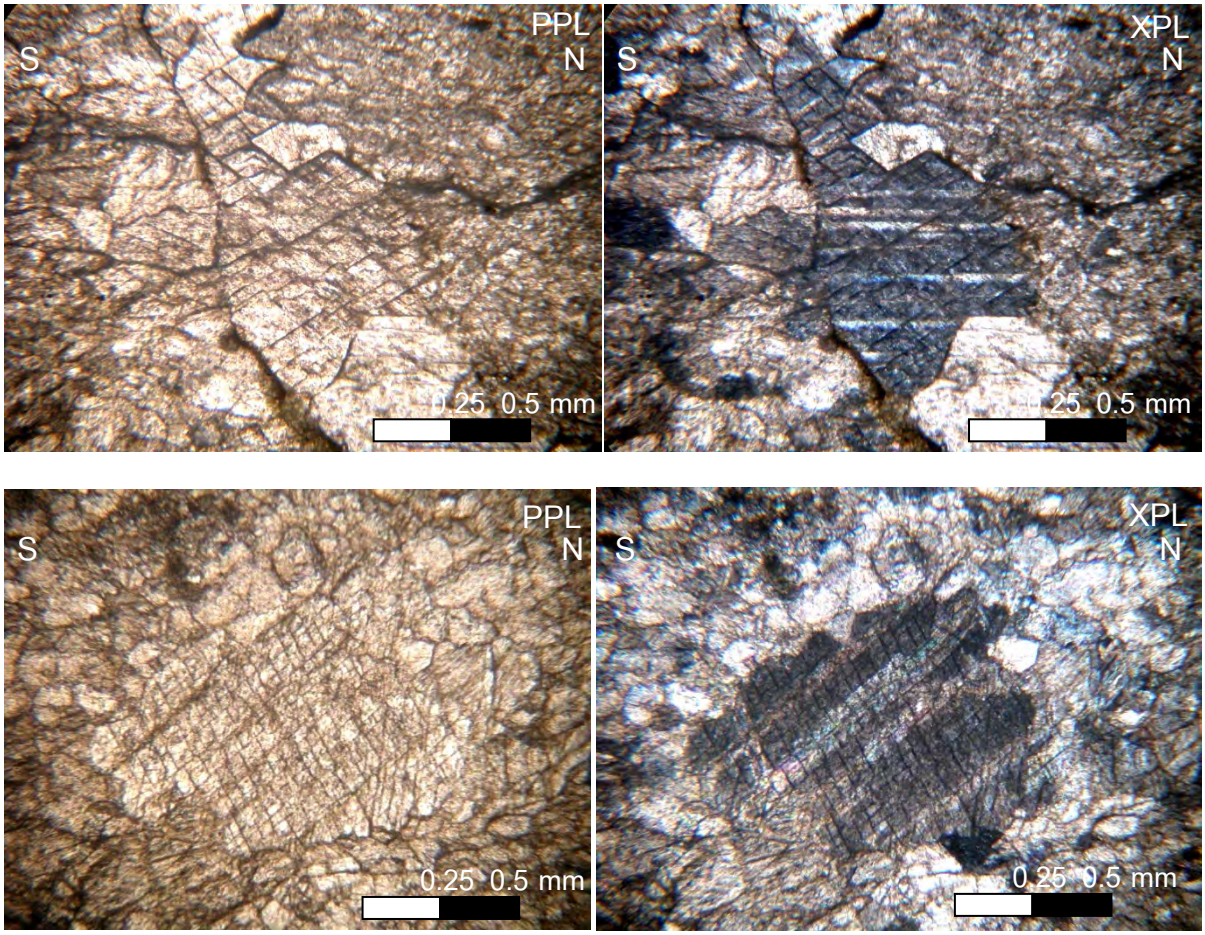

Figure 3.31 Two sets of mutually intersecting micro fractures in calcite. Micro fractures of two sets cut each other. There is no consistent relationship whereby micro fractures of one set terminate on micro fractures of the other set. This micro fractures relate with joint in the field.

Shear band type fragmented porphyroclasts

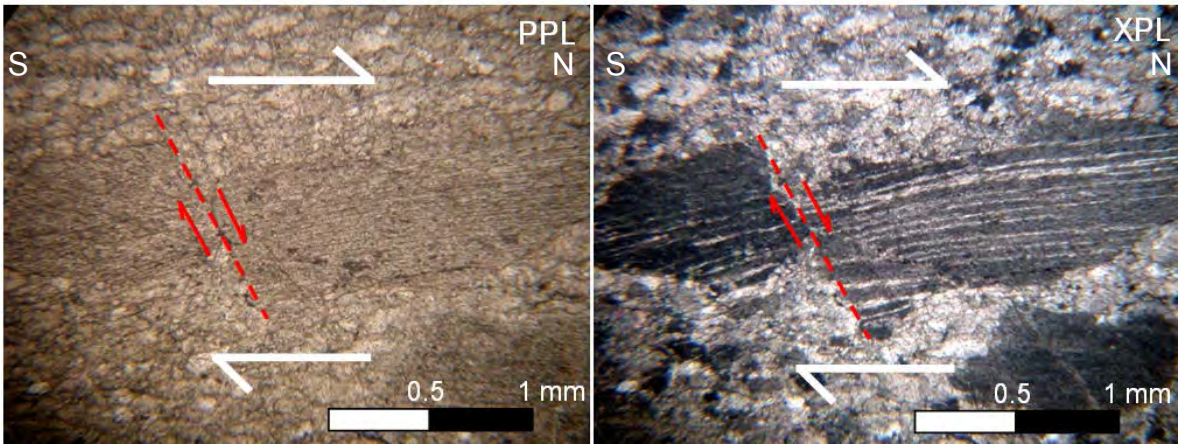

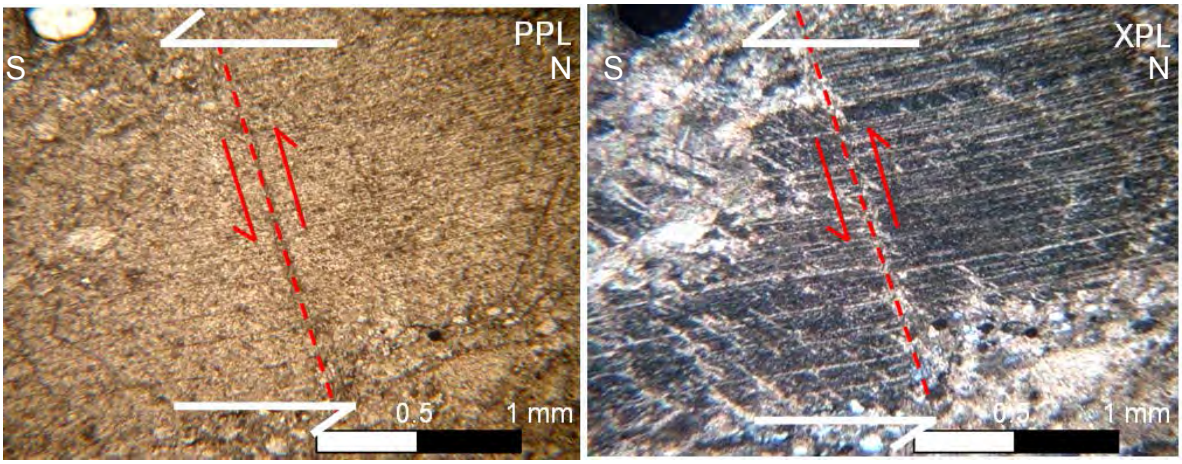

Figure 3.32 Microfaults transecting calcite grain in a section shows sliding in vertical movement which have normal (**a.**) and reverse (**b.**). Sense of sheared is dextral (**a.**) and sinistral (**b.**).

Pressure solution

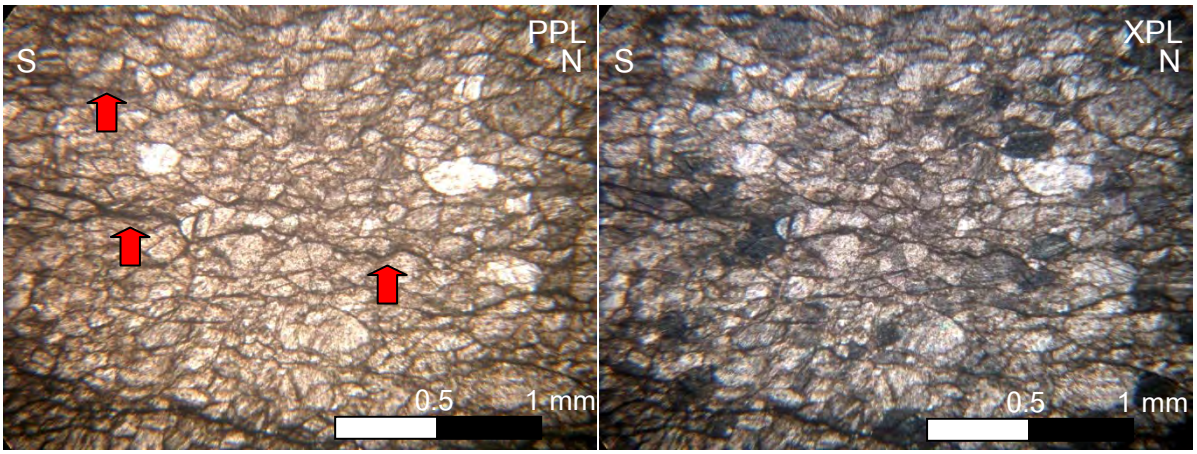

Figure 3.33 In Uthai Thani limestone, pressure solution is common that indicate low-grade metamorphic deformation. Pressure solution is usually active throughout a rock volume on the grain scale, leading to development of foliations and grain-scale dissolution and deposition features. The surfaces are normally highly indented and consist in three dimensions of surfaces mud in grain boundary (red arrow). Compressive strength is perpendicular with surfaces mud.

Stylolites

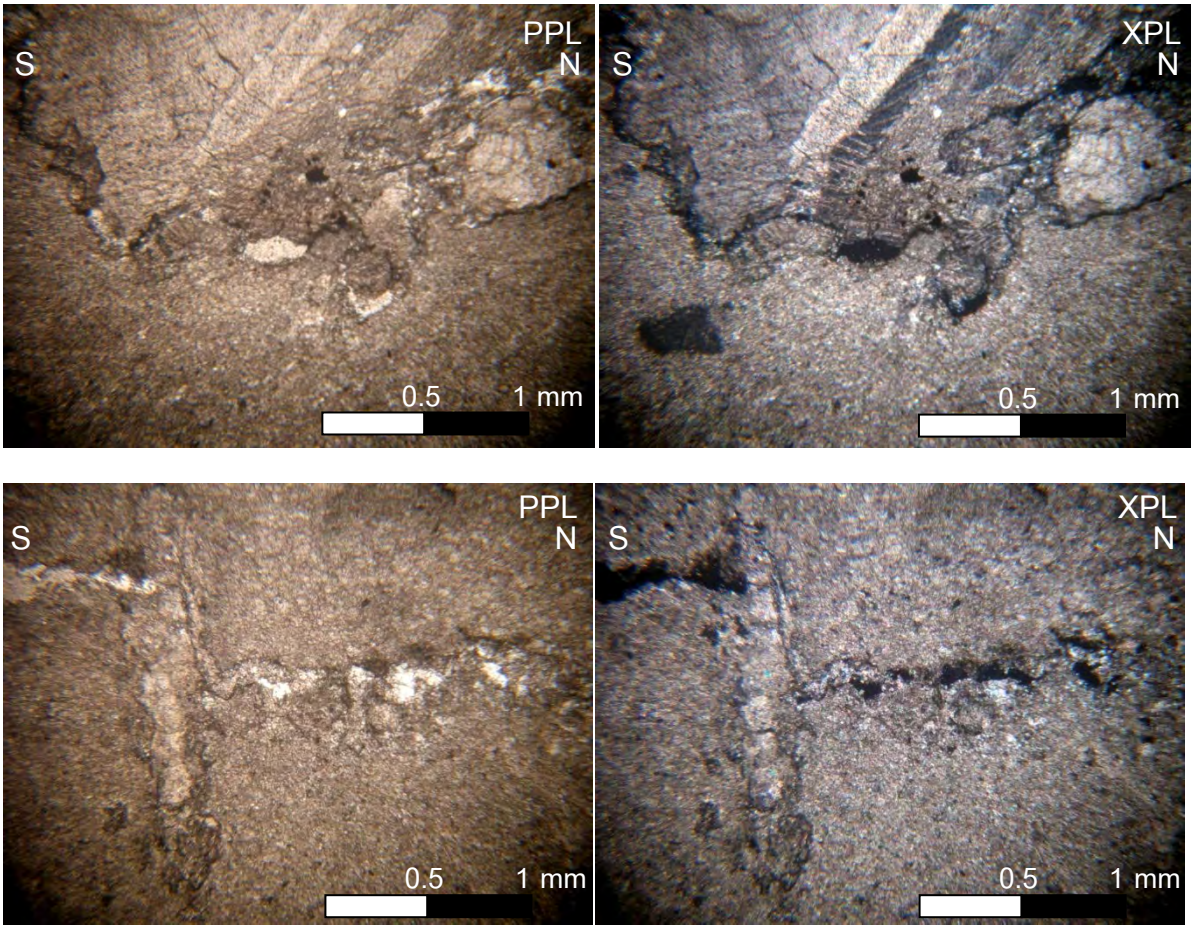

Figure 3.34 Stylolites formed by pressure solution. The surfaces are normally highly indented and consist in three dimensions of interlocking teeth of wall rock. These surfaces are therefore known as stylolites.

Kink bands

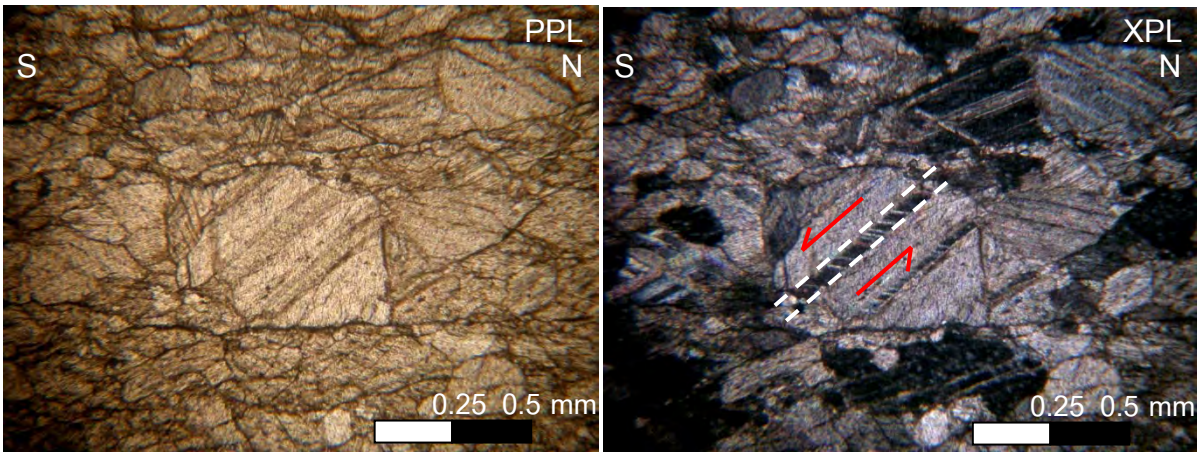

Figure 3.35 Kinking is common in crystals with a single slip system at low temperature. Sense of shear is sinistral kink fold. The kink bands are revealed by differences in absorption colour, owing to their orientation differences.

Twin boundary migration recrystallisation

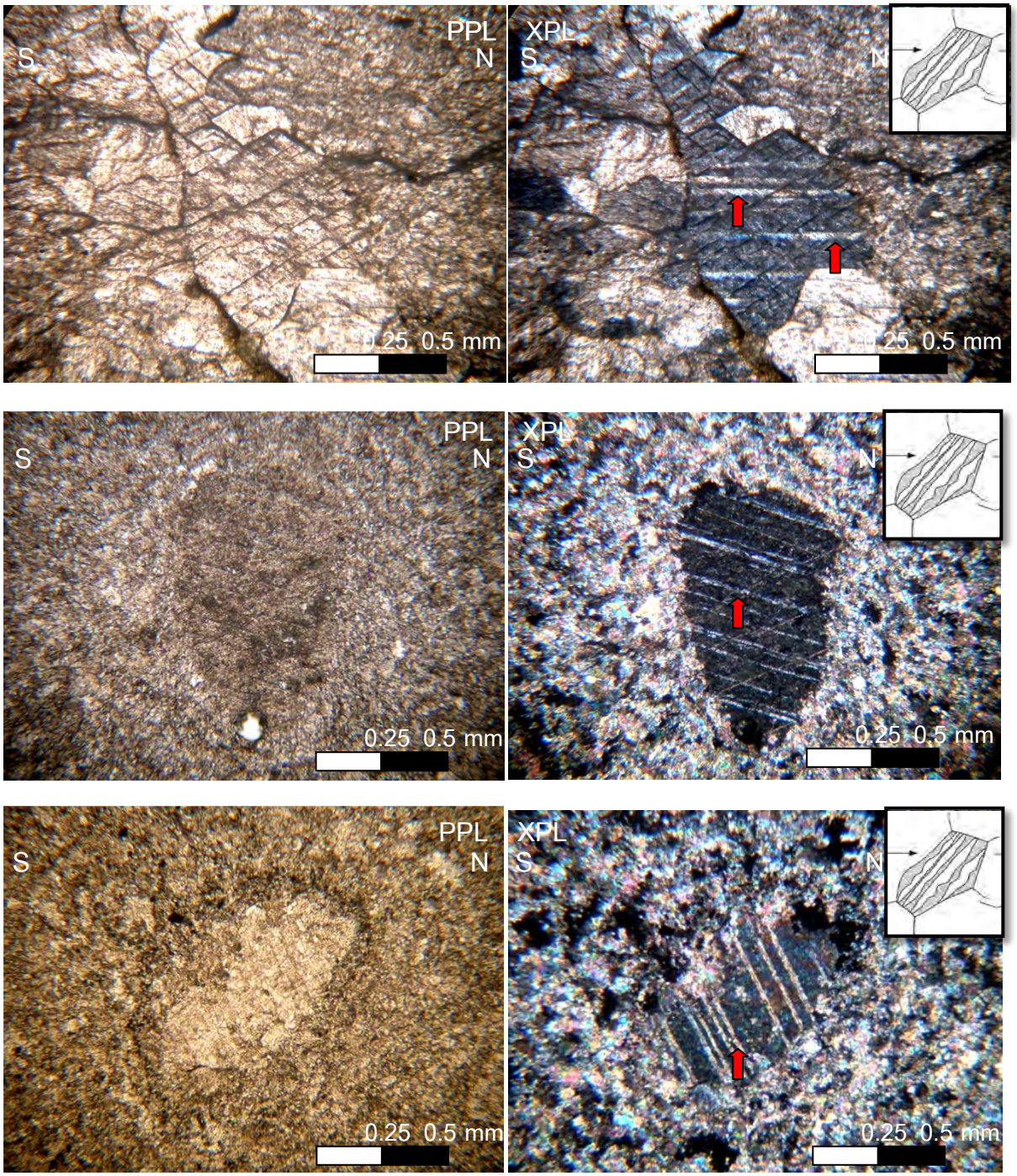

Figure 3.36 Deformation twins are commonly wedge-shaped or tabular or tapered. Twin boundary is not sharp but curve. The small picture in right corner shows boundary migration

recrystallisation in calcite, which can sweep whole crystals by migration of twin boundaries (Ramsay, 1967and Hobbs et al., 1988).

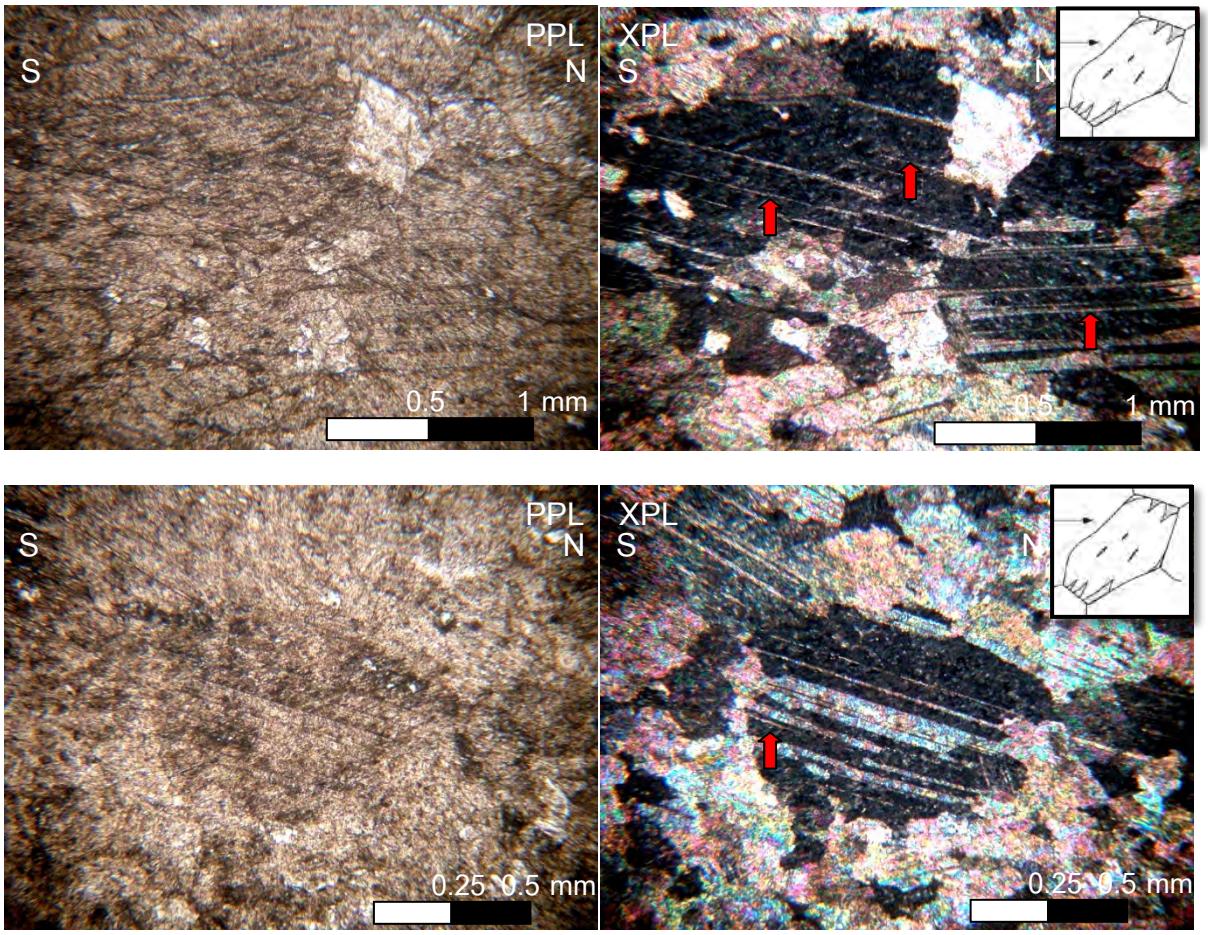

Figure 3.37 Deformation twins are commonly wedge-shaped or tabular or tapered. Some calcite twin absents in middle but in grain boundary still remain. The small picture in right corner shows boundary migration recrystallisation in calcite, which can sweep whole crystals by migration of twin boundaries. It is higher stage than figure 3.36 (Ramsay, 1967and Hobbs et al., 1988).

Temperature gauges

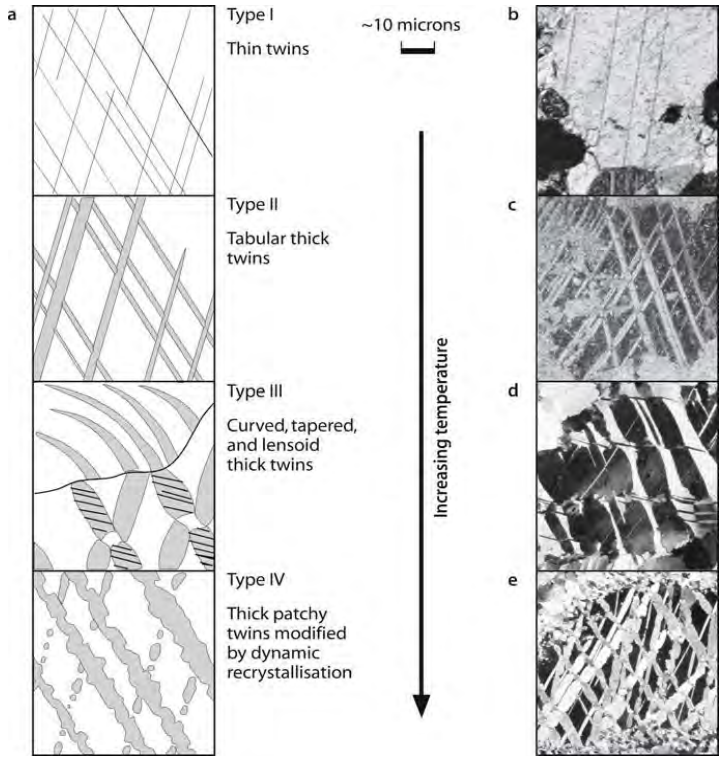

Figure 3.38 a Schematic illustration of the influence of temperature on deformation by calcite twinning (after Burkhard 1993; Ferrillet al. 2004). **b–e** Photomicrograph examples of different twin types (all in crossed-polarized light).**b** At temperatures below 200 C and dominate below 170 C. Narrow straight twins indicate Type I. **c** At temperatures dominate above 200 C up to 300 C. Wider twins which can be optically resolved ;Type II. **d.** At temperatures above 200 C, Type III intersecting twins and bent twins are present. **e.** At temperatures above 250 C, twins obtain serrated boundaries due to twin boundary migration recrystallisation; Type IV (Ramsay, 1967and Hobbs et al., 1988).

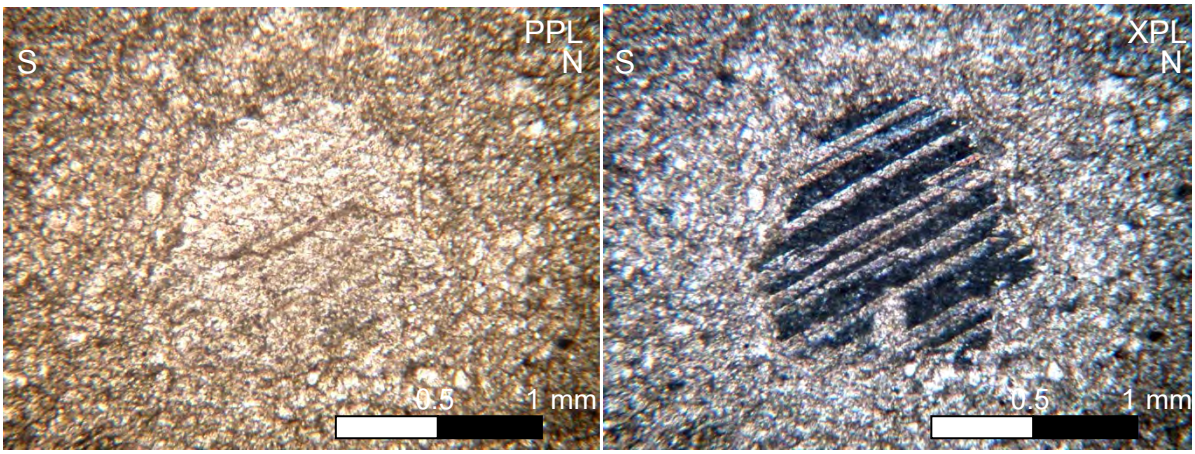

Figure 3.39 Calcite grain has thick twin. Wider twins can be optically resolved; Type II. At temperatures dominate above 200 °C up to 300 °C that is a deformation temperature.

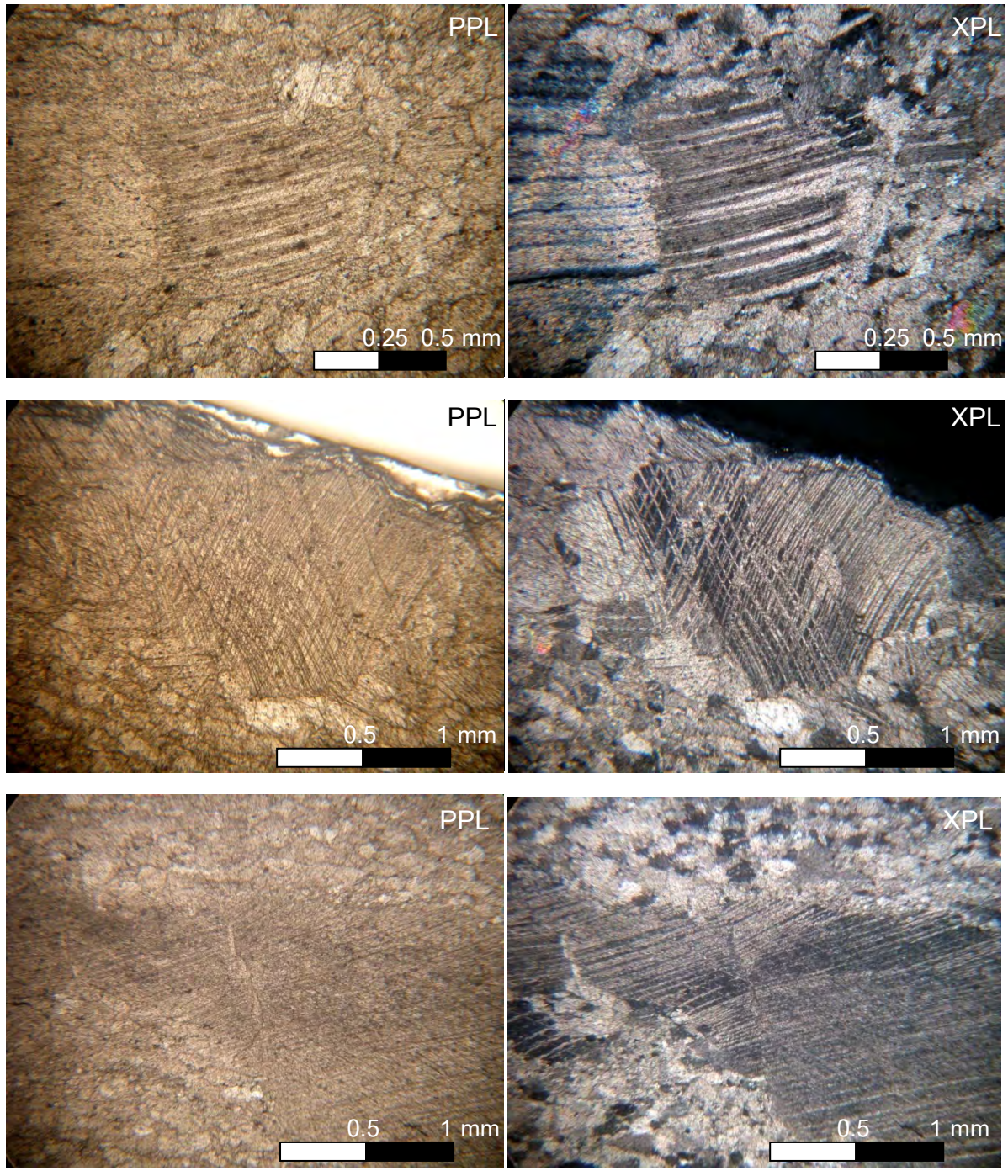

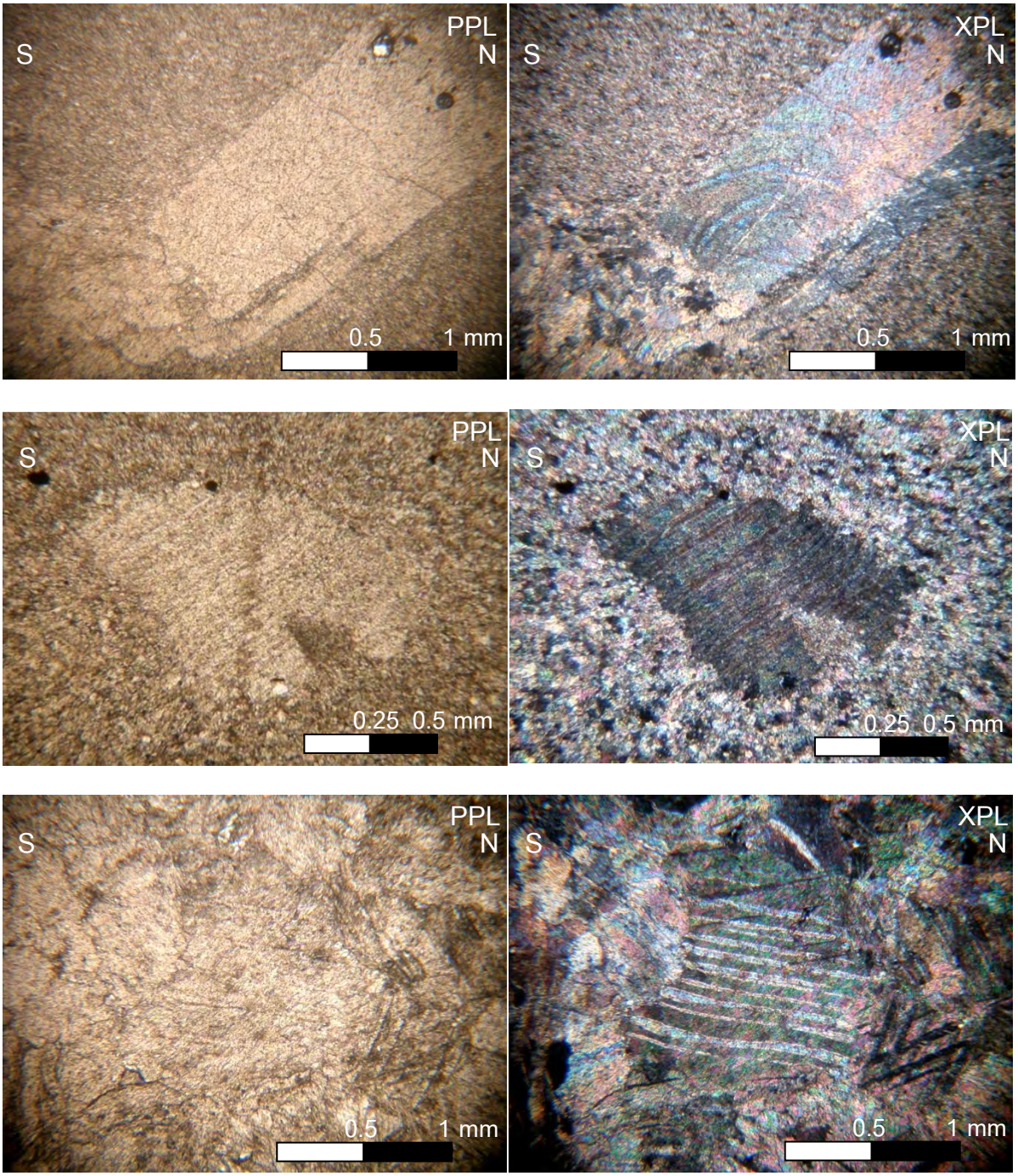

Figure 3.40 Calcite twin become curved, tapered and lensoid thick twins; Type III. The temperature above 200 °C is a deformation temperature.

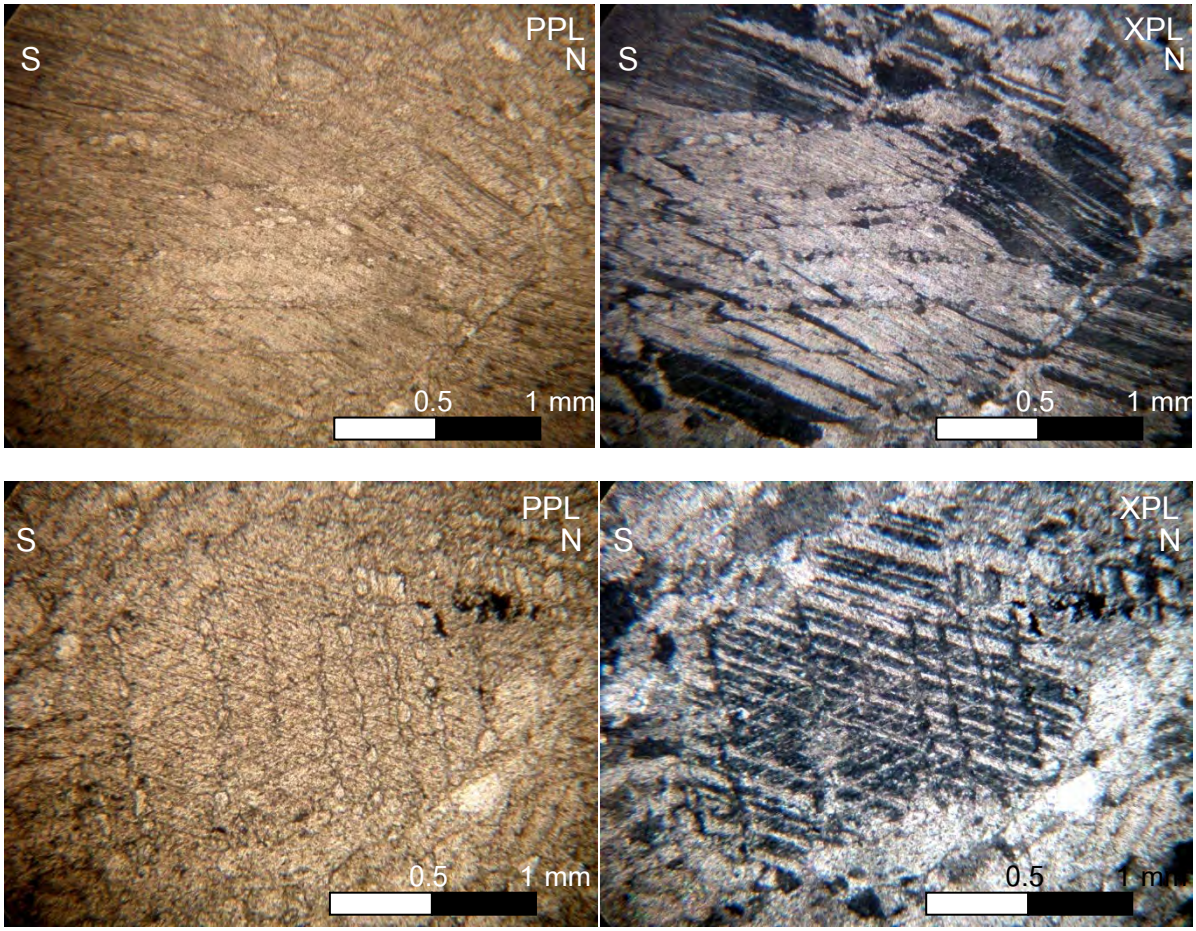

Figure 3.41 Calcite twins obtain serrated boundaries due to twin boundary migration recrystallisation; Type IV. At temperatures above 250 °C that is a deformation tempurature.

Geometric temperature gauges could give independent data on temperature besides the classical petrological geothermometers and may be less easily modified by retrogression and later deformation than mineral composition. One of the most encouraging temperature gauges is twin geometry in calcite. In Uthai Thani limestone Ridge mostly shows geometric deformation of calcite twinning in Type III which indicate temperatures above 200 °C.

Undulose extinction in calcite

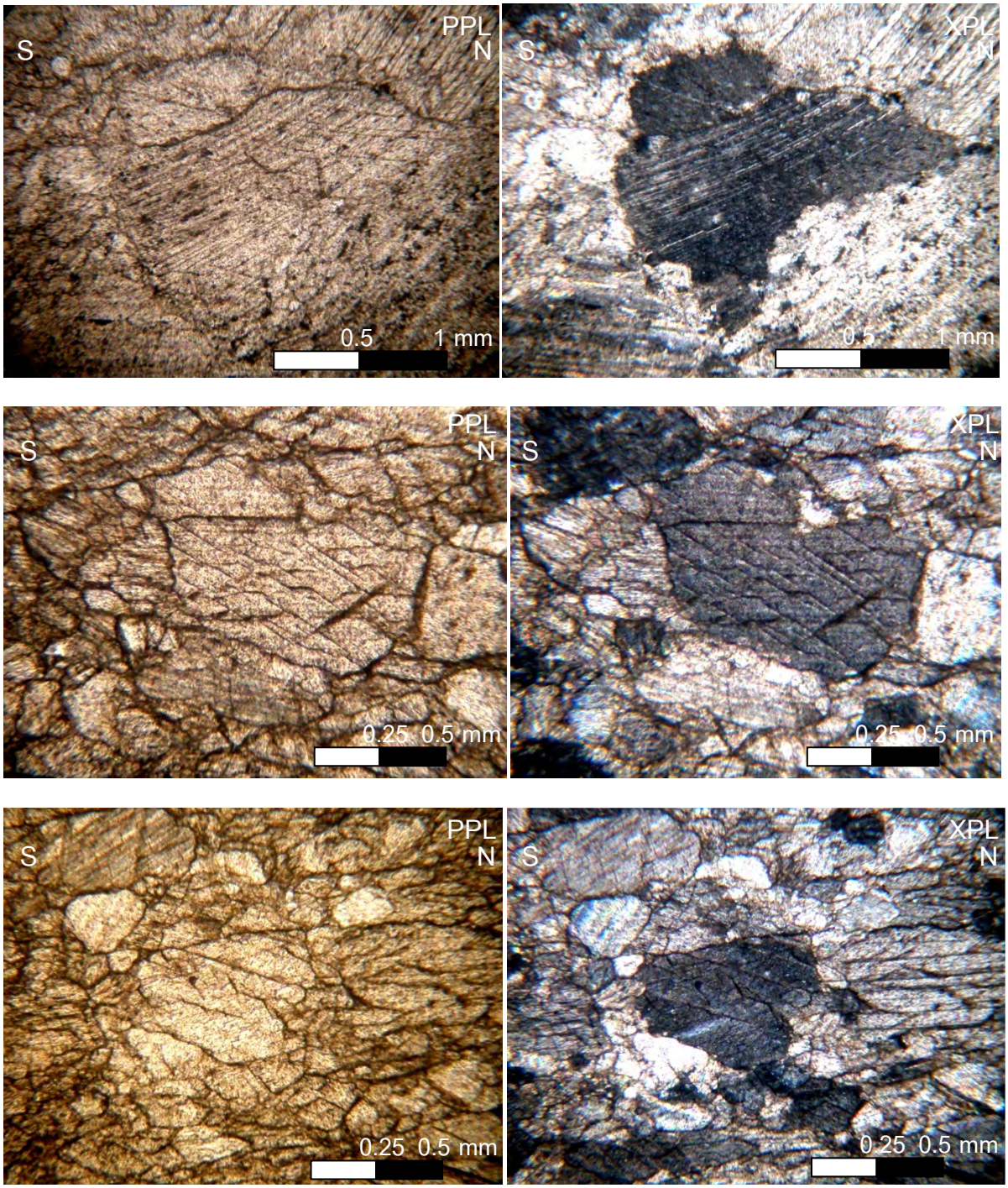

Figure 3.42 Undulose extinction is occurred in deformation calcite grain. Dislocations distributed over the crystal give rise to undulose extinction.

Bulging (BLG) Recrystallisation

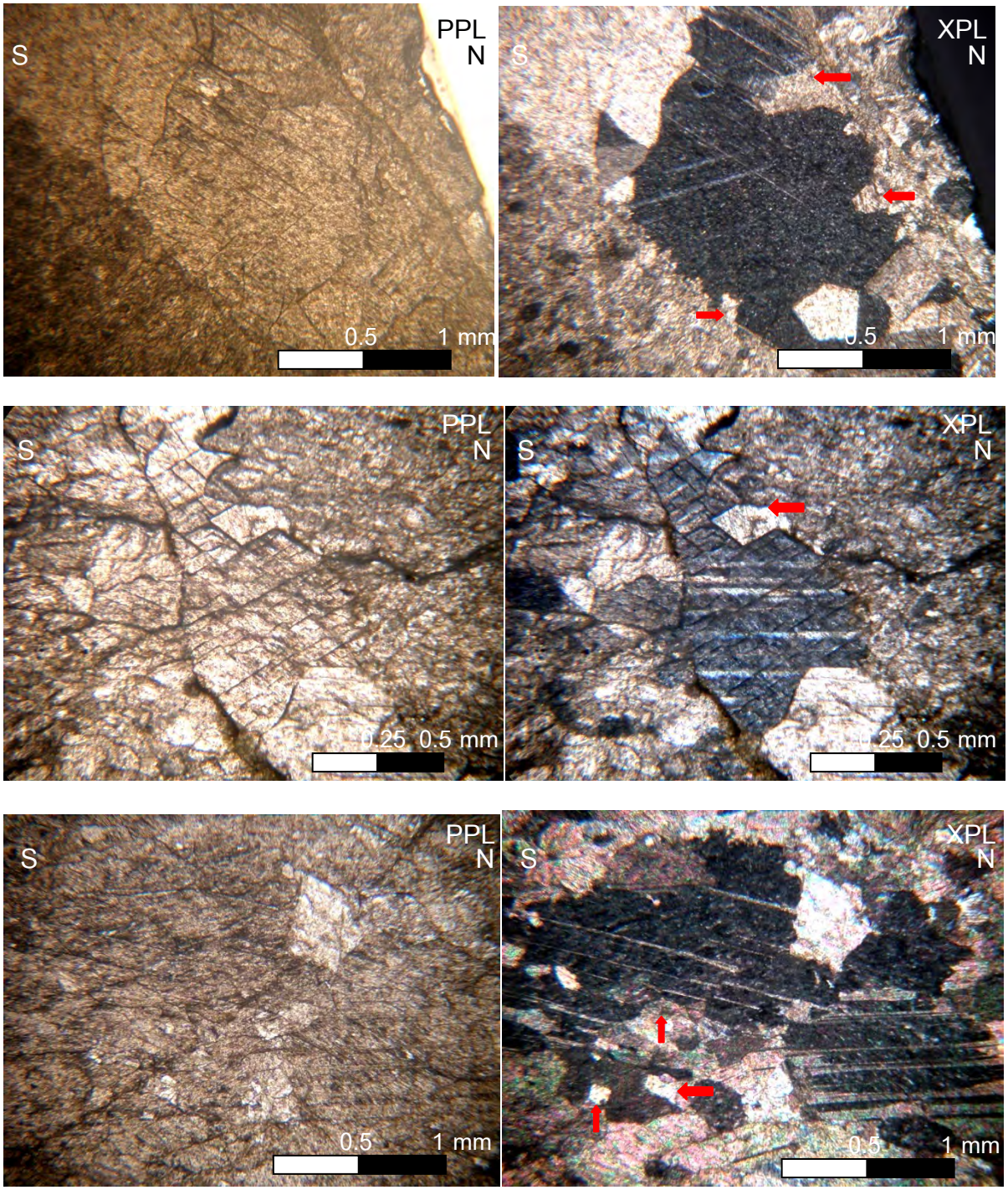

Figure 3.43 In calcite grain boundary show bulging (BLG) recrystallisation. At low temperature, the grain boundary may bulge into the crystal with high dislocation density and form new, independent small crystals

Finally, evidence from microscopic scale in thin section reasonable conform to mesoscopic scale in field observation

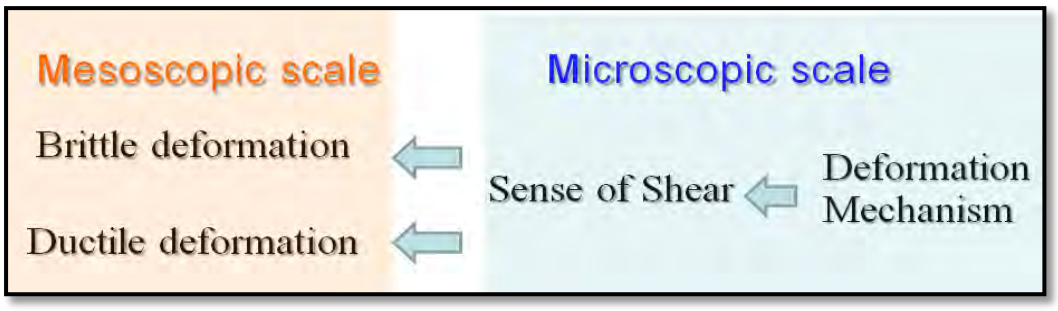

Figure 3.44 Diagram show relationship between evidence from microscopic scale and mesoscopic scale

Chapter 4

Discussion

The 3 main scales of interpretation are composed of macroscopic scale, Mesoscopic scale, and microscopic scale that result of remote sensing interpretation, field observation and microstructure study. Those things bring about to discuss and interpret in terms of structural style and structural evolution of Uthai Thani limestone ridge.

4.1 Structural style

Remote sensing interpretation both in Landsat 5 satellite images and SRTM digital elevation model (DEM) show major lineament trends to N-S composite and minor NE-SW and ENE-WSW (Fig. 3.3 and 3.5). Appearance and trend of ridge in satellite images and DEM is controlled by characteristic of the rocks and structures. The major lineament trends conform to orientation of bed and fault and minor trends conform to fracture and joint.

From the field observation, the evidences of mesoscopic scales can be combined for the structural style of the Uthai Thani limestone ridge. The limestone was developed by sinistral ductile shear motion that was shown by sigma texture in calcite and chert nodule with strain shadow in outcrops. Direction of bedding controlled trend of ridge in N-S that be obvious in stereographic projection (Fig. 3.12). Furthermore, fault accord with the orientation of bedding and fold was found in top of ridge. Those structures fit to the fold model of flexural shear combine with flexural slip (Fig. 4.2). Direction of joint associated with fold model is clear in stereographic projection (Fig. 4.3).

In thin section, microstructure and mineral assemblages can be observed. Calcaleous and calc-silicate protolites include metamorphic index minerals are calcite, quartz and clays that indicated Zeolite facies. Kinematic indicators are both pure shear and simple shear. Pressure solution, non stair stepping ø- objects type and stylolite point to evident of pure shear. In part of simple shear shows mineral orientations, mica fish, sigmoidal texture, strain shadow, stair stepping, trace σ-objects, δ-objects, and shear band type fragmented porphyroclasts. Those evident developed by sinistral ductile shear motion, which conform to ductile deformation in macroscopic and mesoscopic scale. Deformation of limestone widely spread which shown by

stylolites, kink bands, the recrystallisation of twin boundary migration and bulging (BLG) recrystallisation. The temperature gauge of calcite twin geometry indicates temperatures at above 200 °C. Finally, the characteristic of microstructure deformation recognize all texture and the interpretation from petrography. They are related with structural and deforming style in macroscopic and mesoscopic scale (Fig. 4.1).

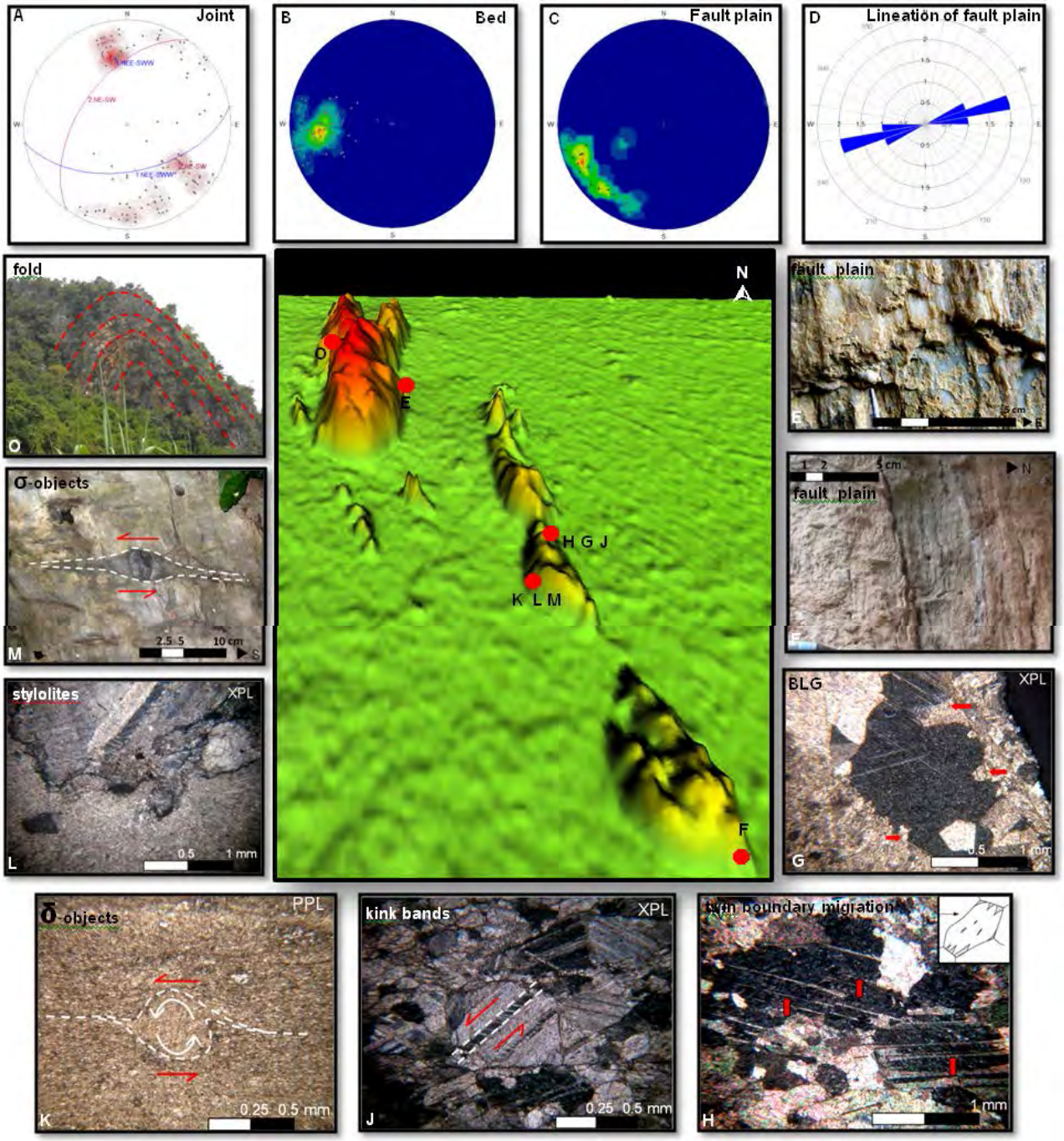

Figure 4.1 Show evident in mesoscopic and microscopic scale in field observation and thinsection that was found in the Uthai Thani limestone ridge. Those evident contribute to the fold model of flexural shear combine with flexural slip (Fig. 4.2); A, B, C, and D show

stereographic projection plotted; E, F, M, and O; G, H, J, K and L show microstructure in thin section.

4.2 Structural Evolution

Eventually, simple analog model of the Uthai Thani limestone ridge has 4 main stages (Fig. 4.4). First of all is digenesis of limestone in Permian. Next is fold stage that is combination with flexural shear and flexural slip. Then the sinistral ductile shear stage is developed on limestone as the affect of Mae Ping fault zone motion. This stage well developed evident of sinistral ductile shear in chert nodule, quartz and calcite grain. Finally, the result from continuous transpressional tectonic of Mae Ping fault zone probably leads to the N-S ridges in Chainat duplex. The reverse fault is possible to associate with uplift process of this ridge and others. This ridge uplifts as the restraining ridge in Chainat Duplex and conform to geometry analog of Smith et al. (2007), Phasongthum (2011), and Kachondham (2011)(Fig. 4.4).

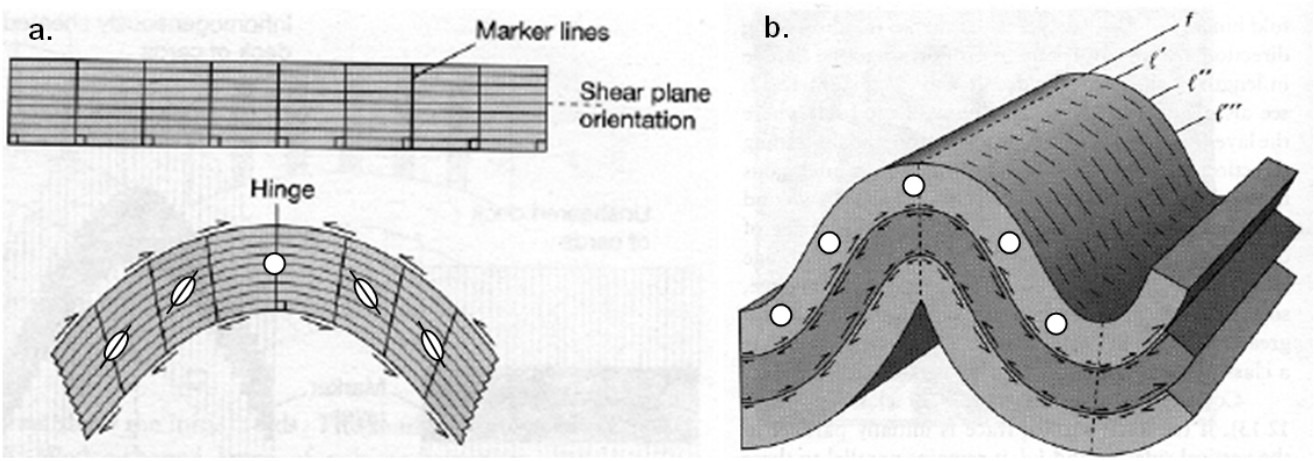

Figure 4.2 Geometry of flexural shear and flexural slip folding (After Twiss and Moores, 1992). **a.** The flexural shear fold is accommodated by simple and pure shear which is stretching into fold. The sense of shear on the rims of fold changes across the fold axial surface and the magnitude of the shear decreases toward the hinge. **b.** The flexural slip fold from an originally planar multilayer, showing relative displacement on layer surfaces. Layers on the convex side of a surface slip toward the hinge line relative to those on the concave side.

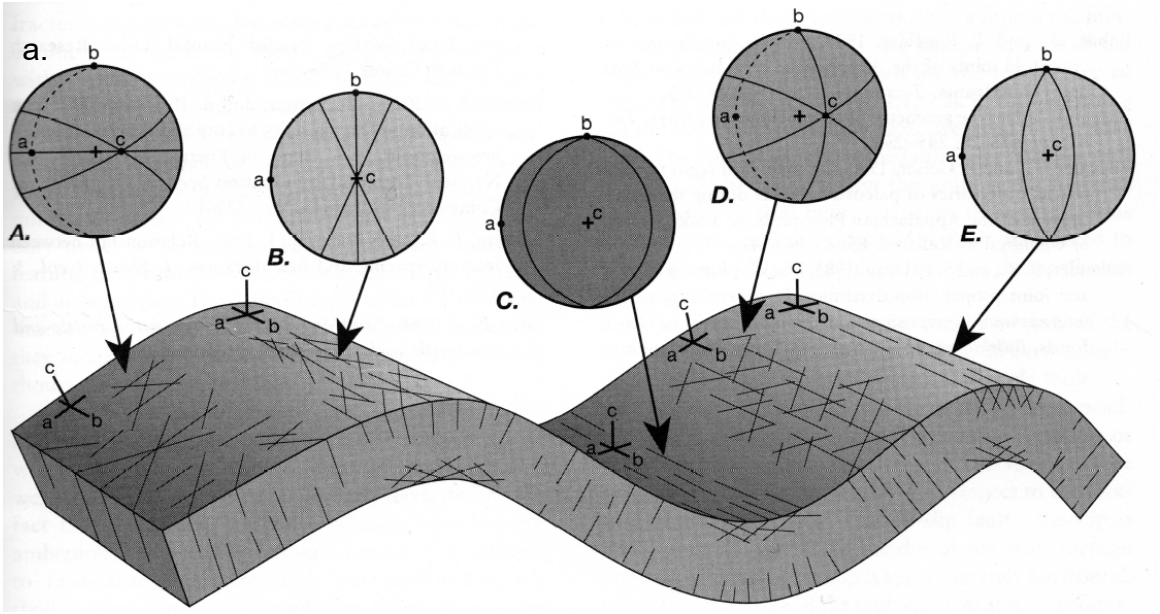

b.

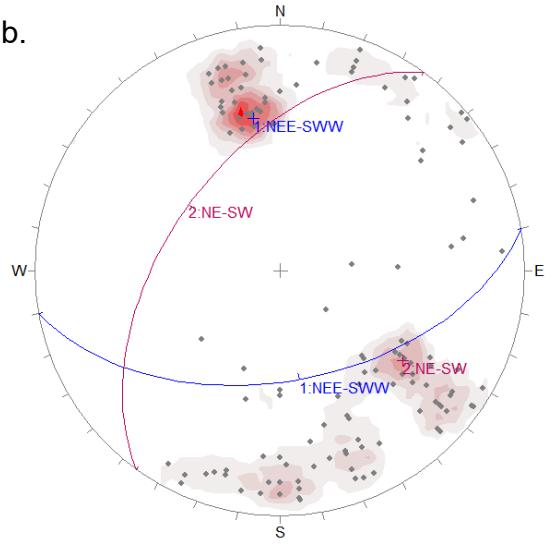

Figure 4.3 a. Fractures associated with folds. The stereographic projections show the orientations of the coordinate system, the bedding where it is not horizontal (dotted great circles), and the fractures (solid great circles) (Twiss and Moores, 1992). **b.** The stereographic projections show the orientations of joint and fracture in study area. They are associated with rim of fold.

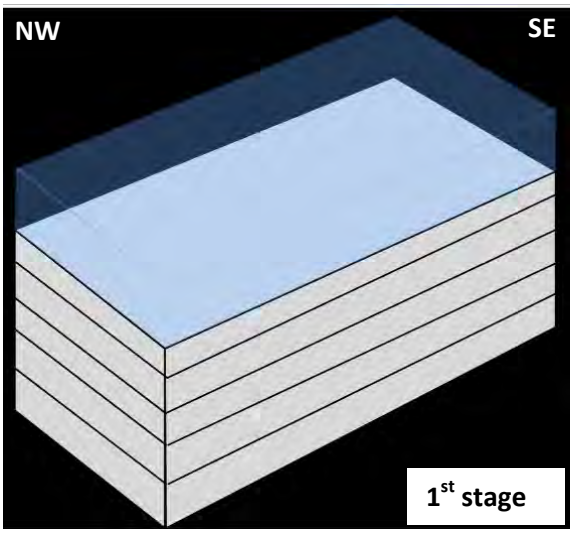

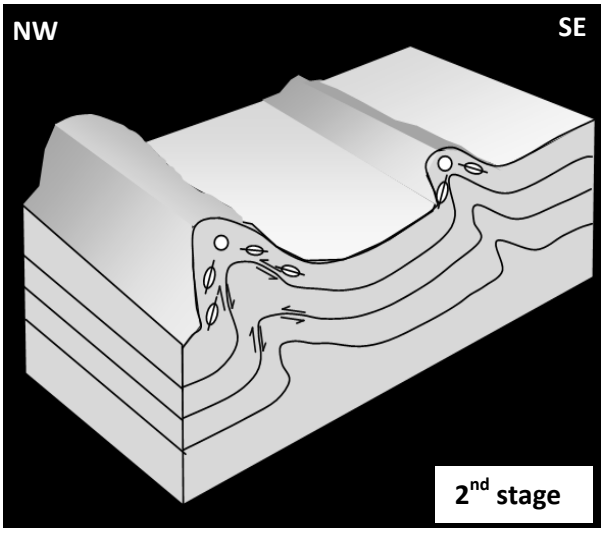

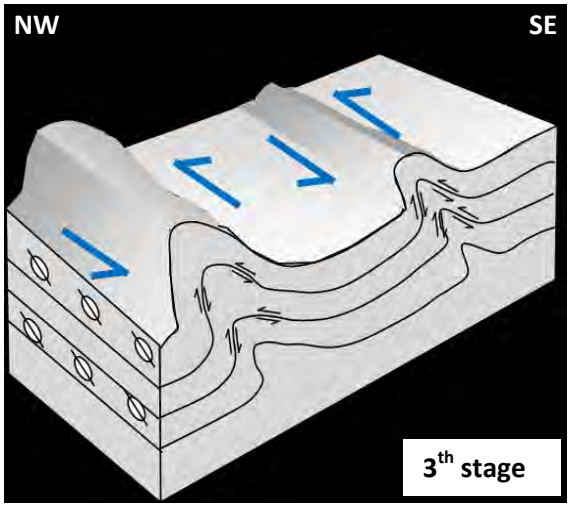

Figure 4.4

1st stage ; Digenesis of limestone in Permian

2nd stage; Fold stage that is combination with flexural shear and flexural slip. The flexural shear show sinistral and dextral shear in each rim of fold.

3th stage ; The sinistral ductile shear stage is developed on limestone as the affect of Mae Ping fault zone motion.

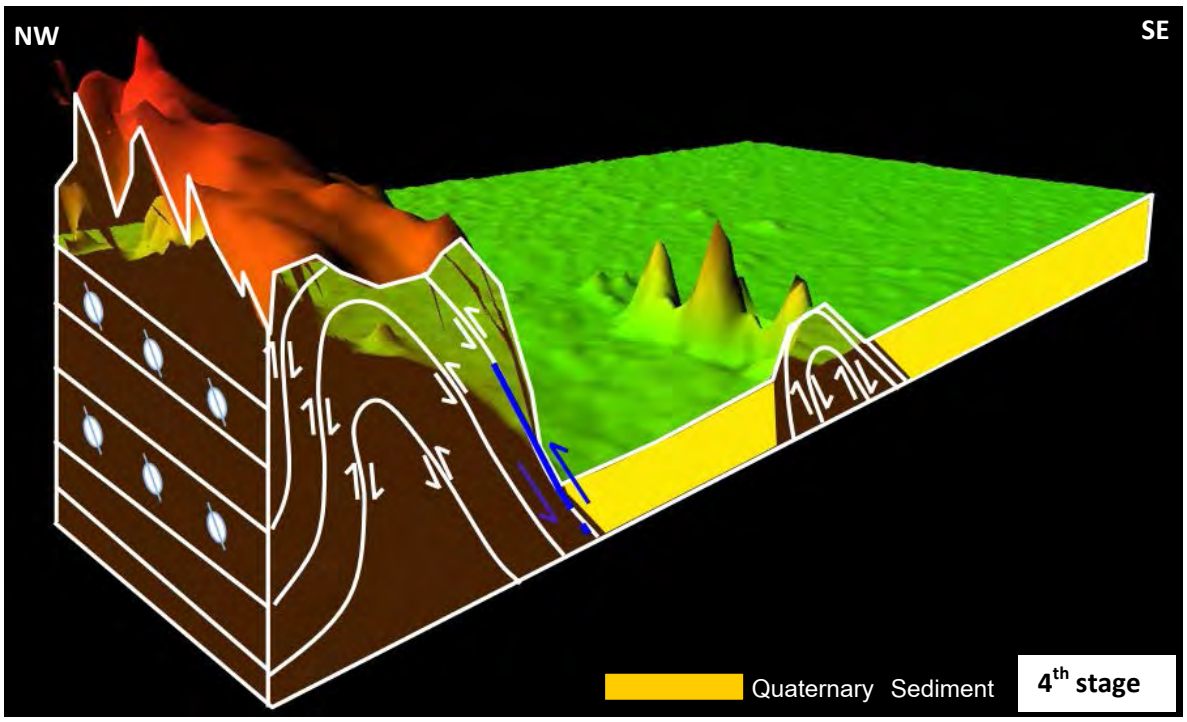

4th stage ; The result from continuous transpressional tectonic of Mae Ping fault zone probably leads to the N-S ridges in Chainat duplex. The reverse fault is possible to associate with uplift process of this ridge and others.

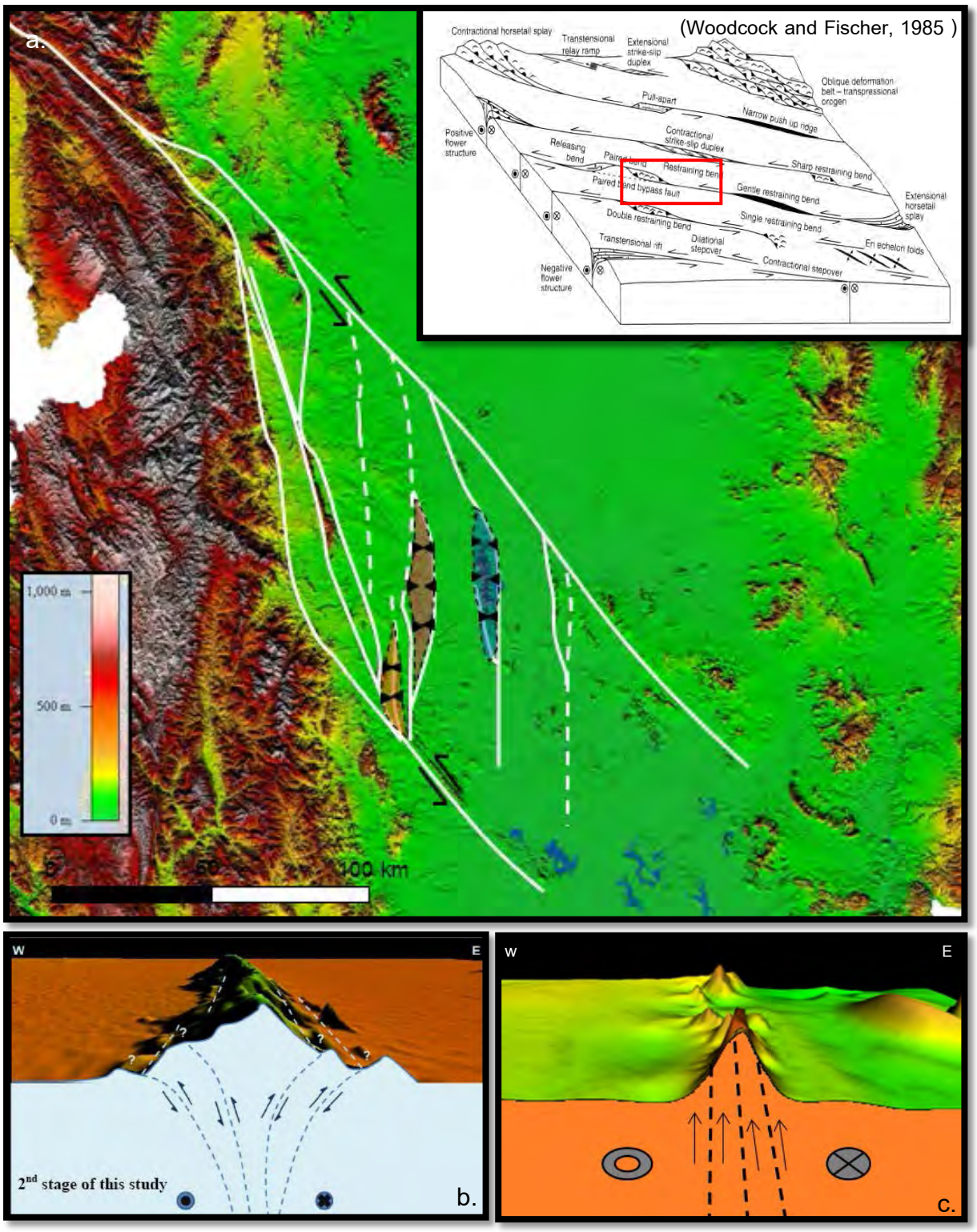

Figure 4.5 **a.** The SRTM digital elevation model show regional scale of northern central plain of Thailand and lineament interpretation to the restraining ben d duplex that modified form Smith et al. (2007). **b.** Model for structural style of the Uthai Thani-Nakhorn Sawan ridge (Phasongthum, 2011) **c.** Model for structural style of the Uthai Thani rhyolite ridge (Kachondham, 2012).

4.3 Tectonics Evolution

The Uthai Thani limestone ridge is remarkable sinistral ductile shear maybe relate with transpressional episode of Mae Ping fault zone. The Mae Ping fault zone has undergone predominantly sinistral strike-slip motion during the Cenozoic (Lacassin et al. 1993, 1997) where the north–south segments would have acted as restraining bends within the overall NW–SE trend. The SRTM digital elevation model and the lineament interpretation have been modified the structural geometry of the duplex from Smith et al. (2007) and Phasongthum (2011), which is composed of a series of north– south-striking ridges, bounded to the north and south by NW–SE-striking faults (Fig. 4.5). Hence, the restraining bends should have experienced considerable strain, uplift and erosion. The Uthai Thani limestone ridge is possible to relate with it because the structural geometry is the same other the north–south ridge in Chinat duplex. But timing of uprift phase not be clear from evident of structure and deformation phase in this ridge.

A correct information from macroscopic, mesoscopic, and microscopc scale, the Uthai Thani limestone ridge shows mainly N-S striking and faulting and sinistral ductile phase inside. Faults are related with uplift phase but are still unclear in timing. Detailed timing of events cannot be determined from structures within the duplex. Morley et al. (2007) and Smith et al. (2007) have been interpreted that uplift phase of Chainat duplex was related to evolution of adjacent rift basins, the Phitsanulok basin which is composed of two sub-basins: the Lahan Graben and the Nong Bua sub-basin. The Lahan Graben lies closest to the Mae Ping fault zone, and shows evidence for Late Oligocene–Early Miocene extension. Extension in the basin had end in the Early Miocene, and this was followed by uplift and widespread erosion. In particular, in the area between both basins, there was cleared basin inversion, which occurred in the late Early Miocene. Inversion created N-S trending anticlines and inverted N-S trending faults. The E-W compression direction of Lahan graben would have stimulated Chainat duplex faults either as reverse and thrusts or sinistral strike-slip faults. The uplift evidence expects in reverse faults or thrust faults that can be observed in western area but normal fault is in same fault plain. Because the vertical movement was occurred more than one, this evident cannot be the strong evidences for uplift phase of the Uthai Thani limestone ridge. If to consider from geometry form parallel N-S ridge in Chainat duplex conform to the Uthai Thani limestone ridge, it will be probably controlled with the main same tectonic episode. Moreover, reverse fault planes show

eastward thrusting, which relate with transpressional episode of Mae Ping fault zone and E-W compression direction of Chainat duplex. Therefore, the reverse fault in this ridge is reasonable to explain the uplift evidences of the Uthai Thani limestone ridge (Fig 4.5).

The Uthai Thani limestone ridge can be observed evident of fold. As usual, folding show different sense of shear in each rim. But in this study in mesoscopic scale and microscopic scale are outstanding with the sinistral ductile shear that relate with the transpressional tectonic of Mae Ping fault zone and Chainat duplex. Based on previous geochrological data by Morley et al. 2007, this sinistral ductile shear episode possible began during post Late Triassic toward Late Oligocene. There are not clearly evidence data to confirm that sinistral ductile shear have begun at early Tertiary. Hence folding stage maybe developed before sinistral ductile shear stage, but after diagenersis of Permian limestone.

In this study if we used comparing with the structural geometry in The Uthai Thani limestone ridge with other ridge. Timing can be approximately predicted form geochrological data in granite in other ridge. Therefore, the geochronological data mainly along Mea Ping fault zone was collected from previous works and the work by Lacassin et al. (1997), and Morley et al., (2007). Uprift phase of Chainat duplex relate with Uplift and inversion of the Lahan sub-basin (Smith et al. 2007) which coincides with the apatite fission-track cooling ages obtained for two granites in the Chainat duplex (22.4+2.8 Ma and 18.2+1.6 Ma) (Morley et al. 2007). The using of 40Ar/39Ar technique, the biotite cooling age for Mea Ping fault suggested that dates of onset and end of sinistral motion were about 33-30 Ma (Lacassin et al., 1997). So Uprift phase of ridges in Chainat duplex include The Uthai Thani limestone ridge was during Oligocene-Late Miocene formed as the restraining ridge. (Table 4.1)

Table 4.1 The table shows summary of tectonic events and structural style in Uthai limestone ridge within Chainat duplex. ▬▬ Certain timing ▪▪▪▪▪ Uncertain timing

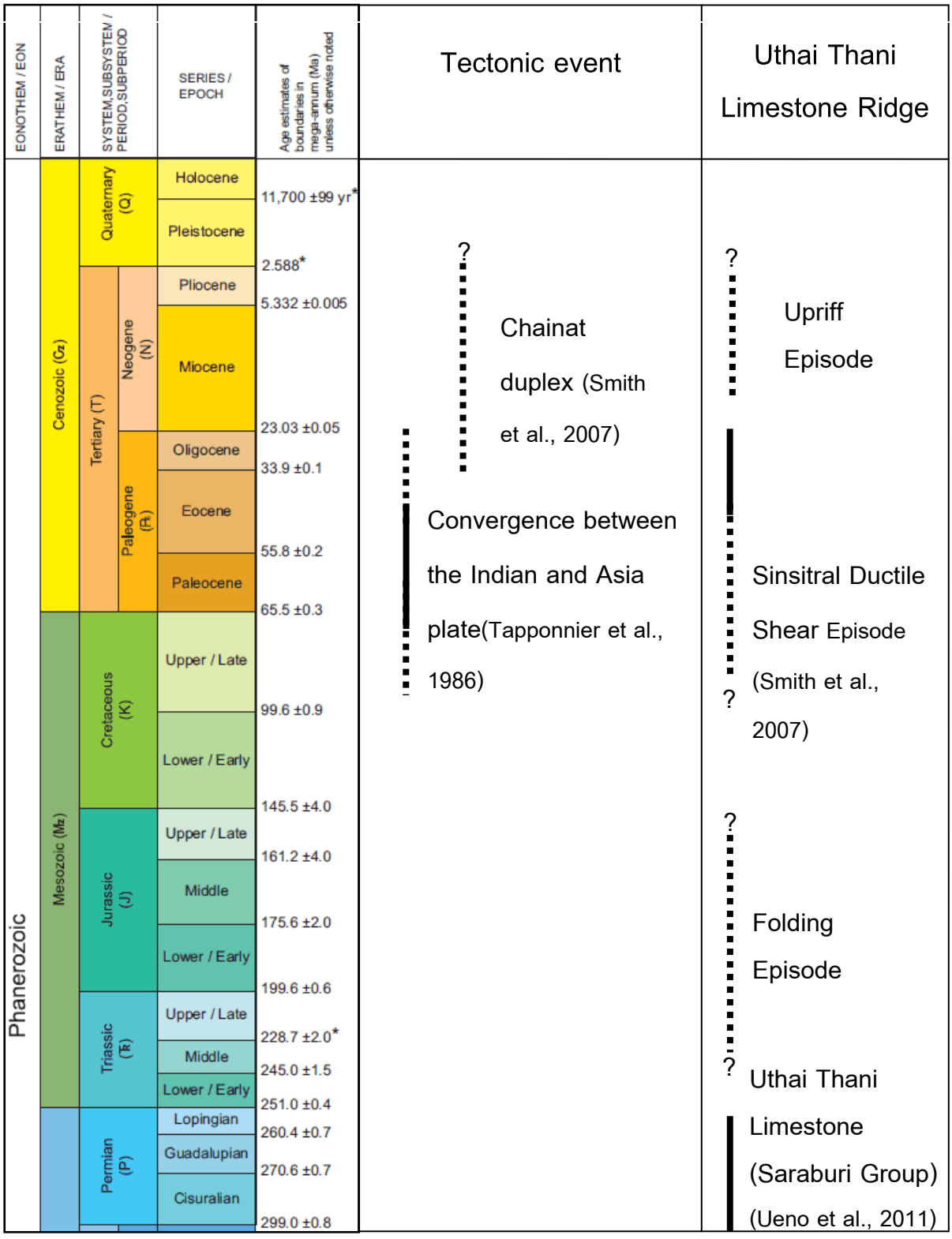

Chapter 5

Conclusion

The 3 main scales of interpretation are composed of macroscopic scale, mesoscopic scale, and Microscopic scale that can be interpreted and discussed in term of structural style and structural evolution of the Uthai Thani limeston ridge. The following conclusions provide from the results of remote sensing interpretation, field observation and microstructure.

- Remote sensing interpretation both in Landsat 7 satellite images and SRTM digital elevation model (DEM) show major lineament in N-S trends that conform with bedding and vertical fault movement
- Fold stage in the Uthai Thani limeston ridge that is combination with flexural shear and flexural slip.
- The sinistral ductile shear developed after fold stage in the Uthai Thani limeston ridge.
- The metamorphism facies in the Uthai Thani limeston ridge can be indicated Zeolite facies and has temperature deformation > 200 °C, based on metamorphic index minerals and calcite twin geometry.
- The Uthai Thani limeston ridge formed as the restraining ridge.
- The Uthai Thani limeston ridge is remarkable sinistral ductile shear maybe relate with transpressional episode of Mae Ping fault zone
- The sinistral ductile shear clearly dominates and deforms Permian limestone in the Uthai Thani limeston ridge. Hence, the sinistral ductile shear episode possible began with post Late Triassic to the end of sinistral movement of Mae Ping Fault during 30-33 Ma.
- The uplift phase might be related with the uplift and inversion of Tertiary basin around Mae Ping fault zone during Early Miocene to Late Miocene, especially Lahan sub-basin in Phitsanulok basin, northern Chainat duplex.
- The major reverse faults can be observed in the Uthai Thani limeston ridge and direction of thereverse faults has same tend of ridge. These evidences can be explained uplift stage of Uthai Thani limeston ridge. These evidences do not clearly for the timing of their evolution.

References

Bunopas, S., 1981, Paleogeographic history of western Thailand and adjacent parts of Southeast Asia: A plate tectonic interpretation, Unpublished PhD Thesis, Victoria University of Wellington, 810.

Bunopas, S., and Vella, P., 1983, Tectonic and geologic evolution of Thailand, In P.Nutalaya, ed., *Proceedings of the Workshop on Stratigraphic Correlation of Thailand and Malasia, Haad Yai, Thailand,* September 8-10, 307-323.

Burkhard, M., 1993, Calcite twins, their geometry, appearance and significance as stress-strain markers and indicators of tectonic regime, *Journal Structure Geology*, 15, 351–368.

Charusiri, P., Daorerk, V., Archibald, D., Hisada, K., Ampaiwan, T., 2002, Geotectonic evolution of Thailand: A new synthesis, *Journal of Geological Society*, Thailand, 1, 1-20.

Charusiri, P and Pum-Im, S., 2009. Cenozoic tectonic evolution of major sedimentary basin in central, northern and the gulf of Thailand. *BEST,* 2(1-2), 40-62 pp.

Department of Mineral Resources., 1976. *Geological map of Thailand,* sheet Changwat Nakhorn Sawan, ND47-3, scale 1:250,000.

Dunham, R. J., 1962, Classification of carbonate rocks according to depositional texture. In: Ham, W. E., ed., Classification of carbonate rocks: American Association of Petroleum Geologists Memoir, 108-121.

Embry, A.F., and Klovan, J.E., 1971, A Late Devonian reef tract on Northeastern Banks Island, NWT: Canadian Petroleum Geology Bulletin, 19, 730-781.

Ferrill, D.A., Morris, P.A., Evans, M.A., Burkhard, M., Groshong, Jr. R.H., Onasch, C.M., 2004, Calcite twin morphology: a low-temperature deformation geothermometer, *Journal Structure Geology* , 26, 1521-1529.

Hall, R., 2002, Cenozoic geological and plate tectonic evolution of SE Asia and the SW Pacific: computer-based reconstructions, model and animations, *Journal of Asian Earth Sciences*, 20, 353-434.

Hinthong, C., Chuaviroj, S., Kaewyana, W., Srisukh, S., Pholprasit, C. and Polachan, S., 1985, Geological Map of Thailand 1:250,000, Sheet Changwat Phra Nakhon Si Ayutthaya (ND 47-8), Geological Survey Division, Department of Mineral Resources, Bangkok.

Hobbs, B.E., 1985, The geological significance of microfabric. In: WenkHR, ed., Preferred orientation in deformed metals and rocks.Academic Press, New York.

Kachondham, N., 2012, Structural Geology of the Uthai Thani Rhyolite Ridge in the Chainat Duplex, Thailand, Unpublished Senior Project, Development of Geology, Science, Chulalongkorn University, Thailand.

Lacssin, R., Hinthong, C., Etal., 1997, Cenozoic diachronic extrusion and deformation of western Indochina: structure and $^{40}Ar/^{39}Ar$ evidence from NW Thailand., *Journal of Geophysical Research*, 102, 10,013–10,037.

Morley, C. K., 2002, A tectonic model for the Cenozoic evolution of strike-slip faults and rift basins in SE Asia, *Tectonophysics*, 347, 189–215.

Morley, C. K., 2004, Nested strike-slip duplexes and other evidence for Late Cretaceous–Palaeogene transpressional tectonics before and during India–Eurasia collision, in Thailand, Myanmar and Malaysia, *Journal of the Geological Society*, London, 161, 799–812.

Morley, C.K., M. Smith, A. Carter, P. Charusiri and S. Chantraprasert., 2007, Evolution of deformation styles at a major restraining bend, constraints from cooling histories, Mae Ping fault zone, western Thailand, *Journal of the Geological Society*, London, 290, 325-349.

O'Leary, H. and Hill, G. S. 1989, Cenozoic basin development in the Southern Central Plains, Thailand, Proceedings of the International Conference on Geology and Mineral Resources of Thailand, Bangkok, Department of Mineral Resources, Bangkok, 1–8.

Passchier, C.W., Trouw, R.A.J., 2005. Microtectonics, 2nd edn. *Springer-Verlag*, Heidelberg, Berlin.

Polachan, S., Pradidtan, S., Tongtaow, C., Janmaha, S., Intarawijitr, K., Sangsuwan, c., 1989, Development of Cenozoic basins in Thailand, Mineral Fuels Division, Unpublished PhD Thesis, Department of Mineral Resources, Thailand.

Prasongthum, P., 2011, Structural Geology of the Uthai Thani-Nakhorn Sawan Ridge in the Chainat Duplex, Thailand, Unpublished Senior Project, Development of Geology, Science, Chulalongkorn University, Thailand.

Ramsay, J.G., 1967, Folding and fracturing of rocks.,McGraw Hill, New York.

Sabins, F.F. Jr, 1996, Remote Sensing: Principles and Interpretation, 3rd edn., New York: W.H. Freeman.

Smith, M., Chantraprasert, S., Morley, C.K. and Cartwright, I., 2007, Structural geometry and timing of deformation in the Chainat duplex, Thailand, In Cunningham, W.D., Mann, P., Eds., Tectonics of Strike-slip Restraining and Releasing Bends, *Journal of the Geological Society*, London, Special Publications, 290, 305–323.

Tapponnier, P., Peltzer, G., Armijo, R., 1986, On the mechanism of collision between India and Asia. In, Coward, M.P., Ries, A.C., Eds., Collision Tectonics, *Journal of the Geological Society*, London, Special Publications, 19, 115-157.

Twiss, Robert J. and Moores, Eldridge M., 1992, Structural Geology W. H. Freeman and Company, 37-126.

Ueno, K., Miyahigashi, A., Kamata, Y., Kato, M., Charoentitirat, T. and Limruk, S., 2011, Geotectonic subdivision of the Central Plain of Thailand: A perapective from Permian and Triassic successions, *Japan Geoscience Union Meeting 2011*, 37.

Woodcock, N.H. and Fischer, M., 1985, Strike-slip duplexes, *Journal of the Structural Geology,* 8, 725–735.

Appendix

Appendix A: Field observation

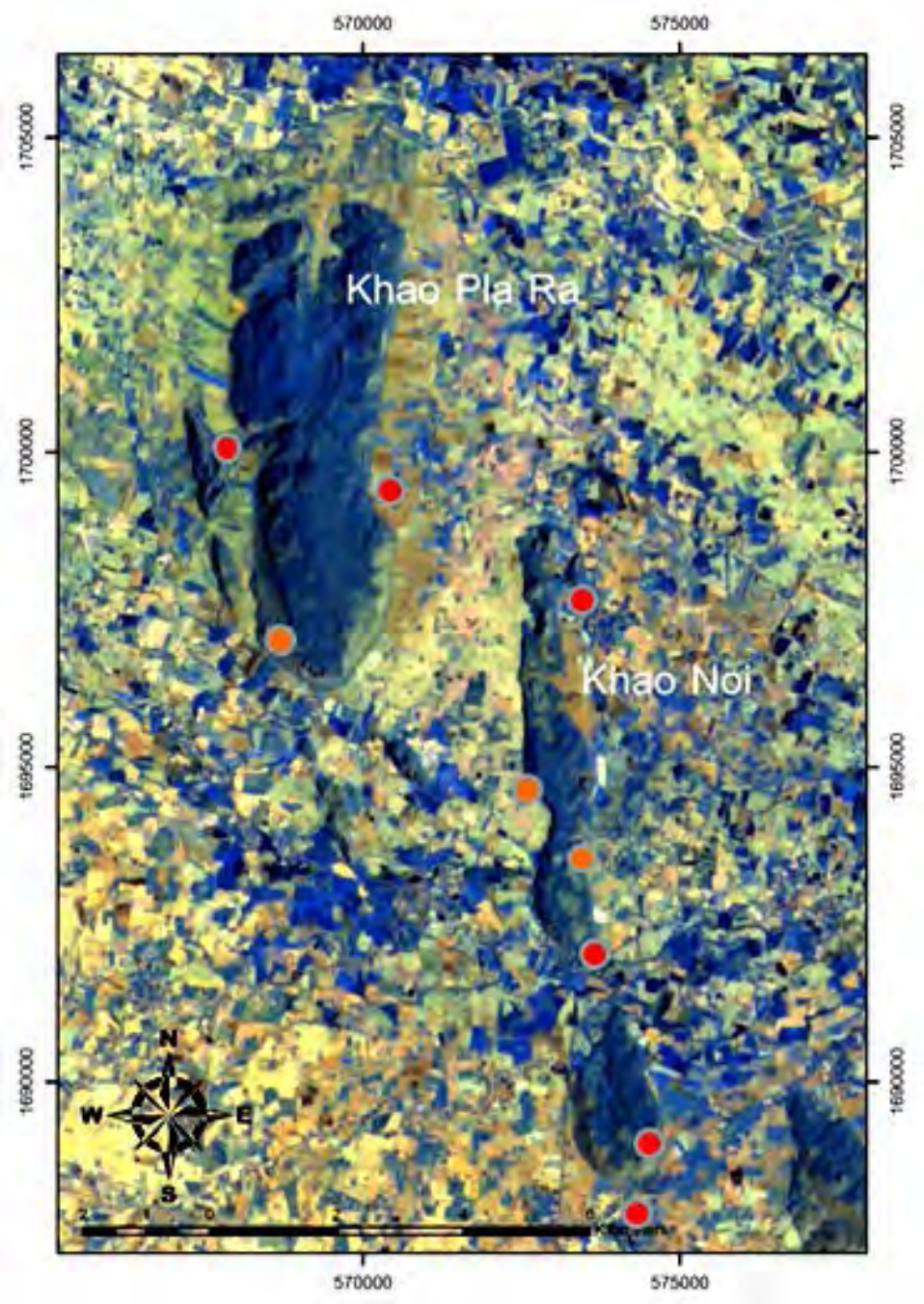

There are 9 study area

- Field observation
- Rock oriented sampling

Appendix B: Field Structural Measurement Data

Aptitude of bed

dip	dipdirection	dip	dipdirection	dip	dipdirection	dip	dipdirection
65	80	80	80	60	80	50	85
47	56	57	100	88	80	80	75
65	78	76	105	36	75	70	85
56	85	35	110	50	85	55	85
80	70	52	100	80	100	60	97
65	83	48	80	32	65	67	82
55	88	60	85	80	65	65	83
60	95	60	95	65	75	65	78
65	80	60	85	85	65	58	90
65	83	55	80	77	85	48	90
60	75	40	93	89	97	85	77
59	90	40	90	75	95	60	95
48	90	80	100	80	98	55	88
88	75	32	120	60	65	60	80
59	90	12	105	68	85	55	105
46	60	45	100	84	75	80	80
60	85	80	80	80	60	50	75
55	104	65	80	75	80	50	75
55	100	70	70	65	80	80	105
50	115	55	80	48	60	56	70
55	112	50	90	65	80	80	65
85	85	60	80	70	85	55	80
77	85	50	75	70	75	52	100
75	80	50	97	60	80	48	80
55	98	45	98	60	90	60	90
80	105	75	88	75	95		

Aptitude of lineation of fault plain

dip	dipdirection	dip	dipdirection	dip	dipdirection	dip	dipdirection
70	330	75	360	60	310	85	215
40	316	75	306	55	344	70	160
68	345	81	25	68	340	62	232
41	316	72	299	55	335	62	161
50	300	75	355	80	338	88	229
74	310	80	335	75	3	40	268
75	15	45	320	78	310	65	260
85	25	68	335	80	360	70	220
80	30	47	316	72	310	74	160
65	360	52	305	78	355	75	170
75	340	75	310	24	265	65	165
83	355	80	10	60	262	58	160
65	308	73	15	75	170	55	173
60	350	80	5	74	160	50	178

60	300	75	360	75	217	70	165
65	5	70	350	60	160	55	168
58	308	82	355	50	160	54	170
77	20	70	315	55	173	60	165
85	300	65	335	54	170	75	210
80	315	62	302	75	170	50	160
50	305	68	358	50	170	73	250
35	20	65	308	54	170	80	235
40	360	75	18	55	173	65	168
50	305	86	305	75	200	75	175
85	305	82	315	50	160	77	200
55	310	55	305	80	265	65	185
47	325	45	15	88	231	80	200
48	300	42	360	54	165	75	165
20	310	50	305	80	175	83	213
35	49	75	305	75	190	70	163
67	340	55	315	62	180	65	230
56	335	47	335	85	200	65	165
79	340	48	305	75	163	80	230
85	215	70	160	88	229	70	220
70	160	62	232	40	268	74	160
62	232	62	161	65	260	75	170
65	165	75	210	65	185	65	165
58	160	50	160	80	200	80	230
55	173	73	250	75	165	55	168
50	178	80	235	83	213	54	170
70	165	65	168	70	163	60	165
77	200	75	175	65	230		

Aptitude of Fault

dip	dipdirection	dip	dipdirection
80	80	80	70
85	75	40	60
30	70	63	20
65	75	72	25
70	70	80	60
78	20	70	35
72	70	70	40
70	60	75	45
75	45	63	50
65	75	70	60
78	50	78	65

Aptitude of lineation of fault plain

Plunge	trend	Plunge	trend
81	83	160	18
172	83	165	20
175	75	165	65
81	83	83	60
70	83	150	68
155	15	75	55
170	20	145	70
165	63	80	80
75	57	170	75
120	68	175	75
50	52	75	80
145	82	70	82

Appendix C: Microtectonic

Simple Shear

a.

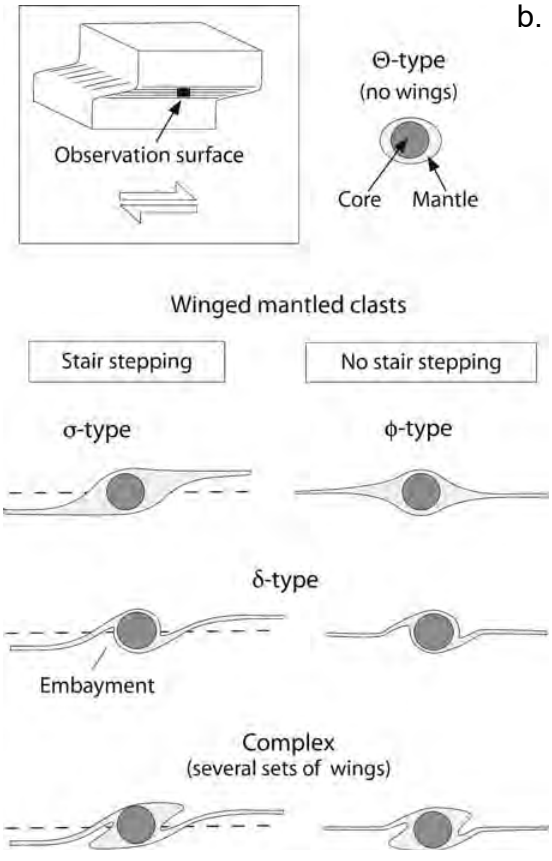

b.

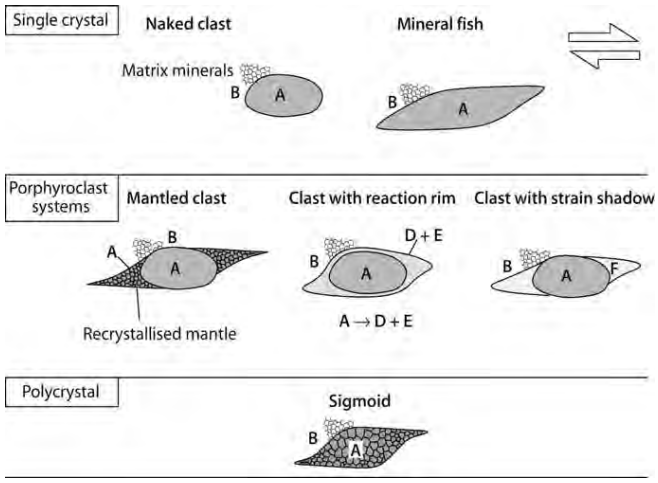

a. Classification of shear type. Dextral sense of shear. b. Schematic diagram of the principal types of objects encountered in thinsection. This includes large single crystal shapes such as naked clasts and mineral fish, single crystal porphyroclasts with rims such as mantles, reaction rims or strain shadows, and polycrystalline aggregates such as sigmoids. *A*, *B*, etc. refer to mineral types (Passchier and Trouw, 2005).

Shear band type fragmented porphyroclasts

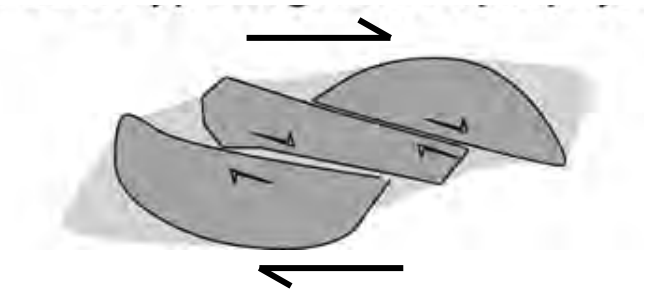

Shear band type fragmented porphyroclasts. The geometry depends on the bulk shear sense and the initial orientation of microfaults in the grains, which may be partly controlled by crystallographic directions in the porphyroclasts. (Passchier and Trouw, 2005)

Stylolites

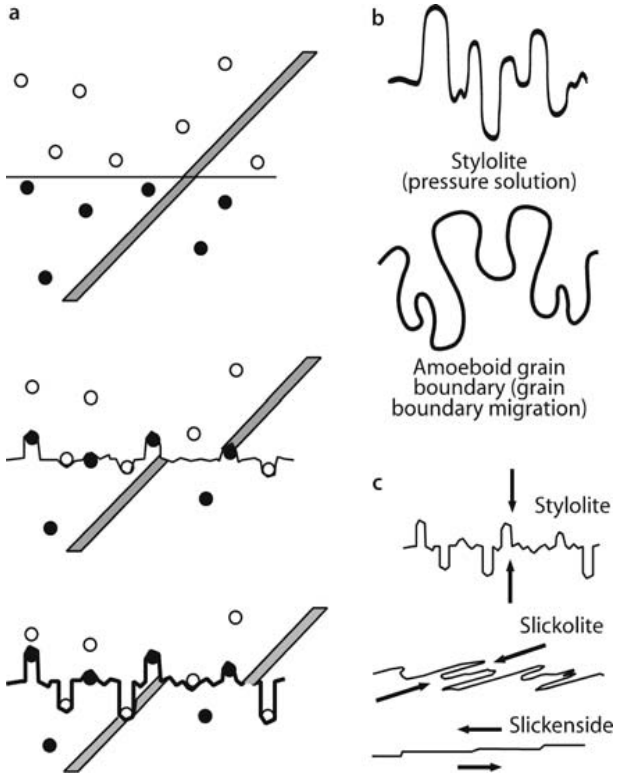

a Development of a stylolite in rocks with insoluble inclusions; material behind inclusions may be protected from solution and form interlocking *teeth*. **b** Stylolites formed by pressure solution differ from amoeboid grain boundaries formed by grain boundary migration in that they have teeth with parallel sides that allow the two halves to be “pulled apart”. **c** Explanation of the terms stylolite, slickolite and slickenside. In a stylolite, teeth and inferred shortening direction are normal to the plane, in slickolites oblique and in slickensides parallel (Ramsay, 1967and Hobbs et al., 1988).

Kink bands

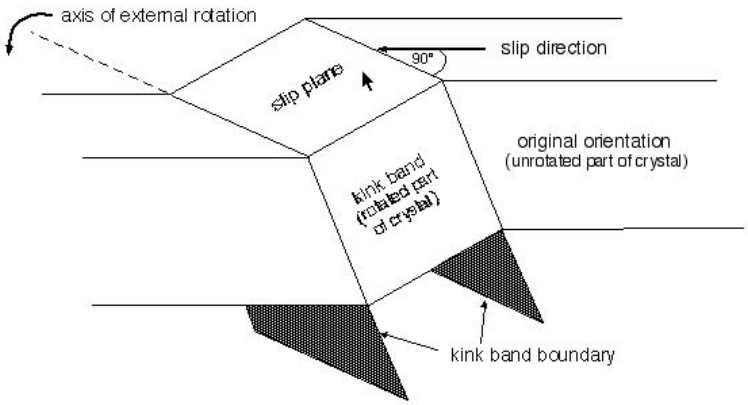

Schematic illustration of kinking resembles twinning (Passchier and Trouw, 2005)

Twin boundary migration recrystallisation

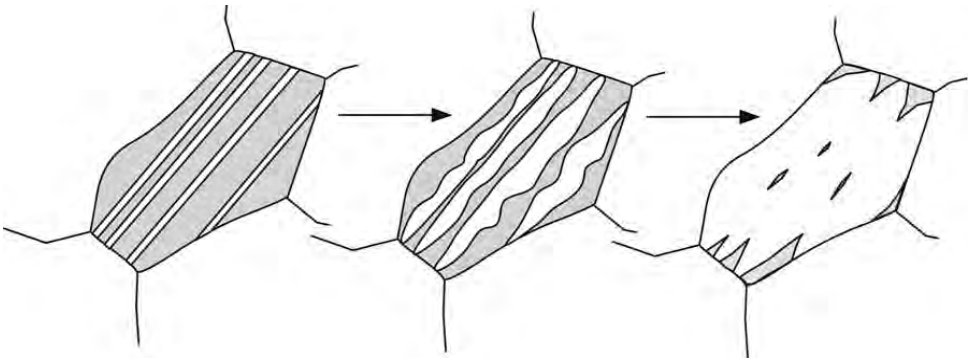

Twin boundary migration recrystallisation in calcite can sweep whole crystals by migration of twin boundaries. Grain boundaries are not affected by this recrystallisation mechanism (Ramsay, 1967and Hobbs et al., 1988).

Undulose extinction in calcite

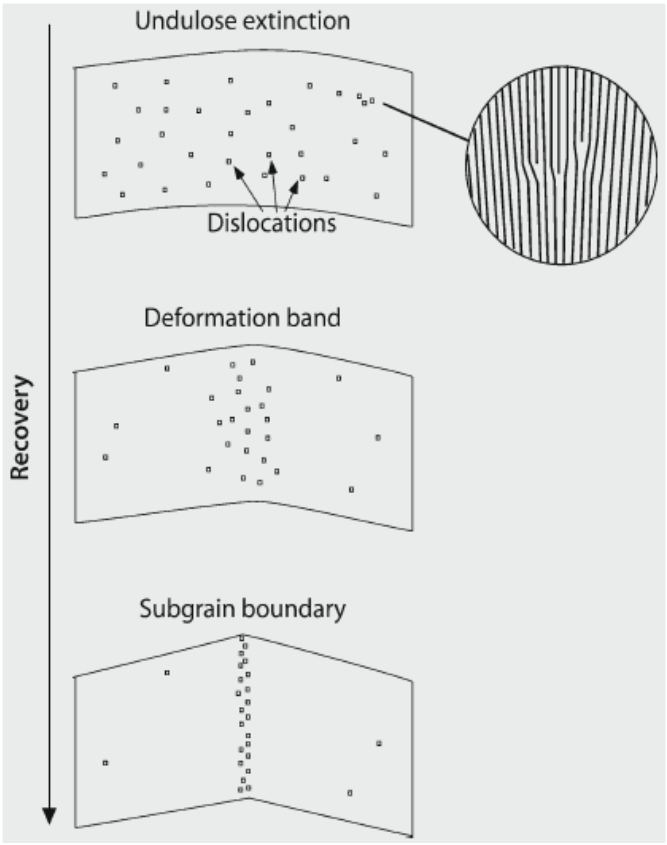

Schematic illustration of the recovery process. **a.** undulose extinction, **b.** deformation bands and eventually, **c.** subgrain boundary (Passchier and Trouw, 2005)

Bulging (BLG) Recrystallisation

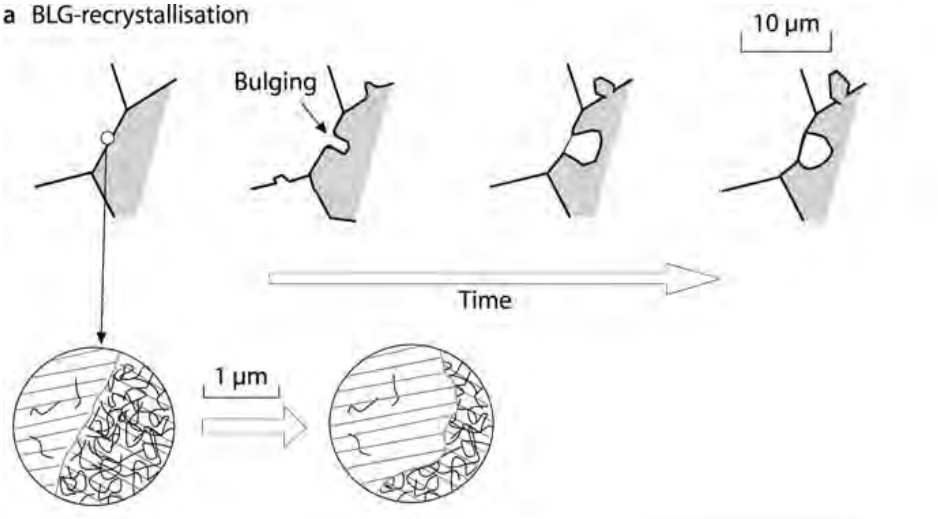

Process of low-temperature grain boundary migration or bulging (BLG) recrystallisation. At low temperature, grain boundary mobility may be local, and the grain boundary may bulge into the crystal with high dislocation density and form new, independent small crystals. Old grains may be little deformed or show fractures (at low temperature) or deformation lamellae and undulose extinction. Remains of old grains are commonly surrounded by moats of recrystallised grains, a feature known as a core-and-mantle structure (Passchier and Trouw, 2005).